HIGH FREQUENCY BEAM DIFFRACTION BY APERTURES AND REFLECTORS

by

GIBREEL A. SUEDAN

M. SC., CALIFORNIA INSTITUTE OF TECHNOLOGY

A THESIS SUBMITTED IN PARTIAL FULFILMENT OF

THE REQUIREMENTS FOR THE DEGREE OF

DOCTOR OF PHILOSOPHY

in

THE FACULTY OF GRADUATE STUDIES

DEPARTMENT OF ELECTRICAL ENGINEERING

We accept this thesis as conforming

to the required standard

THE UNIVERSITY OF BRITISH COLUMBIA

JUNE 1987

In presenting this thesis in partial fulfilment of the requirements for an advanced degree at the University of British Columbia, I agree that the Library shall make it freely available for reference and study. I further agree that permission for extensive copying of this thesis for scholarly purposes may be granted by the head of my department or by his or her representatives. It is understood that copying or publication of this thesis for financial gain shall not be allowed without my written permission.

Department of ELECTRICAL ENGINEERING

The University of British Columbia
1956 Main Mall
Vancouver, Canada
V6T 1Y3

Date Sept. 28, 1987

ABSTRACT

Most solutions for electromagnetic wave diffraction by obstacles and apertures assume plane wave incidence or omnidirectional local sources. Solutions to diffraction problems for local directive sources are needed. The complex source point representation of directive beams together with uniform solutions to high frequency diffraction problems is a powerful combination for this. Here the method is applied to beam diffraction by planar structures with edges, such as the half-plane, slit, strip, wedge and circular aperture.

Previously used restrictions to very narrow beams and paraxial regions, are removed here and the range of validity increased. Also it is shown that the complex source point method can give a better approximation to broad antenna beams than the Gaussian function.

The solution derived for the half-plane problem is uniform, accurate and valid for all beam orientations. This solution can be used as a reference solution for other uniform or asymptotic solutions and is used to solve for the wide slit and complementary strip problems.

Uniform solutions for omidirectional sources are developed and extended analytically to become solutions for directive beams. The uniform theory of diffraction is used to obtain uniform solutions where there are no simple exact solutions, such as for the wedge and circular aperture. Otherwise rigorously correct solutions at high frequencies for singly diffracted far fields are used, such as for the half-plane, slit and strip. The geometrical theory of diffraction and equivalent line currents are used to include interaction between edges.

Extensive numerical results including the limiting cases; e.g. plane wave incidence, line and point sources are given. These solutions are compared with previous solutions, wherever possible and good agreement is evident.

Beam diffraction by a wedge with its edge on the beam axis is analysed. This solution completes a previous asymptotic solution which is infinite on the shadow boundaries and inaccurate in the transition regions. Finally, the diffraction by a circular aperture illuminated by normally incident acoustic beam, is derived and the singularity along the axial caustic is removed using Bessel functions and a closed form expression for multiple diffraction is derived.

ACKNOWLEDGMENTS

I wish to express my heart felt gratitude to Dr. E. V. Jull for both his academic and personal assistance, advice and encouragement throughout the course of this investigation. I am also indebted to him for taking the time to read and evaluate my thesis through his invaluable suggestions.

Full recognition and thanks to the Libyan people for their generous financial support throughout my years of study. The computing support provided by the Natural Sciences and Engineering Research Council (NSERC) of Canada, is gratefully acknowledged.

I wish to thank the general office staff of the Department of Electrical Engineering at the University of British Columbia for their kind help and cooperation.

Special thanks and deep appreciation to my family who waited patiently during my long course of study.

TABLE OF CONTENTS

LIST OF FIGURES

CHAPTER I

INTRODUCTION AND LITERATURE REVIEW

1.1 Introduction

Electromagnetic wave diffraction by conducting reflectors and by apertures in conducting screens has been studied extensively for many years. Solutions for plane wave incidence, or a distant source, and isotropic local sources in real space, have been obtained for the half-plane, for the wedge, for the slit and complementary disc (see Bowman et al., 1969). Of the two categories of solutions, low frequency and high frequency or asymptotic solutions, this thesis is concerned with the latter. Uniform asymptotic solutions for the half screen and wedge have been obtained for omnidirectional local sources (e.g. Boersma and Lee, 1977; Kouyoumjian and Pathak, 1974). Uniform asymptotic solutions are useful in the diffraction solutions for directive beams considered in this thesis.

Diffraction by simple shapes when illuminated by directive local sources such as Gaussian beams and antenna beams, using different techniques, recently, has been extensively studied. One of these techniques is the beam field representation by a current distribution. Anderson (1978) applied this technique to solve for antenna beam diffraction by a conducting half-plane. The difficulty of obtaining the current distribution, which represents the effect of the antenna beam exactly or approximately, is one of the disadvantages of this approach. Another is the difficulty of solving the resulting boundary value

problem. Certainly the accuracy depends on the field representation and on the approximations made to solve the integral involved. However, this approach gives continuous fields at the shadow boundaries.

The Kirchhoff method is another technique used to solve for Gaussian beam diffraction by half-screen (Pearson et al., 1969). Because of double integration introduced in this method, asymptotic solutions are complicated and numerical solutions very costly when large scatterers are assumed. Another shortcoming is poor accuracy in the region off the beam axis. However, it predicts no singularity on the caustic axis.

The Boundary Diffraction Wave Theory (BDWT) proposed by Miyamoto and Wolf (1962), overcomes the problem of a double integration in the Kirchhoff method, but makes the integrand (the vector potential) more complicated. Consequently the integration becomes very difficult in addition to the difficulty in obtaining the vector potential itself. This approach has the same accuracy as the Kirchhoff method or less when the vector potential is approximate. Using the BDWT, Otis and Lit (1975) gave the solution to 2-dimensional Gaussian beam diffraction by a half-screen and the 3-dimensional case was given by Takenaka and Fukumitsu (1982). The single diffraction by a circular aperture when illuminated by a normally incident Gaussian beam was obtained by Otis et al. (1977) and corrected by Takenaka et al. (1980). Also the same problem was solved by Belanger and Couture (1983), using the BDWT with the Gaussian beam represented by a complex source point.

The Inhomogeneous (evanescent) Wave Tracking (IWT) proposed by Choudhary and Felsen (1973) and refined by Einziger and Raz (1980), is another approach used to solve the problem of directive fields. The main advantage of this method is that it gives a physical explanation of the propagation and scattering mechanism. Because of the difficulty of obtaining the phase paths, it has been rarely used. Choudhary and Felsen (1974) applied the IWT method to the problem of Gaussian beam relfection by a conducting circular cylinder. Reflection by a parabolic refelctor was given by Hasselmann and Felsen (1982). Also Felsen (1976) studied the propagation of Gaussian beams in free space using the same method.

The Complex Ray Tracing (CRT) method was invented to overcome the difficulty of determining the phase paths in the IWT method by tracing the directive fields in the complex space. This technique was applied by tracing the Gaussian beam in free space by Keller and Streifer (1971), Deschamps (1971, 1972) and Williams (1973). Ghione et al. (1984) used the CRT method to study the radiation from large apertures with tapered illuminations. Scattering of evanescent plane waves by a conducting circular cylinder was given by Wang and Deschamps (1974). Also Chione et al. (1984) applied the same technique to a reflector antenna illuminated by a beam field.

The CRT method is an optical (asymptotic) solution valid only for high frequencies. The representation of directive beams with complex source points along with using existing (exact or approximate) solutions for real sources, which is called the Complex Source Point (CSP) method,

can give (exact or asymptotic) solutions to many canonical and less simple problems involving directive sources, with no extra effort, provided analytical continuation into complex space is possible.

The only difficulty with the CRT and CSP methods, especially for non-planar surfaces, is to find an a-priori selection rule to distinguish the relevant from spurious ray contributions. Now this can be done by studying the saddle points and steepest descent paths (Ghione et al., 1984). Otherwise these techniques are easy to apply, accurate, and need no integral evaluation in asymptotic solutions. Furthermore these techniques are uniform on the shadow boundaries, except for asymptotic solutions when the beam axis passes through the diffracting edge. The CSP method uses existing solutions, so it needs less effort and it can be used for exact solutions. Because of the above, the CSP method is adopted everywhere in this thesis.

The asymptotic solutions for the Gaussian beam diffraction by a conducting wedge (Felsen, 1976) and by a half-screen (Green et al., 1979), are invalid when the beam axis passes through the diffracting edge or when broad beams are assumed. They are inaccurate in the transition regions and singular on the shadow boundaries.

One of the goals here is to obtain a uniform solution for the wedge using the Uniform Theory of Diffraction and the CSP representation, and for the half-screen, based on a simple solution exact in the far field limit, using the CSP method. A more simple convenient formula for the shadow boundary locations also will be derived. solution to 2-dimensional antenna beam diffraction by a slit, including double

diffraction, and complementary conducting strip will be given. This problem has not been studied before. Finally beam diffraction by circular aperture for normal incidence, including interaction between the edges, is analyzed using the UTD and CSP representation. For all the above examples, numerical results include the limiting cases of plane wave incidence or isotropic sources.

1.2 General Assumptions

Through all the subsequent analysis, the following are assumed:

a) The time dependence is harmonic ($\exp[j\omega t]$) and is suppressed.

b) The medium is homogeneous, isotropic, nondispersive and non-dissipative.

c) The frequencies are very high and observation points are in the far field of the scatterer ($kr \gg 1$).

d) Perfect conductors (screen, half-screen, etc.)

e) Scalar fields (U) are assumed.

f) Soft boundary conditions are assumed.

1.3 Literature Review

Scattering by simple reflectors and apertures as a half-plane, wedge, circular aperture, parabolic and paraboloidal antennas, and circular cylinders when illuminated by directive sources, which are approximately Gaussian beams in the paraxial region, have been studied by many researchers using the different techniques summarized below. As

only the complex source point method of secton 1.3.8 is used in this thesis, the reader may choose to omit sections 1.3.1-1.3.7.

1.3.1 Beam Representation by Current Distributions

By this method, the incident beam is represented by a non-uniform current sheet distribution. Then the boundary value problem of current element in presence of the scatterer is solved by integrating the obtained solution over the whole current sheet. Then the integral is evaluated numerically or asymptotically. The solution with this approach is continuous at the shadow boundaries. This approach is different from physical optics and spectral theory of diffraction. Anderson (1978) used this technique to solve antenna beam diffraction by a conducting half-screen.

1.3.2 Spectral Theory of Diffraction

The basic concepts of the spectral theory of diffraction (STD) proposed by Mittra et al. (1976), were illustrated by the familiar conducting half-plane illuminated by plane wave. The principal contribution of STD is the introduction of the spectral diffraction coefficient which is defined as the Fourier transform of the current induced on the scatterer. This coefficient is associated with the integral representation of the scattered and total fields. Although the spectral diffraction coefficient tends to infinity at the shadow boundaries, the fields obtained by the STD are finite. The scattered field can be constructed by convolving, in the space domain, the induced

current and the radiated field of an elementary point or line source current (Green's function). The total field is the sum of the scattered field and, whenever applicable, the incident field. When the integrals involved in the scattered and total fields are asymptotically evaluated using the saddle point technique, the leading term yields Keller's GTD field.

Arbitrary incident fields, also can be assumed using the STD technique by applying the superposition principal. The spectrum of the incident arbitrary field is multiplied by the spectral diffraction coefficient of the plane wave then integrating over the entire spectrum to give a double integral representation of the scattered and total fields. This integral may be evaluated asymptotically or numerically. Rahmat-Sammii and Mittra (1977) give detailed calculations and applications.

1.3.3 Kirchhoff-Fresnel Method

In this method the total field behind an aperture in a conducting plane is given in terms of the double integral of the incident field and its derivative in the plane of the aperture. This integration is taken over the aperture (Born and Wolf, 1974, p. 375-386). Then the integral is evaluated numerically or asymptotically to yield the total field.

Pearson et al. (1969) applied this technique to the diffraction of a fundamental-mode Gaussian beam (Kogelnik, 1965) by a semi-infinite conducting screen. An asymptotic soluction in the Fresnel limit was derived.

1.3.4 Boundary Diffraction Wave Theory

Through the use of Stoke's theorem and an associate potential vector, Miyamoto and Wolf (1962) showed that, in general, the Kirchhoff surface integral, mentioned in the previous seciton, can be split into two separate line integrals. One represents a wave originating from the boundary of the diffracting aperture called the boundary diffraction wave (BDW) and the other represents the geometrical wave originating from the source. The latter is zero if the observation points lie in the shadow region. The total field is given by the sum of the BDW and geometrical wave fields. The BDW method has the same limitations and approximations as the Kirchhoff-Fresnel method.

Application of the technique to a Gaussian beam with cylindrical symmetry (Siegman, 1971, Ch. 8) normally incident on a circular aperture in a conducting plane is given by Otis (1974) under the paraxial far field approximations.

1.3.5 Uniform Asymptotic Theory of Diffraction

A uniform asymptotic theory of diffraction (UAT) which provides the correct asymptotic solution for an arbitrary incident field on a half-plane has been developed by Alhuwalia et al. (1968) and Lewis and Boersma (1969), corrects defects of the geometricl theory of diffraction (GTD); such as singularities at the shadow boundaries and at the diffracting edge. It also provides higher order terms in the diffracted field expansion.

Boersma and Lee (1977) applied UAT to the problem of cylindrical wave from a line source parallel to the edge of a conducting half-plane. In their approach all fields are expanded asymptotically in inverse powers of the wave number which is assumed large. The coefficients of expansion are derived by substituting in the reduced wave equation. The postulated total field is a uniform asymptotic expansion based on the exact solution of a plane wave incident on a half-plane, so the UAT reduces to the exact solution of plane wave diffraction by a half-plane.

Excluding the caustic points at the source and its image, the UAT solution for the total field is finite and continuous at all observation points. Away from the shadow boundaries, the leading term of the UAT solution reduces to the GTD solution. Since the UAT solution remains finite at the diffracting edge, it can also be used for near-field calculations. Unlike the GTD where the diffraction coefficient is taken from the Sommerfield's half-plane solution, the diffraction coefficient of UAT is derived by enforcing the edge condition.

The UAT has been extended to electromagnetic diffraction by a curved wedge by Lee and Deschamps (1976) but there it is approximate. The main disadvantage of the UAT is its complexity in determining higher order terms, when very directive incident fields are assumed and when interaction between edges are significant. In such cases the uniform geometrical theory of diffraction by Kouyouimjian and Pathak (1974), which gives less accurate results, may be used instead.

1.3.6 Inhomogeneous (Evanescent) Wave Tracking

Here inhomogeneous waves, such as Gaussian beams, can be tracked from the source or the initial surface to the observation point via the scatterer, totally in real space. By solving the differential equations for the real and imaginary parts of the phase and amplitude functions, which result from satisfying the reduced wave equation, the total field can be completely determined. Neglecting the wave length squared term in the above differential equations enables one to calculate the phase independently from the amplitude. The solution obtained in this way is approximate, but the accuracy increases with decreasing the wave length. For details see Choudhary and Felsen (1973), Felsen (1976) and Einziger and Raz (1980).

The inhomogeneous wave tracking method is applied to Gaussian beam reflection by conducting circular cylinder as given by Choudhary and Felsen (1974) without including diffraction from edges.

1.3.7 Complex Ray Tracing

Since it has been noted that a Gaussian beam can be represented in terms of a bundle of complex rays, by Deschamps (1971) and Keller and Streifer (1971), complex ray tracing (CRT) was introduced and complex geometrical optics has been developed. In the CRT method, the phase, amplitude and space coordinates are allowed to take complex values, as in the IWT method. The mathematical basis of this method is the process of analytic continuation. The tracing of the field from the complex source to the real observation point via the scatterer (complex in general) is in complex space. The study of a Gaussian beam, simulated

by a complex line or point source, and propagation in free space from an assigned initial field distribution have been extensively dealt with (Ghione, Montrosset and Orta, 1984).

The eikonal and transport equations used in the IWT method are applicable here. Without separating the phase and amplitude functions into real and imaginary parts, the differential equations can be solved by the method of characteristics to obtain the phase and amplitude of the total field.

1.3.8 Complex Source Point

In the complex ray tracing method, asymptotic solutions are obtained for high frequency (large wave numbers) and far fields. But the Complex Source Point (CSP) method can be used to obtain exact as well as asymptotic solutions for low or high frequencies and near or far fields, as long as solutions to corresponding real sources exist and can be analytically continued into complex space.

On assigning complex values to the source coordinate locations of an oscillating isotropic point or line source, one may generate a highly collimated field that behaves in the vicinity of its maximum (beam axis) like a 3-dimensional (point source) or 2-dimensional (line source) Gaussian beam (Deschamps 1971, Jones 1979; Couture and Belanger 1981, Albertsen et al., 1983, and Felsen 1976, 1984). This implies that the CSP substitution converts point or line source Green's functions for propagation and diffraction in various environments into field solutions for incident Gaussian beams. Thus without further effort, the whole rigorous and asymptotic solutions yield the field response for beam

excitation, provided that there can be an analytic continuation of the solutions from real to complex space.

Let us take, as an example, the evolution of a 2-dimensional Gaussian beam using the CSP. The field of an isotropic point source in free space, is given by Green's function G(R) which is a solution to the wave equation

$$G(R) = \frac{e^{-jkR}}{R} \quad , \tag{1.1}$$

where R is the distance between the source and observation point, which can be real or complex. For a wave propagating in the z-direcion, let the source be located at (0,0,-jb) where b is a real positive number. Then

$$R = [\rho^2+(z+jb)^2]^{1/2} \quad ; \quad \rho^2 = x^2+y^2 \quad , \quad \text{Real}(R)\geq 0 \tag{1.2}$$

From (1.2), R is a multivalued function and vanishes at the branch line z=0, ρ=b. To make R single valued and G(R) analytic, a branch cut (surface) at z=0 and $\rho \leq b$ should be introduced (see Fig. 1.1a).

In the paraxial region ($\rho^2 << z^2 + b^2$) and for z>0, R can be simplified to

$$R \simeq j\left[b - \frac{b\rho^2}{2(z^2+b^2)}\right] + z\left[1 + \frac{\rho^2}{2(z^2+b^2)}\right] \tag{1.3}$$

Inserting (1.3) in (1.1) gives

$$G(\rho,z) \simeq \frac{e^{kb}}{\sqrt{z^2+b^2}} \cdot e^{-(\rho/w)^2} \cdot e^{-jB(\rho,z)} \tag{1.4}$$

where w is the e^{-1} half beam width and B(ρ,z) is the phase

$$w = [2(z^2 + b^2)/kb]^{1/2} \tag{1.5}$$

$$B(\rho,z) = \frac{z}{b}[kb + (\rho/w)^2] + \tan^{-1}(b/z) \tag{1.6}$$

The propagating wave, defined by (1.4), is subject to an exponential decay perpendicular to the z-axis proportional to ρ^2. Thus a Gaussian beam is formed in the paraxial region. For b>>z, the wave propagates parallel to the z-axis with distortion of the wave front; and for b<<z the phase paths (locus of e^{-1} points) are hyperboloids given by

$$(\rho/w_o)^2 - (z/b)^2 = 1, \qquad (1.7)$$

where w_o is the e^{-1} half-beam width at the beam waist (z=0). $w_o=(2b/k)^{1/2}$ is often called the spot size at the beam waist (see Fig. 1.1b).

This derivation is also valid for two dimensional fields. The implications of this are that field solutions for two or three-dimensional Green's functions can be continued analytically into complex space to provide the solutions for directive beams. This can be applied to both numerical and analytical solutions, or to either low or high frequency diffraction solutions. At low frequencies beam diffraction can also be solved numerically. At high frequencies, numerical methods generally are inefficient or fail and the geometrical theory of diffraction together with the complex source point method provides the most convenient solution for beam diffractions.

For higher modes of Gaussian beams, see Shin and Felsen (1976), Hashimoto (1985) and Luk and Yu (1985). Representation of more complicated beams has been studied by Mantica et al. (1986), and wave solutions under complex space-time shifts has been, lately, proposed by Einziger and Raz (1987).

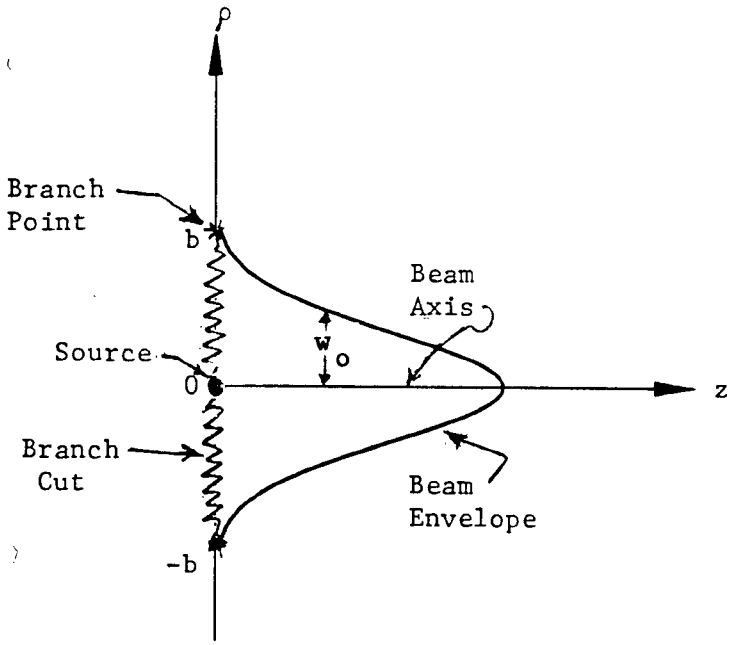

Fig. 1.1a Branch cut and branch points of the CSP

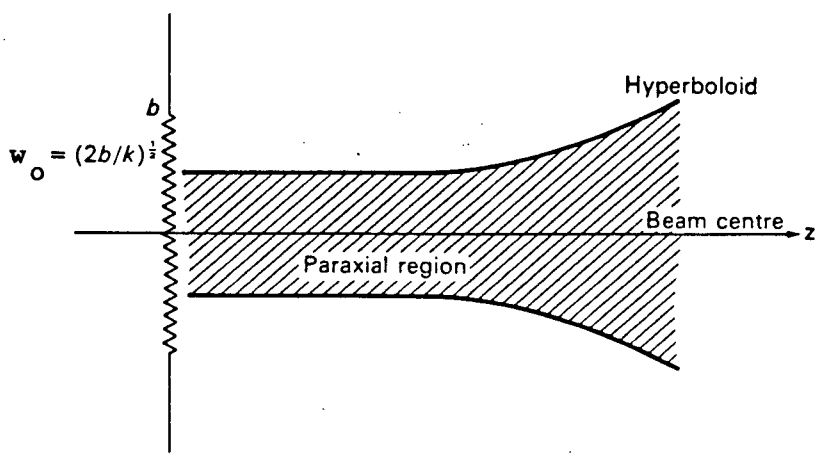

Fig. 1.1b The paraxial region of a Gaussian beam

1.4 Overview of the Thesis

An introduction is given in Section (1.1) and some of existing work in the literature on the representation and diffraction of directive source fields by simple shapes is summarized in Section (1.3).

In Chapter II, beam evolution from a Complex Source Point (CSP) is given in polar coordinates. This is more convenient than representation in cartesian coordinates and directly relates the beam parameters (orientation and directivity) to the complex coordinates of the source. The beam field generated by the CSP, a Gaussian beam and a typical antenna aperture are compared and illustrated. Derivation of more complicated beams; e.g. a beam with sidelobes, is also achieved.

Chapter III is devoted to obtaining a simple solution, uniform everywhere and for all beam orientations, for antenna beam diffraction by a half-screen, based on the exact far field solution of line source diffraction by a half-screen. A comparison of this solution with the asymptotic solution given by Green et al. (1979) is illustrated. Also a simpler formula for shadow boundary location is derived. Results obtained here are used in Chapter IV of the problem of beam diffraction by a slit in a conducting plane and by a complementary strip.

In Chapter V, beam diffraction by a conducting wedge, when the beam axis passes through the edge, is derived using the UTD. Shadow boundaries are obtained and numerical results for different angles of incidence and wedge angles are given.

In the above examples, only 2-dimensional beams and straight edges are assumed. In Chapter VI, a 3-dimensional beam diffracted by a

circular aperture in a perfectly conducting plane, including multiple diffraction. Normal incidence, i.e. the beam axis coincident with the aperture axis, is assumed. Numerical results for different beam waists, including the plane wave as a limiting case, are given. The latter is compared with Keller's solution (1957).

A summary, conclusions and recommendations for future work are given in Chapter VII.

Appendix A contains an evaluation of Fresnel integrals with complex arguments in terms of error functions and some important properties of Fresnel integrals are given.

In Appendix B, the real and imaginary parts of r_s, the complex distance from the source to the edge, in terms of the real distance of the source and the incident beam parameters are derived.

For comparison reasons the asymptotic solution of Gaussian beam diffraction by conducting half-screen, and the shadow boundary positions given by Green et al. (1979) are summarized in Appendix C.

Appendix D, shows the singularity cancellation in the wedge diffraction coefficient at the shadow boundaries, when illuminated by a real line source or a beam source its axis passing through the edge.

Appendix E contains the analysis of beam diffraction by a conducting parabolic reflector.

In Appendix F, the derivation of arctangent of a complex number, in the proper quadrant is given in terms of a complex angle in the first quadrant, that can be determined by the UBC computer functions.

Appendix G is a list of computer programs for the problems discussed in Chapters II-VI and in Appendix E.

CHAPTER II

COMPLEX SOURCE POINT METHOD

By assigning complex values to the source coordinate locations of a time harmonic isotropic point or line source in a homogeneous unbounded medium, one may generate a collimated field that behaves like a 3-dimensional (point source) or 2-dimensional (line source) directive beam. This implies that the complex source point substitution converts point or line source Green's functions (wave equation solutions) for propagation and diffraction in various environments into field solutions for incident directive beams. Thus, without further effort, the whole rigorous and asymptotic diffraction solutions yield the field response for beam excitation, provided there can be an analytic continuation of the solutions from real space to complex space.

2.1 Beam Evolution from a Complex Line Source

Fig. 2.1a shows a 2-dimensional line source at r_o, Θ_o from the origin of coordinates. The fields are uniform in the z direction and represent an omnidirectional cylindrical wave. The field intensity at any observation point r, Θ which is a solution of wave equation may be written as

$$U^i = \sqrt{\pi/2}\, e^{-j\pi/4} H_o^{(2)}(kR) \simeq \frac{e^{-jkR}}{\sqrt{kR}} \quad ; \quad kR >> 1 \quad , \qquad (2.1)$$

where R is the distance of the observation point from the source.

$$R = [r^2 + r_o^2 - 2rr_o \cos(\Theta - \Theta_o)]^{1/2} \tag{2.2}$$

In the far field ($r>>r_o$), $R \simeq r - r_o \cos(\Theta - \Theta_o)$ applies in the phase term and $R \sim r$ in the amplitude term of (2.1) giving

$$U^i \simeq \frac{e^{-jk[r-r_o \cos(\Theta-\Theta_o)]}}{\sqrt{kr}} \quad ; \quad 0 < \Theta_o < \pi \tag{2.3}$$

By making the source coordinates (r_o, Θ_o) complex (r_s, Θ_s) the omnidirectional wave becomes a directive beam uniform in the z direction.

$$\bar{r}_s = \bar{r}_o - j\bar{b} \tag{2.4}$$

where $\bar{r}_s$, $\bar{r}_o$ and $\bar{b}$ are the complex source position, real source position and beam parameter vectors given in polar coordinates as $\bar{r}_o = (r_o, \Theta_o)$, $\bar{r}_s = (r_s, \Theta_s)$ and $\bar{b} = (b, \beta)$, where b defines the sharpness of the beam and β defines its orientation. All angles are measured from the x-axis. r_s and r_o are measured from the origin while b is measured from the real point source as shown in Fig. 2.1.

$$r_s = [r_o^2 + 2r_o(-jb) \cos(\beta-\Theta_o) + (-jb)^2]^{1/2}; \ \mathrm{Re}(r_s) > 0 \tag{2.5}$$

$$\Theta_s = \cos^{-1}\left[\frac{r_o \cos\Theta_o - jb \cos\beta}{r_s}\right] \tag{2.6}$$

where $b > 0$ and $0 \leq \beta \leq 2\pi$. Replacing r_o, Θ_o by r_s, Θ_s in (2.3) gives

$$U^i \simeq \frac{e^{-jk[r-r_s \cos(\Theta-\Theta_s)]}}{\sqrt{kr}} \quad ; \quad r >> |r_s| \tag{2.7}$$

$$r_s \cos(\Theta \mp \Theta_s) = r_s \cos\Theta_s \cos\Theta \pm r_s \sin\Theta_s \sin\Theta \tag{2.8a}$$

and from (2.4),

$$r_s \cos\Theta_s = r_o \cos\Theta_o - jb\cos\beta \quad , \qquad (2.8b)$$
$$r_s \sin\Theta_s = r_o \sin\Theta_o - jb\sin\beta$$

Using these in (2.8a) yields

$$r_s \cos(\Theta \mp \Theta_s) = r_o \cos(\Theta \mp \Theta_o) - jb\cos(\Theta \mp \beta) \qquad (2.8c)$$

Substitute (2.8c) in (2.7) to get

$$U^i \simeq \frac{e^{-jk[r - r_o\cos(\Theta-\Theta_o)]}\; e^{kb\cos(\Theta-\beta)}}{\sqrt{kr}} \qquad (2.9)$$

By comparing equation (2.9) with (2.3) we find that (2.9) represents an omnidirectional cylindrical wave (first term) modulated by a beam pattern $\exp[kb\cos(\Theta-\beta)]$ with its maximum in the direction $\Theta=\beta$ and minimum in the direction $\Theta=\beta+\pi$.

2.2 Half Power Beam Width

To calculate the half power beam width (HPBW), we normalize the field of (2.9) to its peak value.

$$\left|\frac{U^i(r,\Theta)}{U^i(r,\beta)}\right| = e^{-kb[1 - \cos(\Theta-\beta)]} \qquad (2.10)$$

At $\Theta-\beta = \frac{HPBW}{2}$ the normalized field amplitude of (2.10) equals $1/\sqrt{2}$.

$$e^{-kb[1 - \cos(\frac{HPBW}{2})]} = \frac{1}{\sqrt{2}} \qquad (2.11)$$

Thus the half power beam width is related to the beam parameter kb by

$$HPBW = 2\cos^{-1}\left(1 - \frac{\ell n\sqrt{2}}{kb}\right) \; ; \; kb \geq \frac{\ell n\sqrt{2}}{2} \qquad (2.12)$$

(2.12) shows that as kb increases the beam width decreases. If $kb < \frac{1}{4} \ln 2$ the beam does not decay to the half power point.

Special Case:

r_s and Θ_s are complex unless b=0, corresponding to a real source or $\beta=\Theta_o$ or $\Theta_o + \pi$. To show the last case substitute for $\beta=\Theta_o$ or $\Theta_o+\pi$ in (2.5) and (2.6) to get

$$r_s = r_o \mp jb \quad ; \quad \beta = \Theta_o, \ \Theta_o+\pi \tag{2.13a}$$

and

$$\Theta_s = \Theta_o \tag{2.13b}$$

Therefore Θ_s becomes real whenever the beam axis lies along r_o.

2.3 Comparison with Gaussian and Typical Aperture Beam Patterns

Since near the beam axis, $\Theta-\beta$ is small, we can write

$$\cos(\Theta-\beta) \simeq 1 - \frac{(\Theta-\beta)^2}{2} \tag{2.14}$$

Using (2.14) in (2.10) gives

$$\left|\frac{U^i(r,\Theta)}{U^i(r,\beta)}\right| \simeq e^{\frac{-kb(\Theta-\beta)^2}{2}} \tag{2.15}$$

Showing, as is well known (Green et al. (1979) and Hasselman (1980)), that a complex source point provides a beam which is Gaussian in the paraxial region. It is important to appreciate that this complex source point representation of a beam is not limited to the paraxial region.

Fig. 2.2a shows the far field radiation pattern of a source at $kr_o=8$ for several values of the kb corresponding to half power beam widths ranging from 68.5°(kb=2) to 10.4°(kb=85).

In Fig. 2.2b the broken curve is a typical aperture antenna beam pattern, that of an inphase cosinusoidal distribution in an aperture of width 2a. Its normalized pattern is

$$\left|\frac{U^i(r,\Theta)}{U^i(r,\beta)}\right| = \frac{\cos[ka\,\sin(\Theta-\beta)]}{1-[\frac{2ka}{\pi}\sin(\Theta-\beta)]^2} \tag{2.16}$$

For ka=4, its half-power beam width is 55.7°. The solid curve in Fig. 2.2b is a complex source point pattern of the same beam width (HPBW=55.7° or kb≈3) with

$$kb = \frac{\ell n\sqrt{2}}{[1-\cos(\frac{HPBW}{2})]} \tag{2.17}$$

The dashed curve in Fig. 2.2b is a Gaussian beam with the same beam width.

$$\left|\frac{U^i(r,\Theta)}{U^i(r,\beta)}\right| = e^{-\ell n\sqrt{2}[\frac{2(\Theta-\beta)}{HPBW}]^2} \tag{2.18}$$

All three curves overlap in the paraxial region ($\Theta-\beta$ small). At angles well off the beam axis, there is some difference, specially for broad beams (kb small), between (2.10) and (2.18) but here the complex source point pattern given by (2.10) is a slightly better approximation to (2.16). The complex source point representation appears to be a valid approximation to an antenna main beam pattern over the forward angular range ($|\Theta-\beta| < \pi/2$). Of course it cannot represent pattern sidelobes.

2.4 Multiple Complex Line Sources

More complicated beams such as beams with sidelobes also can be derived by using the complex source point method. By putting more than one source at different complex locations and changing the real locations r_o, Θ_o and the beam parameters b,β we get a variety of beam shapes.

Let us have M sources located at M complex positions. The mth source is located at r_{om}, Θ_{om} and its corresponding beam parameters are b_m, β_m as shown in Fig. 2.1b. Then the far field due to the mth complex source U_m^i is given by (2.9) and rewritten here as

$$U_m^i \simeq \frac{e^{-jk[r-r_{om}\cos(\Theta-\Theta_{om})]}}{\sqrt{kr}} \; e^{kb_m\cos(\Theta-\beta_m)} \; ; \; r \gg r_{om}, b_m \qquad (2.19)$$

Then the resultant far field, due to the M weighted sources, U^i is

$$\begin{aligned} U^i &= \sum_{m=1}^{M} Q_m U_m^i \\ &\simeq \frac{e^{-jkr}}{\sqrt{kr}} \sum_{m=1}^{M} Q_m \cdot e^{jkr_{om}\cos(\Theta-\Theta_{om})} \cdot e^{kb_m\cos(\Theta-\beta_m)} \end{aligned} \qquad (2.20)$$

where Q_m are the weighting factors.

In Fig. 2.3 the field due to 3 line sources is derived for different beam parameters b,β while the real locations are kept constant, $\Theta_{o1}=0$, $\Theta_{o2}=\pi/2$, $\Theta_{o3}=\pi$, $kr_{o1}=kr_{o3}=1$, $kr_{o2}=0$. The weighting factor $Q_2=1$ while Q_1 and Q_3 are variables (positive or negative, greater or less than 1). Because sources 1 and 3 are symmetric with respect to source 2, the fields shown in Fig. 2.3 are symmetric. Asymmetric fields

also can be derived from asymmetric sources. A beam which resembles a line source diffracted by a slit and a beam with first sidelobes which looks like a plane wave diffracted by a slit are shown in Fig. 2.3. More sidelobes can be derived if more complex sources are included.

In this chapter we studied the line source. The point source is very much the same with term $\frac{1}{\sqrt{kr}}$ is replaced by $\frac{1}{kr}$ and two dimensions is replaced by three dimensions.

A general description of multiple complex source point representation of beams has been given by Hashimoto (1985).

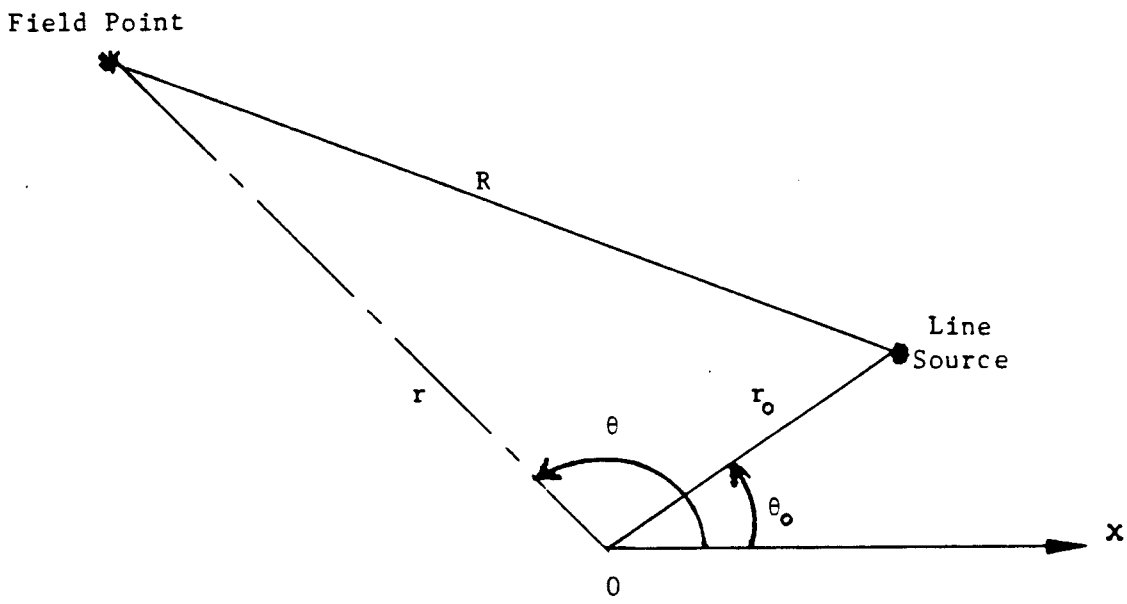

Fig. 2.1a Geometry of a complex line source and real far field point

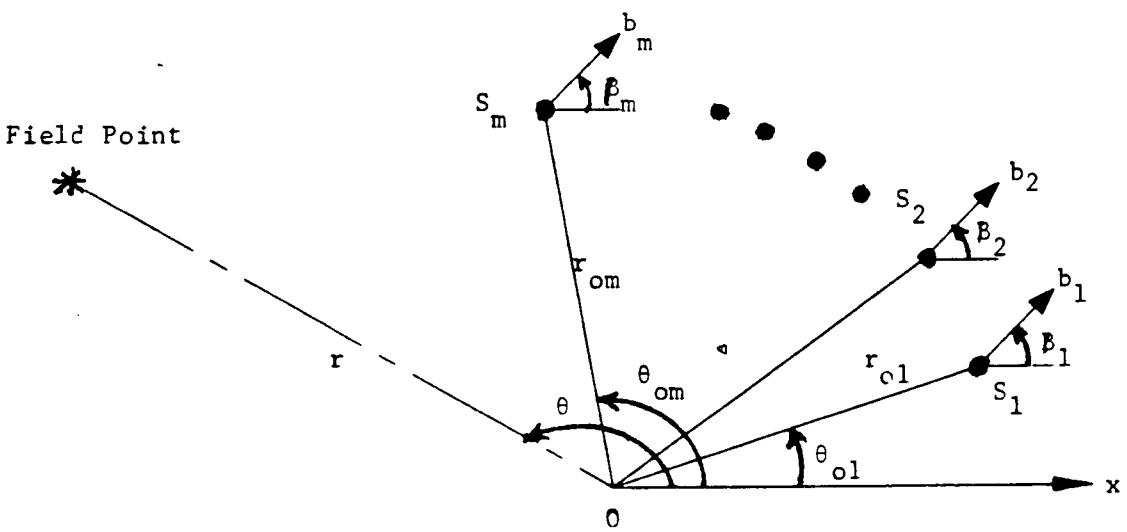

Fig. 2.1b Geometry of multiple complex line sources and real far field point

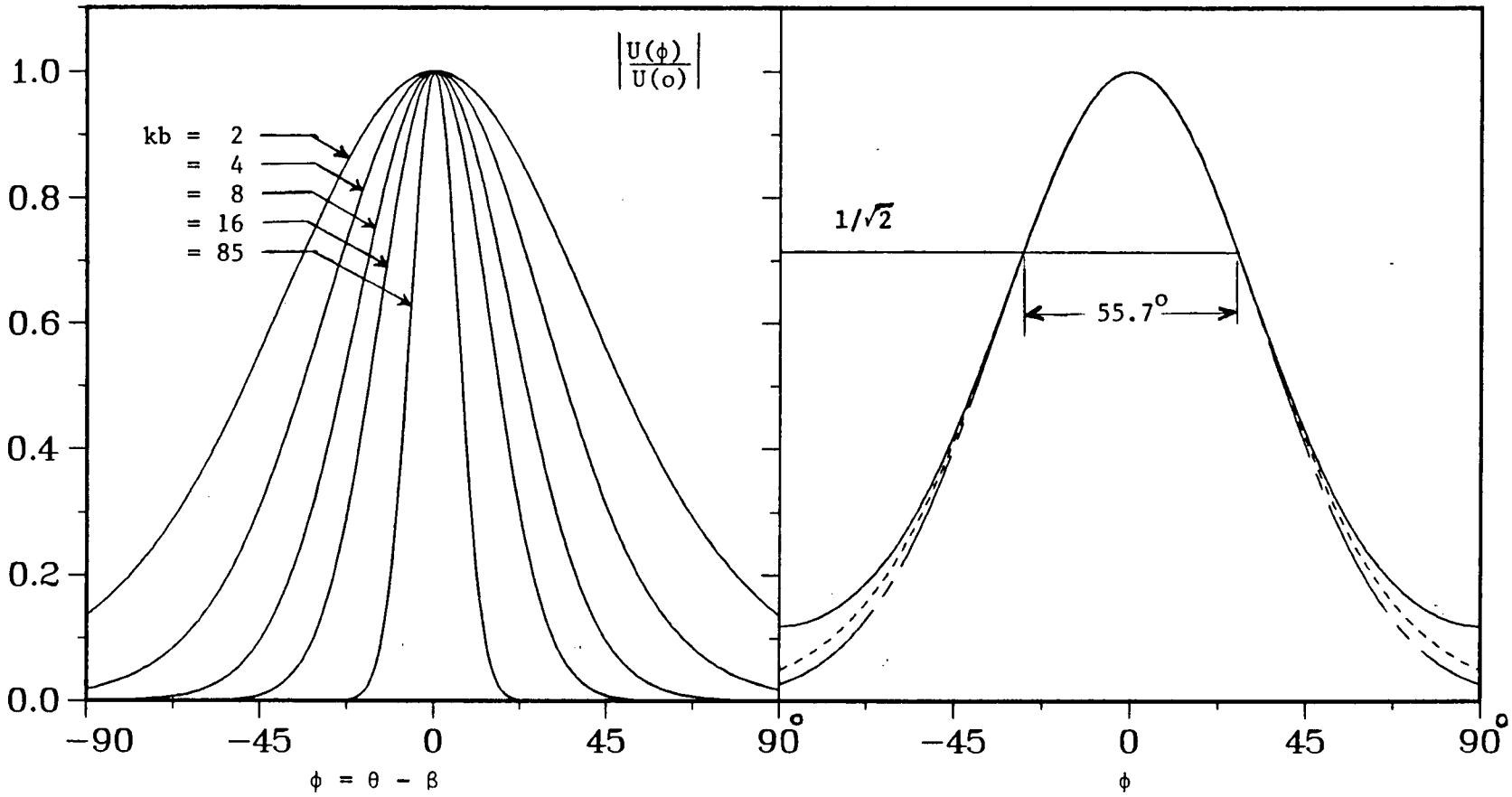

Fig. 2.2a Normalized radiation patterns with different beam widths using the Complex Source Pont method (r>>b)

Fig. 2.2b Comparison of radiation patterns with 55.7° beam width

——— typical aperture antenna (2.16, ka=4)
– – – – Complex Source Point (2.10, kb=3)
— – — Gaussian (2.18, HPBW=55.7°)

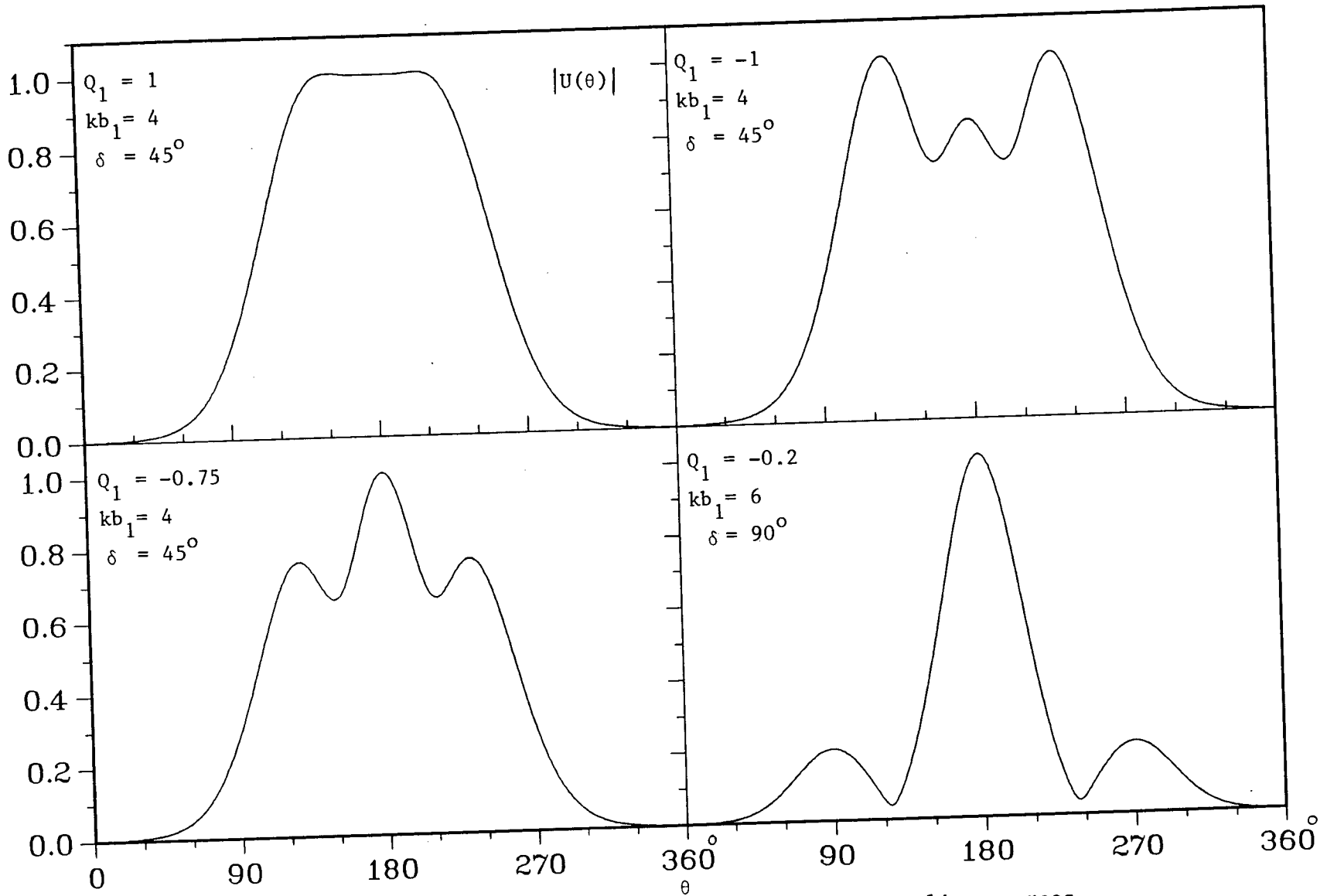

Fig. 2.3 Normalized patterns of multiple complex line sources

($\beta_2=180^o$, $Q_2=1.0$, $b_1=b_2=b_3$, $Q_1=Q_3$, $\beta_1=\beta_2-\delta$ and $\beta_3=\beta_2+\delta$)

CHAPTER III

BEAM DIFFRACTION BY A CONDUCTING HALF-PLANE

The total far field diffraction by a conducting half-screen of a beam is derived from the exact far field solution given by Born & Wolf (1978) and Clemmow (1950) for a real line solution and compared with the asymptotic solution given by Green et al (1979) (see Appendix C).

3.1 Uniform Solution Far Field Radiation Pattern

Suppose the omnidirectional source given by (2.1) is parallel to the edge of an infinitely thin perfectly conducting half-plane in y=0, x>0 as shown in Fig. 3.1. If $k(r+r_o)>>1$, the total field at any point r,Θ far from the edge ($r>>r_o$) is given exactly as

$$U(r,\Theta) = \frac{e^{-j(kr-\pi/4)}}{\sqrt{\pi kr}} \left\{ e^{jkr_o\cos(\Theta-\Theta_o)} F\left[-\sqrt{2kr_o}\cos\left(\frac{\Theta-\Theta_o}{2}\right)\right] - e^{jkr_o\cos(\Theta+\Theta_o)} F\left[-\sqrt{2kr_o}\cos\left(\frac{\Theta+\Theta_o}{2}\right)\right]\right\} \quad (3.1)$$

where

$$F[w] = \int_w^\infty e^{-j\tau^2} d\tau \quad (3.2)$$

is the Fresnel integral (see Appendix A).

By making the coordinates (r_o,Θ_o) of the source, complex (r_s,Θ_s) as in (2.5) and (2.6), the omnidirectional source becomes a directive beam and the solution in (3.1) is still valid with r_s, Θ_s replacing r_o, Θ_o.

The total far field of a beam diffracted by conducting half-screen for normal and non-normal incidence is given as

$$U(r,\Theta) = \frac{e^{-j(kr-\pi/4)}}{\sqrt{\pi kr}} \left\{ e^{jkr_s \cos(\Theta-\Theta_s)} F[-\sqrt{2kr_s}\cos(\frac{\Theta-\Theta_s}{2})] - e^{jkr_s \cos(\Theta+\Theta_s)} F[-\sqrt{2kr_s}\cos(\frac{\Theta+\Theta_s}{2})] \right\} \quad (3.3)$$

where F[w] is the complex Fresnel integral. The Fresnel integrals provide values finite and continuous across the shadow and reflection boundaries of the source and half-plane. In the asymptotic solution given by Green et al (1979) the field is singular along the boundaries when the beam axis hits the diffracting edge and is inaccurate in the neighbourhood of the shadow boundaries.

Efficient computer subroutines are available for calculating the Fresnel integrals in terms of error functions with the complex arguments (see Appendix A).

3.2 Shadow and Reflection Boundaries

Far from the half-screen edge simple expressions for the shadow and reflection boundaries are to be derived here analogous to those of Green et al (1979). These expressions are simpler and more accurate because only the real part of r_s need be calculated, whereas before real part, imaginary part and absolute value of r_s and real and imaginary parts of Θ_s were used. r_s and Θ_s are the source complex coordinates. These boundaries in general are not straight lines. They depend on the relative position of the half-screen edge with respect to the beam axis

and the source. The shadow and reflection boundaries are straight lines and coincide with those of the source when its coordinates are real, only when the beam axis passes through the edge of the half-screen.

Using the Green et al. (1979) definition of shadow and reflection boundaries, we have

$$\text{Real}(we^{j\pi/4}) = 0 \tag{3.4}$$

where w is the Fresnel integral argument of (3.3) given as

$$w_{\substack{i\\r}} = -\sqrt{2kr_s}\,\cos\left(\frac{\Theta \mp \Theta_s}{2}\right) \tag{3.5}$$

where the subscripts i, r refer to incidence and reflection. (3.4) is satisfied if

$$\text{Imag}\left[(we^{j\pi/4})^2\right] = 0 \tag{3.6}$$

and

$$\text{Real}\left[(we^{j\pi/4})^2\right] \leq 0 \tag{3.7}$$

Letting $r_s = R - jI$ as in Appendix B and using the identities given by (2.8c), it is easy to show that

$$(we^{j\pi/4})^2 = jk[R+r_o\cos(\Theta \mp \Theta_o)] + k[I+b\cos(\Theta \mp \beta)] \tag{3.8}$$

Hence

$$\text{Imag}\left[(we^{j\pi/4})^2\right] = k[R+r_o\cos(\Theta \mp \Theta_o)] \tag{3.9}$$

and

$$\text{Real}\left[(we^{j\pi/4})^2\right] = k[I+b\cos(\Theta \mp \beta)] \tag{3.10}$$

Substituting (3.9) in (3.6) and solving for Θ at the shadow and reflection boundaries, i.e. $\Theta=\Theta_{si}$ and Θ_{sr}, gives

$$\theta_{\substack{si \\ sr}} = \pm\, \theta_o + \cos^{-1}\left(\frac{-R}{r_o}\right) \tag{3.11}$$

since R=Real(r_s) and r_o are real and positive we can write

$$\theta_{\substack{si \\ sr}} = \pm\, \theta_o + [\pi \pm \cos^{-1}\left(\frac{R}{r_o}\right)] \tag{3.12}$$

or the shadow boundary position is

$$\theta_{si} = \theta_o + [\pi \pm \cos^{-1}\left(\frac{R}{r_o}\right)] \quad ; \quad \beta \lessgtr \theta_o + \pi \tag{3.13}$$

and the reflection boundary position is

$$\theta_{sr} = -\theta_o + [\pi \mp \cos^{-1}\left(\frac{R}{r_o}\right)] \quad ; \quad \beta \lessgtr \theta_o + \pi \tag{3.14}$$

From (3.13) and (3.14) we can see the symmetry of shadow and reflection boundaries with respect to the half-screen. This property is valid for omnidirectional and directive sources as well. Adding (3.13) and (3.14) gives

$$\theta_{si} + \theta_{sr} = 2\pi \quad , \text{ for all } \beta \tag{3.15}$$

To satisfy (3.7), substitute for R from (3.9) and (3.6) in (B.6) of Appendix B yielding

$$I = -b\, \frac{\cos(\beta-\theta_o)}{\cos(\theta \pm \theta_o)} \tag{3.16}$$

Expanding $\cos(\beta-\theta o)$ in terms of cosines and sines of $(\theta \pm \beta)$ and $(\theta \pm \theta o)$ and substituting in (3.10) we get

$$\text{Real}\left[(we^{j\pi/4})^2\right] = -kb\, \sin(\theta \pm \beta).\, \tan(\theta \pm \theta_o) \tag{3.17a}$$

From equation (3.13) and Appendix B we can show

$$\pi < \Theta_{si} - \Theta_o < \frac{3\pi}{2} \quad \text{if} \quad 0 < \Theta_{si} - \beta < \pi \tag{3.17b}$$

Hence $\tan(\Theta_{si}-\Theta_o)>0$ and $\sin(\Theta_{si}-\beta)>0$

Also we can show

$$\frac{\pi}{2} < \Theta_{si} - \Theta_o < \pi \quad \text{if} \quad -\frac{\pi}{2} < \Theta_{si}-\beta < 0 \tag{3.17c}$$

Hence, $\tan(\Theta_{si} - \Theta_o) < 0$ and $\sin(\Theta_{si}-\beta) < 0$.

Therefore (3.7) is satisfied for the shadow boundary. Similarly from (3.14) and Appendix B we can satisfy (3.7).

As a check on the above formulas for Θ_{si} and Θ_{sr}, let us discuss the following special cases.

i) Real line source i.e. b=0

from (3.10) $R=r_o$, and

$$\Theta_{\substack{si\\sr}} = \pi \pm \Theta_o \tag{3.18}$$

ii) Beam axis passes through the screen edge

$\beta = \Theta_o + \pi$

from (3.13), $r_s = r_o + jb$ and

$\Theta_{\substack{si\\sr}} = \pi \pm \Theta_o$,

which is the same as the real line source shadow and reflection boundaries.

3.3 Numerical Results for the Half-Plane

The solid curves in Fig. 3.2 and Fig. 3.3 represent the uniform total field calculated from (3.3) with $kr_o=16$ and $\Theta_o=\pi/2$ while the

dashed curves represent the asymptotic total field calculated from Appendix (C.5). The two dimensional beam is normally incident upon the half plane and at a distance $kr_o=16$. The development of a beam from an omnidirectional line source (kb=0) to a directive beam (kb=12) is shown in Fig. 3.2. For the case of kb=0 the pattern oscillations in the illuminated region ($-\pi/2<\phi<0$) are familiar, showing interference between the direct wave from the source and a diffracted wave emanating from the edge. In the shadow region ($0<\phi<\pi/2$) there is only a diffracted field, which decreases with ϕ to become zero on the conductor. As kb increases the above oscillations are suppressed in the illuminated region. This occurs because the incident field is suppressed in the illuminated region as directivity increases.

In Fig. 3.2, where the beam axis passes through the edge, we can see how inaccurate the asymptotic solution becomes near the shadow boundary. When kb increases there is little improvement. On the shadow boundary the asymptotic field is singular for all values of kb in Fig. 3.2.

In Fig. 3.3 where the beam axis is off the edge by an angle δ, the asympototic solution is finite but inaccurate near and on the shadow boundary especially for small kb or δ. In Fig. 3.3 the asymptotic solution improved greatly when the off edge angle increased from 15° to 45° for a fixed kb=12. In the lower graphs of Fig. 3.3 where the off edge angle is fixed to $\delta=30°$, the asymptotic solution improved considerably when kb increased from kb=4 to kb=16. From the above we can conclude that the asymptotic solution is a good approximation to the uniform solution whenever the beam axis is well off the diffracting edge

and the beam is sufficiently directive, i.e. when δ and kb are sufficiently large, for then there is little diffraction by the edge.

Fig. 3.4 shows the far fields for half plane diffraction by a distant line source represented by a solid curve and by a narrow beam source represented by a dashed curve. For $b>>r_o$ the wave uniformly illuminates the diffracting edge and its neighbourhood and in a similar way the distant line source also does. So in Fig. 3.4b we can see the diffracted field components are similar. In Fig. 3.4a the total fields are different in the illuminated region ($-\pi/2<\phi<0$), because far from the source the direct incident wave of the narrow beam is almost zero a few degrees off the beam axis, so the diffracted field is essentially the total field. The direct wave of the distant line source is almost uniform, consequently interference between the direct wave and the diffracted wave occurs and appears as oscillations in the illuminated region.

To obtain numerical values from (3.3) it is necessary to have a Fresnel integral subroutine that can handle complex arguments. A relation between the Fresnel integral and the error function is given in Appendix A. Subroutines for the error function with complex argument are available in the UBC computing center General Library. Also tables of the error function with complex arguments by Gautschi (1964) and tables of the modified Fresnel integral with complex arguments by Clemmow and Munford (1952) agree with our subroutine whenever comparison is possible.

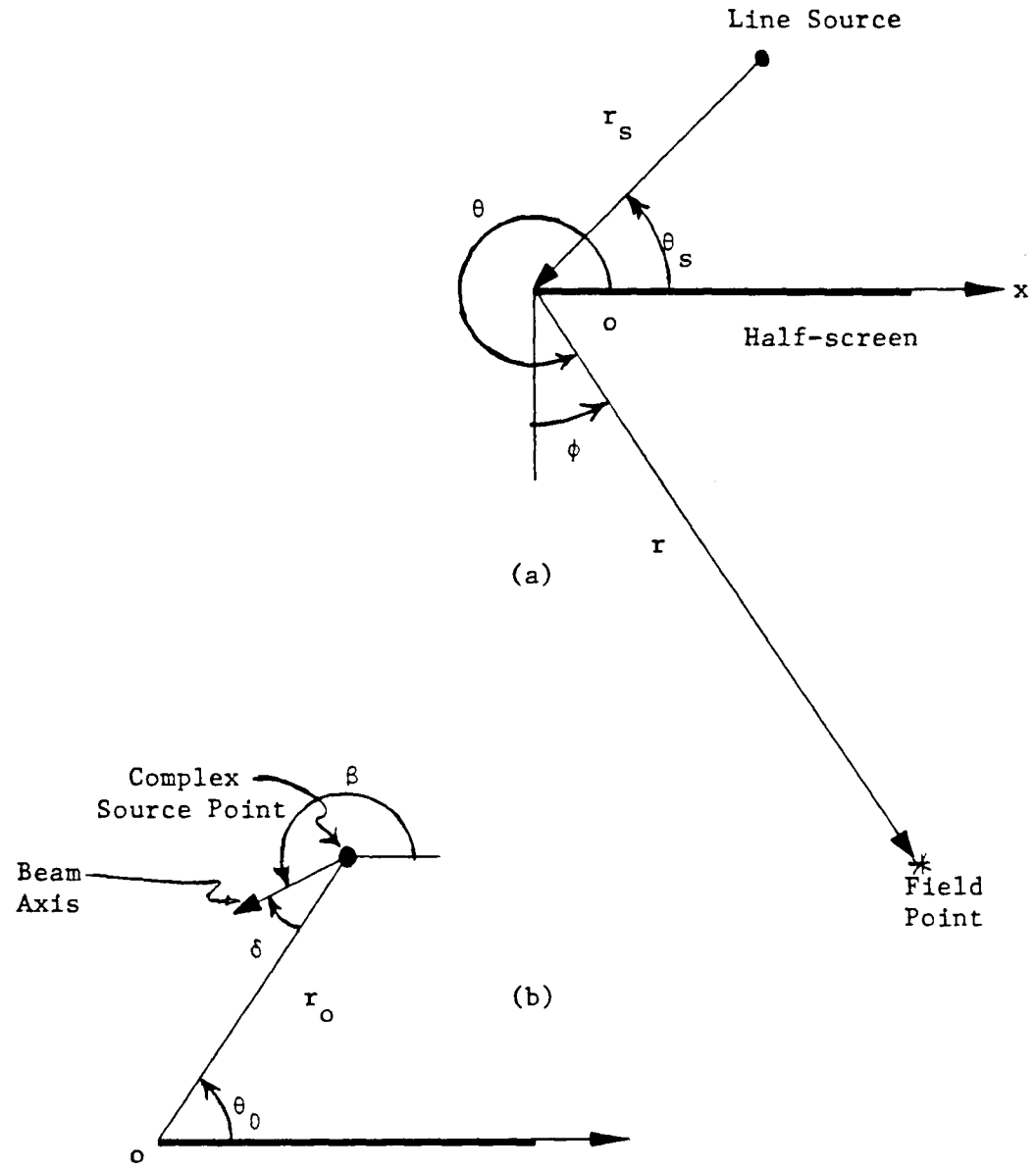

Fig. 3.1 a) Geometry of a complex line source diffraction by a half-plane
b) Beam orientation with respect to the edge.

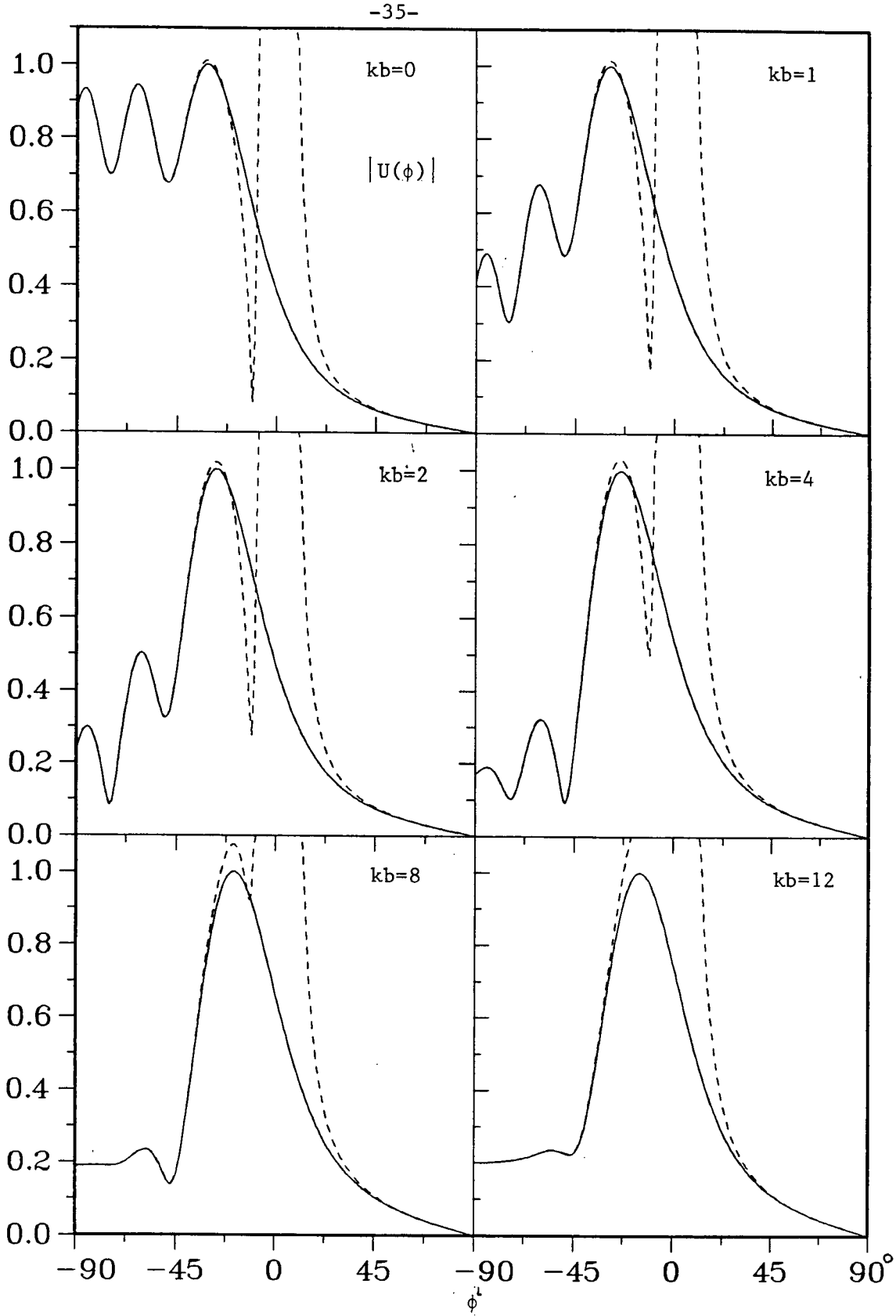

Fig. 3.2 Comparison of uniform (solid, eq. 3.3) and asymptotic (dashed, Green et al., 1979) Solutions ($kr_o=16$, $\theta_o=90^o$, $\beta=270^o$)

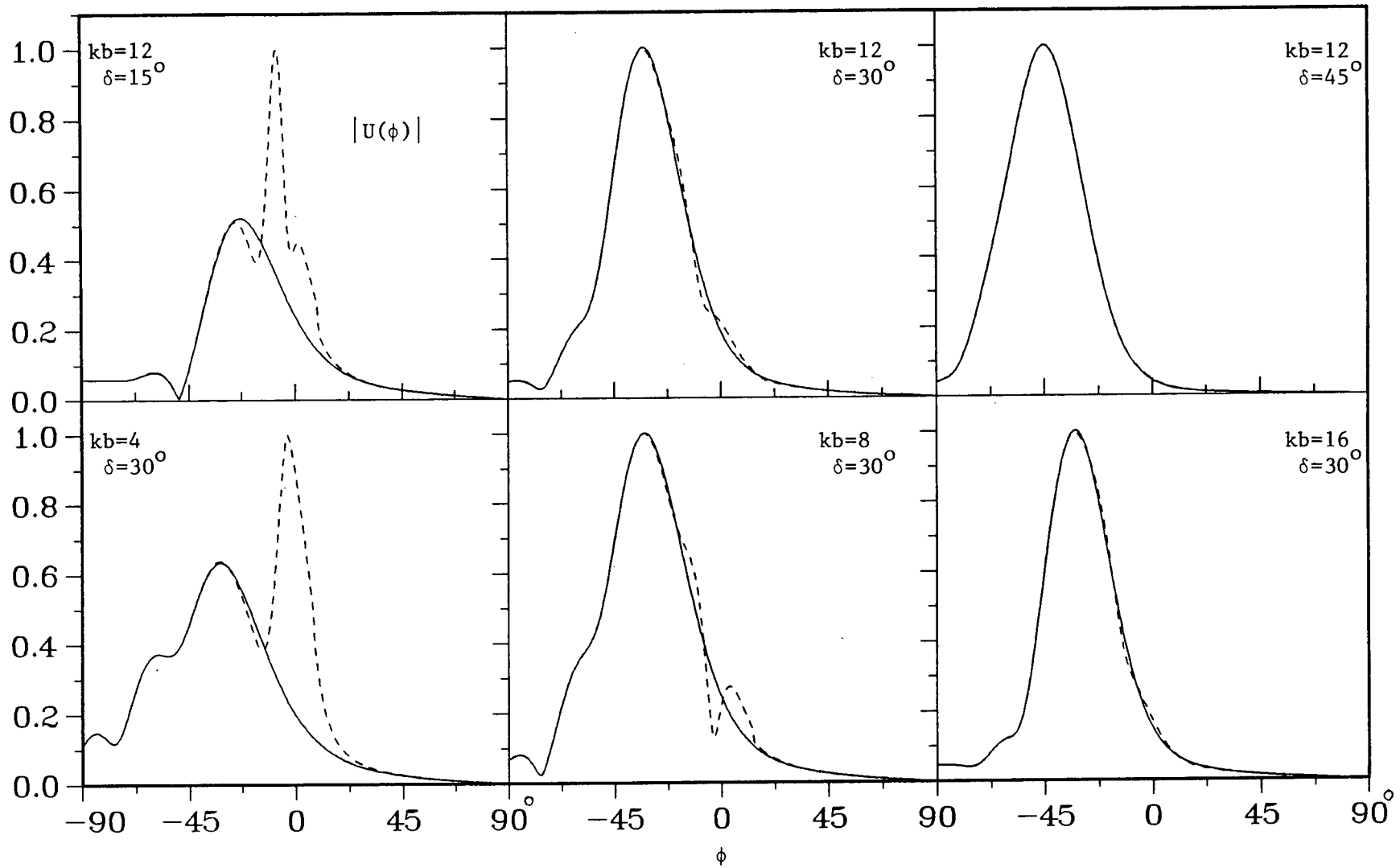

Fig. 3.3 Comparison of the uniform (solid) and asymptotic (dashed) solutions with the beam axis off the edge ($kr_o=16$, $\theta_o=90^o$, $\beta=270^o-\delta$)

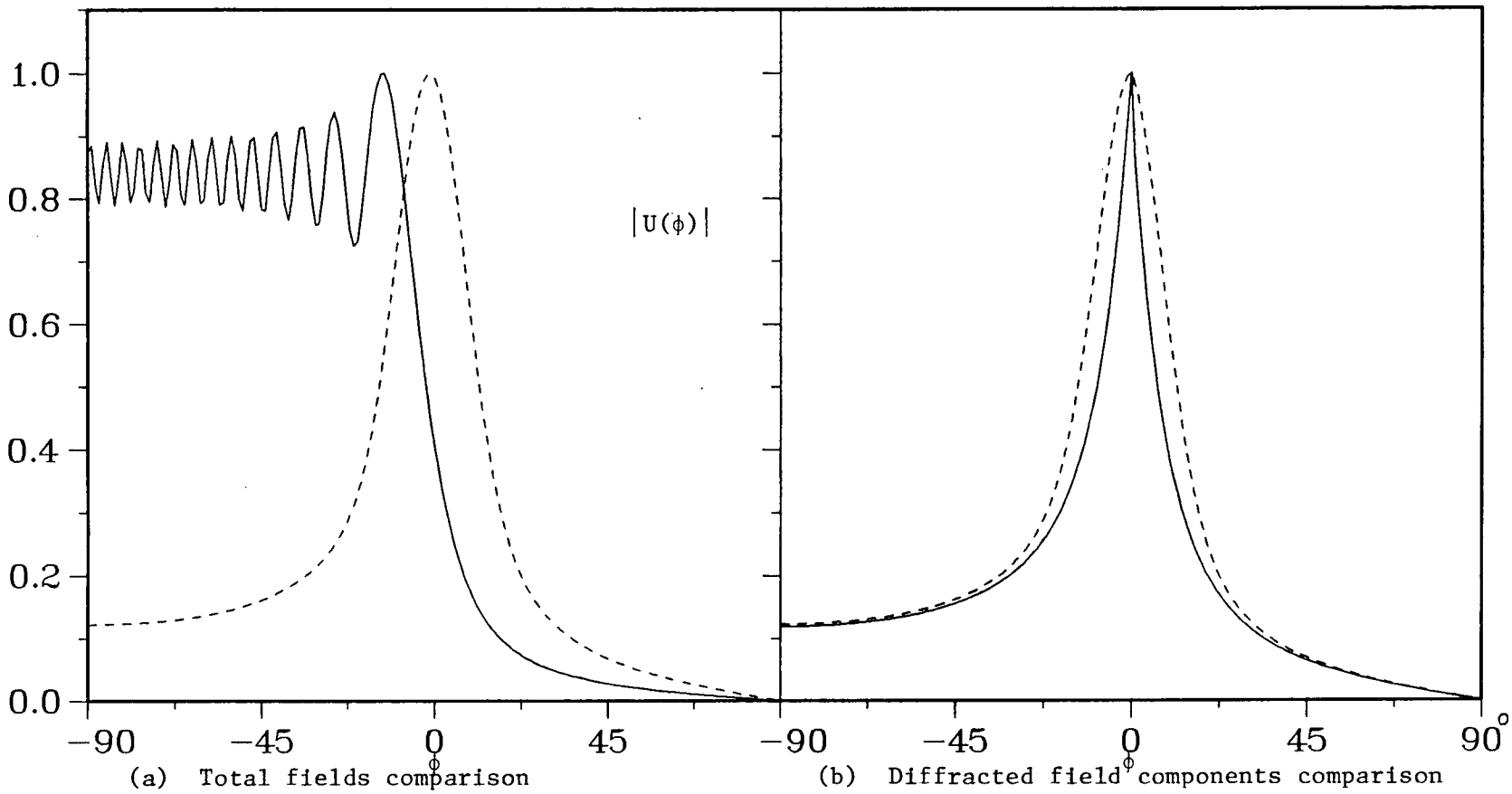

Fig. 3.4 Uniform solution (eq. 3.3) comparison of a distant source (solid) and a limiting beam of large kb

——— kb=o , kr_o=85 , θ_o=90°

– – – – – kb=85 , kr_o=8 , θ_o=90° , β=270°

CHAPTER IV

BEAM DIFFRACTION BY A WIDE SLIT AND COMPLEMENTARY STRIP

4.1 Beam Diffraction by a Wide Slit

With the results for beam diffraction by a half-plane we can solve the problem of beam diffraction by a slit in a conducting plane and its complement, a conducting strip. The slit between two coplanar half-planes with parallel edges, or its complement, the strip, are a traditional test of theories involving multiple diffraction by edges.

4.1.1 Far Field Calculation

Fig. 4.1 shows a line source parallel to a slit in y=0, $|x| \leq a$. With an incident field given by (2.1) the total far field of the half-plane on the right side in isolation $U_1(r_1,\theta_1)$ is given by (3.3) with r_1, θ_1 replacing r, θ and r_{s1}, θ_{s1} replacing r_s, θ_s.

Similarly the total far field of the left half-plane in isolation $U_2(r_2,\theta_2)$ is given by (3.3) with r_2, θ_2 replacing r, θ and r_{s2}, θ_{s2} replacing r_s, θ_s. All the coordinates are shown in Fig. 4.1.

These expressions for the fields of the two half-planes contain both incident and diffracted fields behind the slit. Consequently the total non-interaction far fields for the slit are their sum less an incident field U^i.

$$U_s^t = U_1(r_1,\theta_1) + U_2(r_2,\theta_2) - U^i \tag{4.1}$$

In the far field of the slit ($r \gg a$)

$$r_1 \simeq r - a\cos\theta_1 \quad , \quad \theta_1 \simeq \theta$$

$$r_2 \simeq r - a\cos\theta_2 \quad , \quad \theta_2 \simeq \pi - \theta \; ; \quad 0 < \theta < \pi \tag{4.2a}$$

$$\simeq 3\pi - \theta \; ; \quad \pi < \theta < 2\pi$$

These far field substitutions for r_1, r_2 are used in the exponential terms of U_1 and U_2 while $r_1 \simeq r_2 \simeq r$ is used in the amplitude terms. From Fig. 4.1 we can write the following geometrical relations for r_{s1}, r_{s2}, Θ_{s1}, Θ_{s2}, measured from the two edges in terms of r_s, Θ_s.

$$r_{s_{\frac{1}{2}}} = [r_s^2 + a^2 \mp 2ar_s \cos\Theta_s]^{1/2} \quad ; \quad \text{Real}(r_{s_{\frac{1}{2}}}) > 0 \ , \tag{4.2b}$$

$$\Theta_{s_{\frac{1}{2}}} = \pi - \sin^{-1}\left(\frac{r_s \sin\Theta_s}{r_{s_{\frac{1}{2}}}}\right) \ , \tag{4.2c}$$

where r_s and Θ_s are measured from the centre of the slit and given by (2.5) and (2.6) respectively. We may use the Fresnel integral identity.

$$F[-w] = \sqrt{\pi}\, e^{-j\pi/4} - F[w] \tag{4.3}$$

to include the extra incident field

$$U^i = \frac{e^{-jk[r_1 - r_{s1}\cos(\Theta_1-\Theta_{s1})]}}{\sqrt{kr}} = \frac{e^{-jk[r-r_s\cos(\Theta-\Theta_s)]}}{\sqrt{kr}} \tag{4.4}$$

in a Fresnel integral term. Then the non-interaction far fields of the slit are

$$U_s^t \simeq \frac{e^{-j(kr-\pi/4)}}{\sqrt{\pi kr}} \left[e^{jka\cos\Theta_1} \left\{ - e^{jkr_{s1}\cos(\Theta_1-\Theta_{s1})} F[-w_{i1}] - e^{jkr_{s1}\cos(\Theta_1+\Theta_{s1})} F[w_{r1}] \right\} + e^{jka\cos\Theta_2} \left\{ e^{jkr_{s2}\cos(\Theta_2-\Theta_{s2})} F[w_{i2}] - e^{jkr_{s2}\cos(\Theta_2+\Theta_{s2})} F[w_{r2}] \right\} \right] \quad (4.5)$$

where

$$\begin{matrix} w_{i1} \\ r1 \end{matrix} = -\sqrt{2kr_{s1}}\cos\left(\frac{\Theta_1 \mp \Theta_{s1}}{2}\right) \quad (4.6)$$

and similarly for $\begin{matrix} w_{i2} \\ r2 \end{matrix}$ with subscript 2 replacing 1 in (4.6).

This is an accurate solution for slits sufficiently wide that interaction between edges is negligible. In order to indicate the accuracy it is useful to include also interaction between the slit edges. Earlier results for plane wave incidence using the geometrical theory of diffraction show that single and double diffraction provide accurate results for slit widths ka $\geq$ 2 (Keller (1957), Fig. 9).

4.1.2 Multiple Diffraction Calculation

To include higher order interactions between the edges the field singly diffracted from each edge in the direction of the opposite edge is replaced by the field of a line source of equal amplitude located at the edge from which the singly diffracted field originates. For example

the doubly diffracted field from the left edge is produced by the singly diffracted field from the right edge in the $\Theta_1=\pi$ direction and vice-versa for the right edge. This can be repeated infinitely many times. Adding all contributions from the two edges gives the multiply diffracted fields of the slit.

The singly diffracted component of the field given by (3.3) can be written as

$$U^d = U_e^i \; D(\Theta_s, r_s, \Theta, r) \quad , \tag{4.7}$$

where U_e^i is the incident field calculated at the diffracting edge given by

$$U_e^i \approx \frac{e^{-jkr_s}}{\sqrt{kr_s}} \quad , \; |kr_s| >> 1 \tag{4.8}$$

and $D(\Theta_s, r_s, \Theta, r)$ is the diffraction coefficient of the edge

$$D(\Theta_s, r_s, \Theta, r) = \sqrt{\frac{kr_s}{\pi}}\, e^{j\pi/4} \left\{ -e^{jw_i^2} \; F[-w_i] - e^{jw_r^2} \; F[+w_r] \right\} \frac{e^{-jkr}}{\sqrt{kr}} \tag{4.9}$$

where w_i and w_r are given by (4.6).

Following the same procedure given by Jull (1981, p.91) in calculating multiple diffraction for plane wave incidence on a slit, the multiply diffracted field excluding single diffraction, can be written as

$$U_m^d = \frac{U_{e_1}^i \; D_1^i \; (D_o D_1^f + D_2^f) + U_{e2}^i \; D_2^i (D_o D_2^f + D_1^f)}{(1 - D_o^2)} \tag{4.10}$$

If the line source coordinates are on the slit axis (y-axis), i.e., the source is symmetric with respect to both edges of the slit. Then $r_{s1} = r_{s2}$ and $\Theta_{s1} = \Theta_{s2}$ consequently $U_e^i = U_{e2}^i$ and $D_1^i = D_2^i$. Then (4.10) can be simplified to

$$U_m^d = \frac{U_{e1}^i D_1^i (D_1^f + D_2^f)}{(1 - D_o)} \tag{4.11}$$

where U_{e1}^i is given by (4.8) with r_{s1} replaces r_s and

$$D_o = D(\pi, 2a, \pi, 2a)$$

$$= -\sqrt{4/\pi} \cdot e^{j(2ka+\pi/4)} \cdot F[\sqrt{4ka}] \tag{4.12}$$

$$D_1^i = D(\Theta_{s1}, r_{s1}, \pi, 2a)$$

$$= -\sqrt{2kr_{s1}/\pi ka}\; e^{j(-2ka + \pi/4)} \cdot e^{-jkr_{s1}\cos\Theta_{s1}} \cdot e^{jkr_{s1}} \cdot F[\sqrt{2kr_{s1}}\sin(\frac{\Theta s1}{2})] \tag{4.13}$$

$$D_1^f = D(\pi, 2a, \Theta_1, r_1)$$

$$= -\sqrt{8ka/\pi} \cdot e^{j(2ka + \pi/4)} \cdot e^{-jka\cos\Theta_1} \cdot F[\sqrt{4ka}\,\sin(\frac{\Theta_1}{2})] \cdot \frac{e^{-jkr}}{\sqrt{kr}} \tag{4.14}$$

While D_2^f is given by (4.14) with r_2, Θ_2 replacing r_1, Θ_1.

For a wide range of slit widths (2a), higher order interaction fields of the slit give little or no improvement in accuracy over the first order interaction. In practice it is sufficient to include the first order interaction only. That is partly because the above higher

order interaction calculations are approximate, for the edge diffracted fields are not omnidirectional as assumed. It is also because higher order interaction is weak except for narrow slits, for which the whole process diverges and a different method is required.

Now the total field including multiple diffraction U_m^t is given by

$$U_m^t = U_s^t + U_m^d \quad , \tag{4.15}$$

where U_s^t is given by (4.5) and U_m^d is given by (4.10). The total far field given by (4.15) is continuous and free from shadow boundary singularities because the Fresnel integrals are retained.

4.1.3 Numerical Results for the Slit

The diffraction patterns of Fig. 4.2 are calculated for a line source parallel to and at a height $kr_o = 8$ above a slit of width $2ka=16$. The solid curves are the non-interaction diffraction fields calculated from (4.5) and the dashed curves calculated from (4.15) include higher order interaction between the edges of the slit. Clearly interaction fields are of minor importance for this width of slit.

For an omnidirectional source (kb=0) the incident field has a substantial symmetric phase variation across the aperture resulting in a broad main beam with high shoulders. As the source becomes directive, beam definition improves. For moderate source directivity (e.g., kb=8) the aperture illumination is essentially Gaussian and so is the pattern. For a very directive source (kb=85) the aperture illumination is essentially plane wave and the diffraction pattern is very like that for plane wave illumination of a slit. Fig. 4.3 compares results from

Keller's geometrical theory of diffraction (1957, Fig. 7) and beam diffraction for kb=85. The singly diffracted field patterns are almost identical, but the interaction fields differ. Keller's multiple diffraction field is a summation of all fields resulting from the first term in an asymptotic expansion of the Fresnel integral; higher order Fresnel integral asymptotic expansion terms are omitted. It is also singular at shadow boundaries of the diffracted field, as is evident here at $\phi=\pm 90°$. These are limitations of the geometrical theory of diffraction.

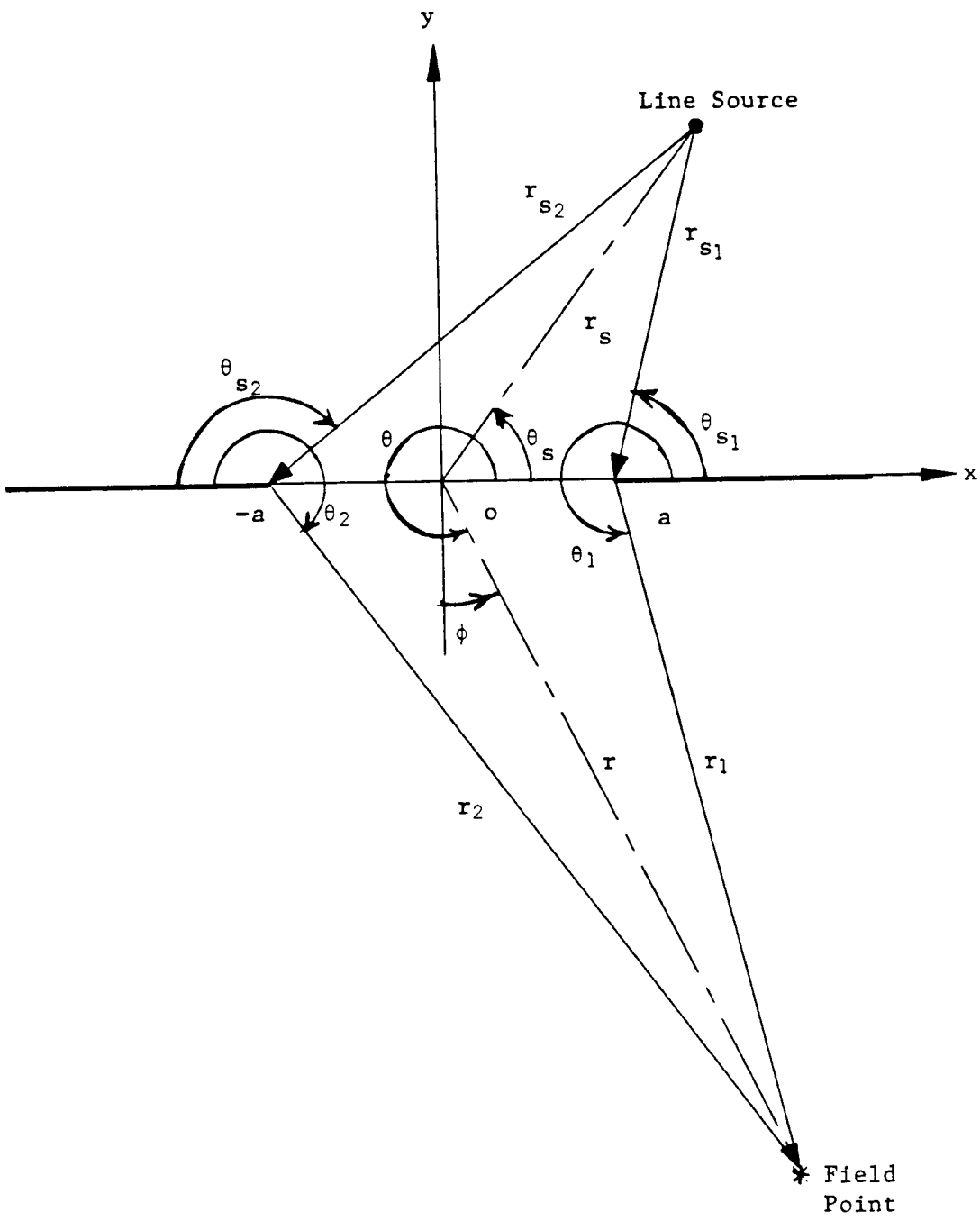

Fig. 4.1 Geometry of complex line source diffraction by a slit

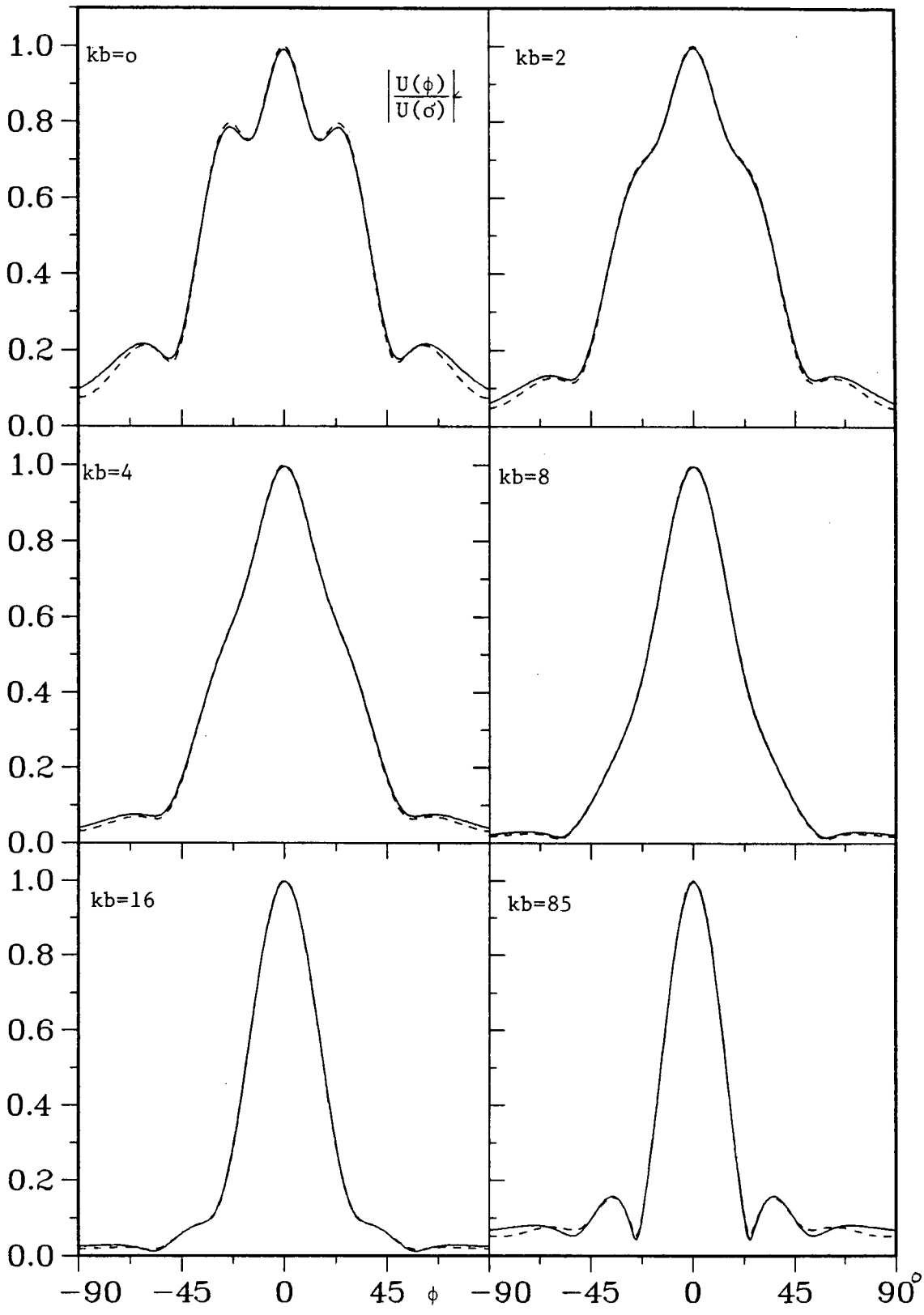

Fig. 4.2 Normalized total field pattern of a beam diffraction by a slit, single (solid) and double (dashed) diffractions

($ka=8=kr_o$, $\theta_o=90^o$, $\beta=270^o$)

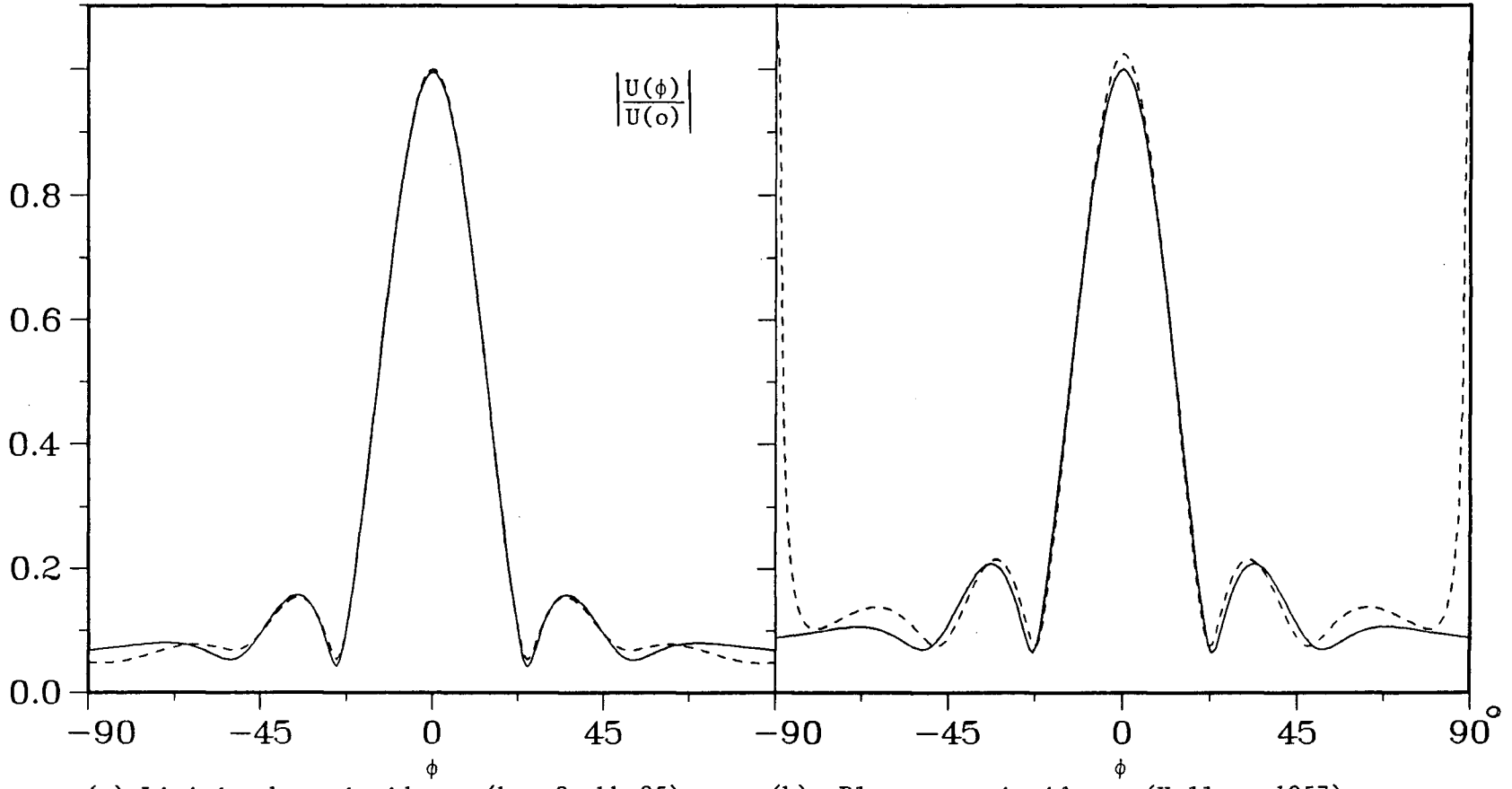

(a) Limiting beam incidence (kr_o=8, kb=85) (b) Plane wave incidence (Keller, 1957)

Fig. 4.3 Comparison of a plane wave and a limiting beam diffraction by a slit (ka=8) (solid) single diffraction and (dashed) multiple diffraction

4.2 Beam Diffraction by a Wide Conducting Strip

As another application of line source diffraction by a half-plane is the line source diffraction by a conducting strip. Fig. 4.4 shows a line source above and parallel to a conducting strip in the y=o plane and $|x| \leq a$.

4.2.1 Far Field Calculation

In the far field of the strip ($r \gg r_o, a$) we use the approximation given by (4.2).

The singly diffracted total field of a line source above a strip can be calculated from the total field of a line source over a half-plane for each of the edges. This total field U_s^t may be written

$$\begin{aligned} U_s^t &= U_1(r_1,\theta_1) + U_2(r_2,\theta_2) - [U^i(r,\theta) + U^r(r,\theta)]; \quad 0<\theta<\pi \\ &= U_1(r_1,\theta_1) + U_2(r_2,\theta_2) \qquad\qquad ; \quad \pi<\theta<2\pi \end{aligned} \tag{4.16}$$

where U_1 is total field of the line source over a half-plane at y=0 and $x \geq -a$ and U_2 is the total field of the same line source over a half-plane at y=0 and $x \leq a$. $U_1(r_1,\theta_1)$ and $U_2(r_2,\theta_2)$ are given by (3.3) with r_1,θ_1 and r_2,θ_2 replacing r,θ, respectively. While U^i and U^r are the incident and reflected fields, respectively. U^i is given by (4.4) and

$$U^r = -\frac{e^{-jk[r_1 - r_{s1}\cos(\theta_1+\theta_{s1})]}}{\sqrt{kr}} = -\frac{e^{-jk[r - r_s\cos(\theta+\theta_s)]}}{\sqrt{kr}} \tag{4.17}$$

Using (4.3), the singly diffracted total field given by (4.16) can be simplified to

For $0<\Theta<\pi$

$$U_s^t = \frac{e^{-j(kr-\pi/4)}}{\sqrt{\pi kr}} \{ e^{jka\cos\Theta_1} (- e^{jkr_{s1}\cos(\Theta_1-\Theta_{s1})} F[-w_{i1}] + e^{jkr_{s1}\cos(\Theta_1+\Theta_{s1})} F[-w_{r1}]) + e^{jka\cos\Theta_2} (e^{jkr_{s2}\cos(\Theta_2-\Theta_{s2})} F[w_{i2}] - e^{jkr_{s2}\cos(\Theta_2+\Theta_{s2})} F[w_{r2}]) \} , \quad (4.18a)$$

and for $\pi<\Theta<2\pi$

$$U_s^t = \frac{e^{-j(kr-\pi/4)}}{\sqrt{\pi kr}} \{ e^{jka\cos\Theta_1} (e^{jkr_{s1}\cos(\Theta_1-\Theta_{s1})} F[w_{i1}] - e^{jkr_{s1}\cos(\Theta_1+\Theta_{s1})} F[w_{r1}]) + e^{jka\cos\Theta_2} (e^{jkr_{s2}\cos(\Theta_2-\Theta_{s2})} F[w_{i2}] - e^{jkr_{s2}\cos(\Theta_2+\Theta_{s2})} F[w_{r2}]) \} \quad (4.18b)$$

Where w_i and w_r are the Fresnel integral arguments given by (4.6).

If interaction fields of the strip edges are calculated in a similar way as for the interaction fields of the slit it is found that they vanish on the conducting strip. Consequently a new diffraction coefficient is required (e.g. Karp and Keller, 1961) based on the normal derivative of the diffracted fields in the direction of the edge opposite. These interaction fields are much weaker than for the slit and so are omitted here.

4.2.2 Numerical Results for the Strip

The field pattern shown in Figs. 4.5 and 4.6 are calculated from (4.18) after normalization to the field on the peak of the pattern.

Fig. 4.5 illustrates the development of a beam solution from an omnidirectional line source (kb=0) at $kr_o=8$, $\Theta_o=\pi/2$ above a strip of width 2ka=16, to a beam source (kb=12) perpendicular to the strip. The total far field is maximum in the illuminated region at $\Theta=\pi/2$ where the reflected field is combined with the diffracted fields from both edges. The diffracted fields from the two edges at the field point $\Theta=\pi/2$ or $3\pi/2$ add in phase. In the shadow region at $\Theta=3\pi/2$ the total field is a relative maximum. As kb increases from 0 to 12 the incident beam becomes narrower and the edges are less illuminated. So the total field behind the strip, which is mainly the diffracted fields from the edges, decreases. The total field in the illuminated region becomes more directive with fewer sidelobes because there is little interaction between the reflected field and the diffracted fields.

Now if the incident beam of kb=8 is off the perpendicular to the strip by an angle δ, as shown in Fig. 4.6, the total field pattern is tilted. As δ increases the total field pattern is tilted more to the same side of the incident beam and it becomes larger behind the strip as shown.

The diffracted field contribution from the right edge is small and the main contribution is from the left edge and the incident field. The diffracted field from the left edge is a maximum when the incident beam axis is directed at the left edge as shown in Fig. 4.6 for the case of $\delta=45°$.

In the lower right graph of Fig. 4.6, the strip width is increased to 2ka=160 as a limit of a plane screen. The resulting total field pattern is a tilted sharp beam making an angle 135° with the strip, and is simply the reflected field.

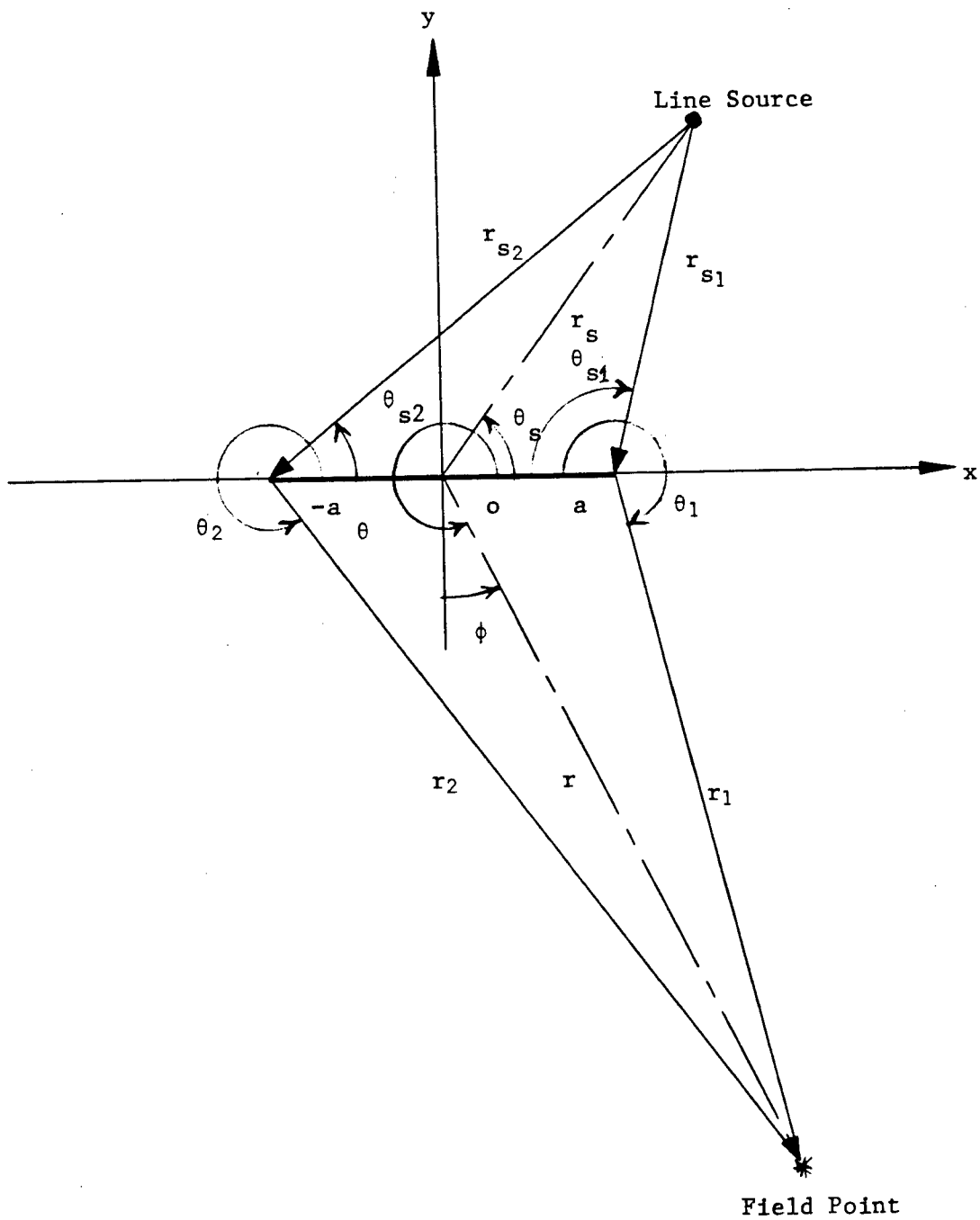

Fig. 4.4 Geometry of a complex line source diffraction by a strip

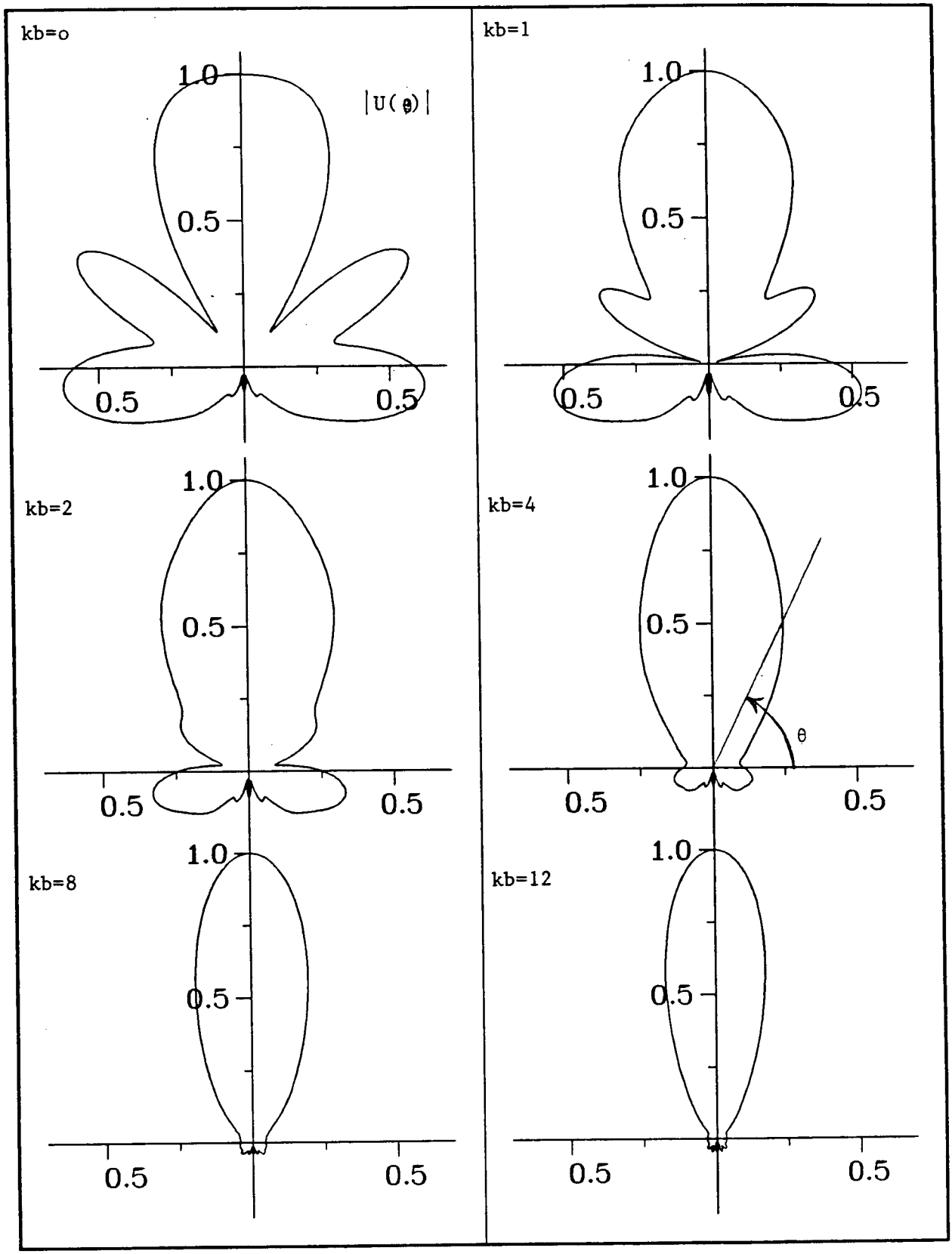

Fig. 4.5 Normalized total field pattern of a beam diffraction by a strip ($ka=8=kr_o$, $\theta_o=90^o$, $\beta=270^o$)

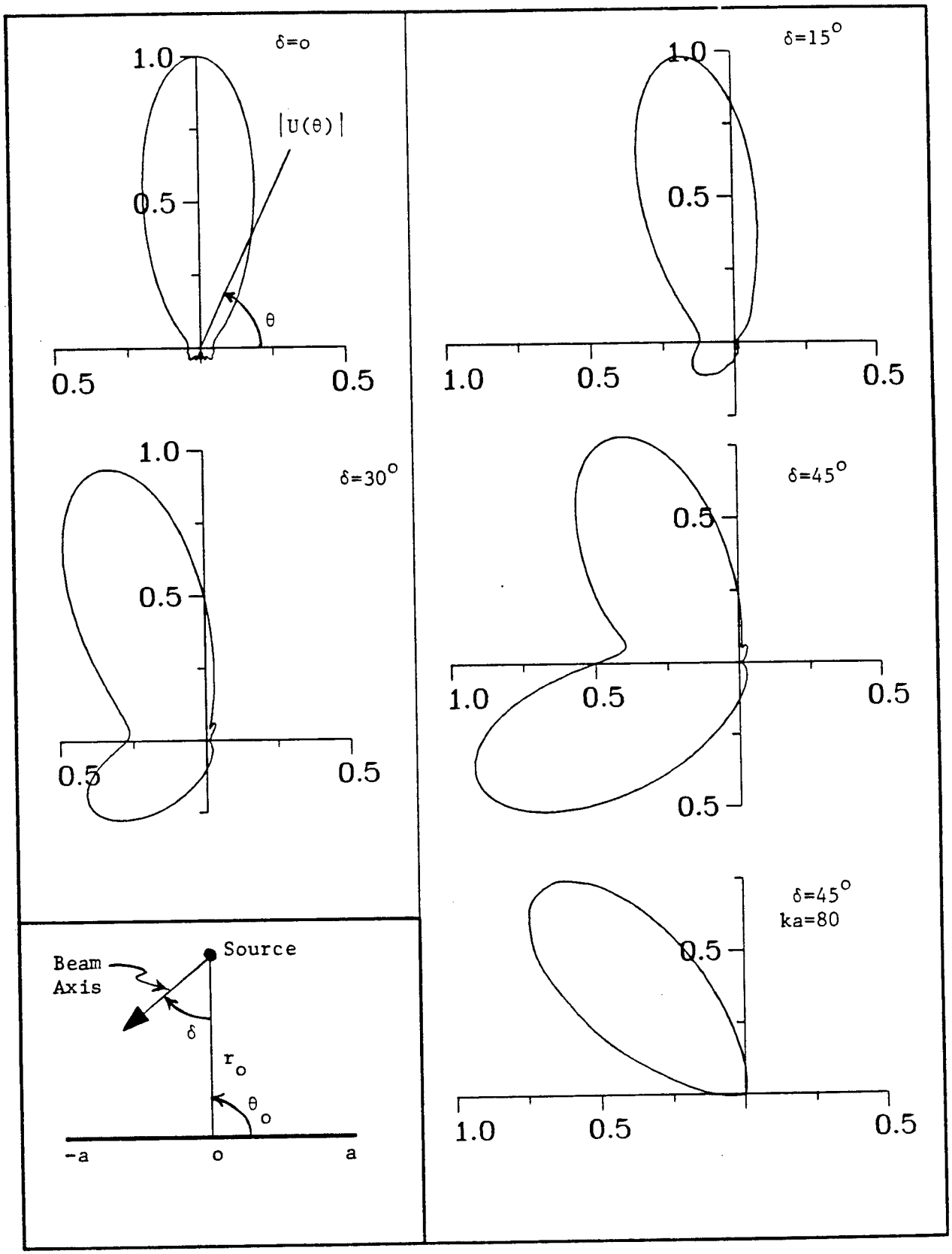

Fig. 4.6 Normalized total field pattern of a beam diffraction by a strip ($ka=kr_o=kb=8$, $\theta_o=90^o$, $\beta=270-\delta$)

CHAPTER V

BEAM DIFFRACTION BY A CONDUCTING WEDGE

A perfectly conducting wedge of exterior angle $n\pi$ is illuminated by a line source at r_o, Θ_o parallel to the edge, as shown in Fig. 5.1. For this configuration, let us have the following limitations:

$$0<\Theta_o<\frac{n\pi}{2} \quad ; \tag{5.1a}$$

$$0<\Theta\leq n\pi \quad ; \tag{5.1b}$$

$$1.5\leq n\leq 2 \quad \text{or} \quad \frac{\pi}{2} \geq \alpha_w \geq 0 \ , \tag{5.1c}$$

where α_w is the interior wedge angle. Since $\Theta = n\pi/2$ is the line of symmetry of the above configuration, the solution for $0<\Theta_o<n\pi/2$ with Θ measured from the upper surface, is the same as that for $n\pi/2<\Theta_o<n\pi$ when Θ is measured from the lower wedge surface. Therefore $\Theta_{sym} = n\pi/2$ is called angle of symmetry.

5.1 Real Line Source Solution

Exterior to the wedge, the total far field U^t is given as

$$U^t = U^i . S(\Theta_{si}-\Theta) + U_1^r S(\Theta_{sr1}-\Theta) + U_2^r S(\Theta-\Theta_{sr2}) + U^d \tag{5.2}$$

Here $S(x)$ is the unit step function, Θ_{si}, Θ_{sr1} and Θ_{sr2} are the shadow boundary, reflection boundary for the upper surface and reflection boundary for the lower surface, respectively. All the boundary angles are measured from the upper surface of the wedge and are given by

$$\Theta_{si} = \pi + \Theta_o \quad ; \tag{5.3a}$$

$$\Theta_{sr1} = \pi - \Theta_o \quad ; \tag{5.3b}$$

$$\Theta_{sr2} = (2n-1)\pi - \Theta_o \; ; \tag{5.3c}$$

U_7^i, U^d, U_1^r, and U_2^r are the incident, diffracted and reflected fields from the upper and lower surfaces, respectively.

$$U^i = \sqrt{\pi/2}\, H_o^{(2)}(kR^i) \simeq \frac{e^{-jkR^i}}{\sqrt{kR^i}} \quad ; \quad kR^i >> 1 \tag{5.4a}$$

$$\simeq e^{jkr_o\cos(\Theta-\Theta_o)} \cdot \frac{e^{-jkr}}{\sqrt{kr}} \quad ; \quad r >> r_o \tag{5.4b}$$

$$U_1^r = -\sqrt{\pi/2}\; H_o^{(2)}(kR_1^r) \simeq -e^{jkr_o\cos(\Theta+\Theta_o)} \frac{e^{-jkr}}{\sqrt{kr}} \tag{5.5}$$

$$U_2^r = -\sqrt{\pi/2}\, H_o^{(2)}(kR_2^r) \simeq -e^{jkr_o\cos[2n\pi - (\Theta+\Theta_o)]} \frac{e^{-jkr}}{\sqrt{kr}} \tag{5.6}$$

The diffracted field is

$$U^d \simeq U_e^i \cdot D(\Theta_o, r_o, \Theta) \frac{e^{-jkr}}{\sqrt{kr}} \quad , \tag{5.7}$$

where U_e^i is the incident field at the edge of the wedge given by

$$U_e^i = \sqrt{\pi/2}\, H_o^{(2)}(kr_o) \tag{5.8a}$$

$$\simeq \frac{e^{-jkr_o}}{\sqrt{kr_o}} \quad ; \; kr_o >> 1 \tag{5.8b}$$

and $D(\Theta_o, r_o, \Theta)$ is the uniform diffraction coefficient given by Kouyoumjian and Pathak (1974), with some modifications, as

$$D(\Theta_o, r_o, \Theta) \simeq \frac{e^{-j\pi/4}}{2n\sqrt{2\pi}} \{[\cot(T_1)\, G(w_1) - \cot(T_2)\, G(w_2)] + [\cot(T_3)\, G(w_3) - \cot(T_4)\, G(w_4)]\}, \qquad (5.9)$$

Here

$$G(w) = 2j\, e^{jw^2}\, w\, F[w] \quad ; \quad \text{Real}(we^{j\pi/4}) \geq 0 \qquad (5.10a)$$

$$= -2j\, e^{jw^2}\, w\, F[-w] \quad ; \quad \text{Real}(we^{j\pi/4}) < 0 \qquad (5.10b)$$

F[w] is the Fresnel integral given by (3.2), and

$$w_{1,2} = -\sqrt{2kr_o}\, \cos\left[\frac{2\pi n M_1^{\mp} - (\Theta \mp \Theta_o)}{2}\right] \qquad (5.11a)$$

$$w_{3,4} = -\sqrt{2kr_o}\, \cos\left[\frac{2\pi\, n\, M_2^{\mp} - (\Theta \mp \Theta_o)}{2}\right] \qquad (5.11b)$$

$$T_{1,2} = \frac{\pi - (\Theta \mp \Theta_o)}{2n} \qquad (5.12a)$$

$$T_{3,4} = \frac{\pi + (\Theta \mp \Theta_o)}{2n} \qquad (5.12b)$$

In (5.11) $M_1^{\mp}$ and $M_2^{\mp}$ are integers which most nearly satisfy the equations.

$$2\pi\, n\, M_1^{\mp} - (\Theta \mp \Theta_o) = -\pi \qquad (5.13a)$$

$$2\pi\, n\, M_2^{\mp} - (\Theta \mp \Theta_o) = \pi \qquad (5.13b)$$

Here we have two cases, depending on whether the reflected field from the lower wedge surface exists or does not, i.e. $\Theta_o \gtrless \Theta_{cr}$, where the critical angle for illumination of the lower wedge surface is $\Theta_{cr}=(n-1)\pi$.

Now the total field u^t can be written as,

for $0<\Theta_o<\Theta_{cr}$; (5.14)

$$\begin{aligned} u^t &= u^d + u^i + u_1^r \quad , \quad 0<\Theta<\Theta_{sr1} \\ &= u^d + u^i \quad , \quad \Theta_{sr1}<\Theta<\Theta_{si} \\ &= u^d \quad , \quad \Theta_{si}<\Theta<n\pi \\ &= 0 \quad , \quad n\pi<\Theta<2\pi \end{aligned} \tag{5.15}$$

and for $\Theta_{cr}<\Theta_o<\Theta_{sym}$; (5.16)

$$\begin{aligned} u^t &= u^d + u^i + u_1^r \quad , \quad 0<\Theta<\Theta_{sr1} \\ &= u^d + u^i \quad , \quad \Theta_{sr1}<\Theta<\Theta_{sr2} \\ &= u^d + u^i + u_2^r \quad , \quad \Theta_{sr2}<\Theta<n\pi \\ &= 0 \quad , \quad n\pi<\Theta<2\pi \end{aligned} \tag{5.17}$$

5.2 Uniform Solution for a Beam Source

To get the two-dimensional beam solution from the omnidirectional line source solution, we replace r_o, Θ_o by r_s, Θ_s in all above equations except (5.1), (5.3), (5.13), (5.14) and (5.16). In (5.1), Θ_o is left as it is and in (5.13), Θ_o is replaced by Real(Θ_s). (5.14) and (5.16) are replaced, respectively, by

$$\Theta_{sr2} \gtrless n\pi \tag{5.18}$$

Finally (5.3) is given by (3.13) and (3.14) and rewritten here as

$$\Theta_{si} = \Theta_o + [\pi \mp \cos^{-1}(R/r_o) \quad , \quad \beta \gtrless \Theta_o+\pi \tag{5.19}$$

$$\Theta_{sr1} = -\Theta_o + [\pi \pm \cos^{-1}(R/r_o)] \quad , \quad \beta \gtrless (\Theta_o+\pi) \quad , \tag{5.20}$$

$$\Theta_{sr2} = -(n\pi - \Theta_o) + [\pi \mp \cos^{-1}(R/r_o)] \quad , \quad \beta \gtrless (\Theta_o+\pi) \quad , \tag{5.21}$$

where r_s and Θ_s are given by (2.5) and (2.6) respectively.

If the edge of the wedge lies on the beam axis, r_s and Θ_s are simplified to

$$r_s = r_o + jb \quad \text{and} \quad \Theta_s = \Theta_o, \tag{5.22}$$

and one of the cotangent functions in (5.9) is singular on the shadow or reflection boundaries, but when multiplied by the corresponding G(w) function, it becomes finite (see Appendix D). Hence the diffraction coefficient given by (5.9) is always finite, unlike the asymptotic solutions. When the beam axis does not pass through the wedge edge, all the cotangent functions are finite everywhere.

5.3 Numerical Results for the Wedge

In all the following figures the source is parallel to the edge and at a distance $kr_o = 16$. Also the edge lies on the beam axis; i.e. $\beta = \Theta_o+\pi$.

In Figs. 5.2, 5.3 and 5.4 the wedge angle $\alpha_w = (2-n)\pi$ is kept constant at $\alpha_w = 90°$ for which n=1.5. Therefore the critical angle Θ_{cr}=90° and the angle of symmetry $\Theta_{sym} = 135°$.

Fig. 5.2 illustrates how the normalized total field varies when the incident field on a right angled conducting wedge changes from

omnidirectional (kb=0) to a directive beam (kb=12). As kb increases two beams appear, one along the reflection boundary at $\Theta_{sr1} = 120°$, and another along the shadow boundary at $\Theta_{si} = 240°$. In the region illuminated by the incident and reflected fields considerable constructive and destructive interference between incident and reflected fields is observed when kb=0. As kb increases this interference decreases because incident and reflected fields become directive. The diffracted field does not change significantly because the edges lie on the beam axis. Since the incident angle $\Theta_o = 60°$ is less than $\Theta_{cr}=90°$, there is no reflected field from the lower wedge surface. In the shadow region ($240°<\Theta<270°$) there is only a diffracted field, which vanishes on the lower wedge surface.

Fig. 5.3 is similar to Fig. 5.2 except the angle of incidence $\Theta_o=120°$ is greater than Θ_{cr} so both faces of the wedge are illuminated. In this case the reflected fields from both wedge surfaces contribute to the total field. Interference between incident, reflected and diffracted fields occurs in $0<\Theta<\Theta_{sr1} = 60°$ and $270°<\Theta<\Theta_{sr2} = 240°$, also between incident and diffracted fields in the region $60°<\Theta<240°$. Here all the region exterior to the wedge is illuminated by incident, diffracted and for $\Theta<60°$ and $\Theta>240°$ reflected fields, so there is no shadow regions when kb is small. When kb is sufficiently large, shadow regions may exist.

In Fig. 5.4 the angle of incidence is chosen to equal the angle of symmetry; i.e. $\Theta_o = \Theta_{sym} = 135°$. The arrangement was used as a partial verification of the validity of our equations and computer programs in this analysis. The symmetry of the field about $\Theta=135°$ is clear. When

kb is sufficiently large, say kb=12, two directive beams appear at $\Theta=\Theta_{sr1} = 45°$ and $\Theta_{sr2} = 225°$. These are the reflected fields from the upper and lower wedge surfaces respectively. But when kb=0 or is small, say kb=2, the interference between reflected, incident and diffracted fields are more significant in the regions $0<\Theta<45°$ and $225°<\Theta<270°$. Most of the total far field in the region $45°<\Theta<225°$ when kb is small, but not zero, is due to the diffracted field. All of it is diffracted field when kb is sufficiently large, because the reflected fields from both wedge surfaces do not contribute to the total field in this region.

Fig. 5.5 shows how the total fields for an omnidirectional source (kb=0) and a beam source (kb=4) change with the interior wedge angle α_w. For $\Theta_o=120°$, the wedge angle is changed from $\alpha_w=90°$(n=1.5) to a half-plane $\alpha_w=0°$(n=2), comparing the case of half-plane solution to the beam diffraction by half plane solution given in chapter 3, gives another check on the validity and accuracy of our analysis and computer programs. From Fig. 5.5 we can notice that the total field in the region closer to the upper wedge surface; i.e. $\Theta<n\pi/2$, is not significantly affected with the change of wedge angle because in this region the incident and reflected fields do not change with the wedge angle. In the region closer to the lower surface; i.e. $(\frac{n\pi}{2} < \Theta < n\pi)$, the total field is noticeably changed with the change of the wedge angle, because the reflected field changes significantly with the change of the wedge angle.

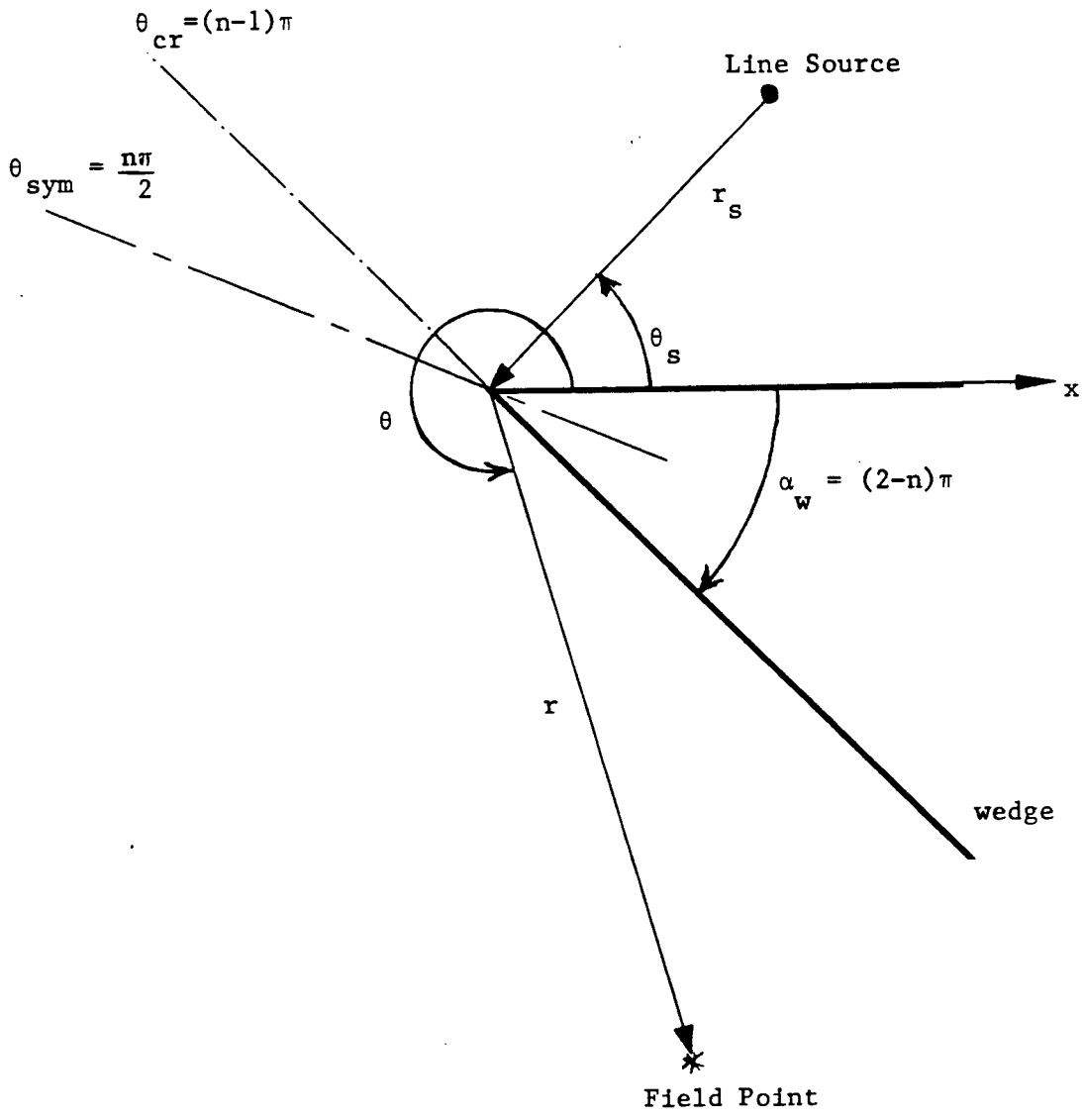

Fig. 5.1 Geometry of a complex line source diffraction by a wedge

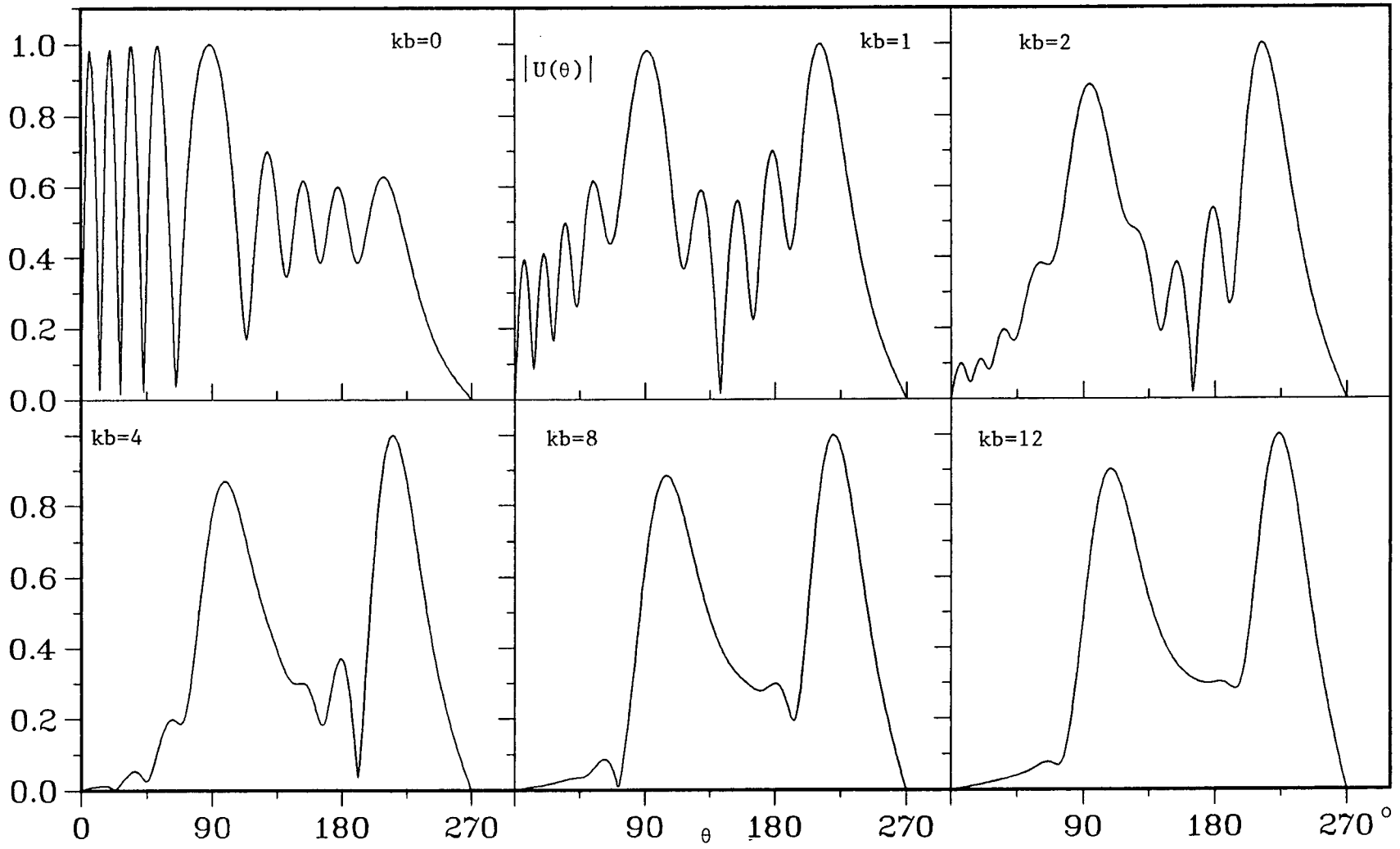

Fig. 5.2 Normalized total field pattern of a beam diffraction by a wedge ($kr_o=16$, $\theta_o=60^o<\theta_{cr}$, $\alpha_w=90^o$, $\beta=180^o+\theta_o$)

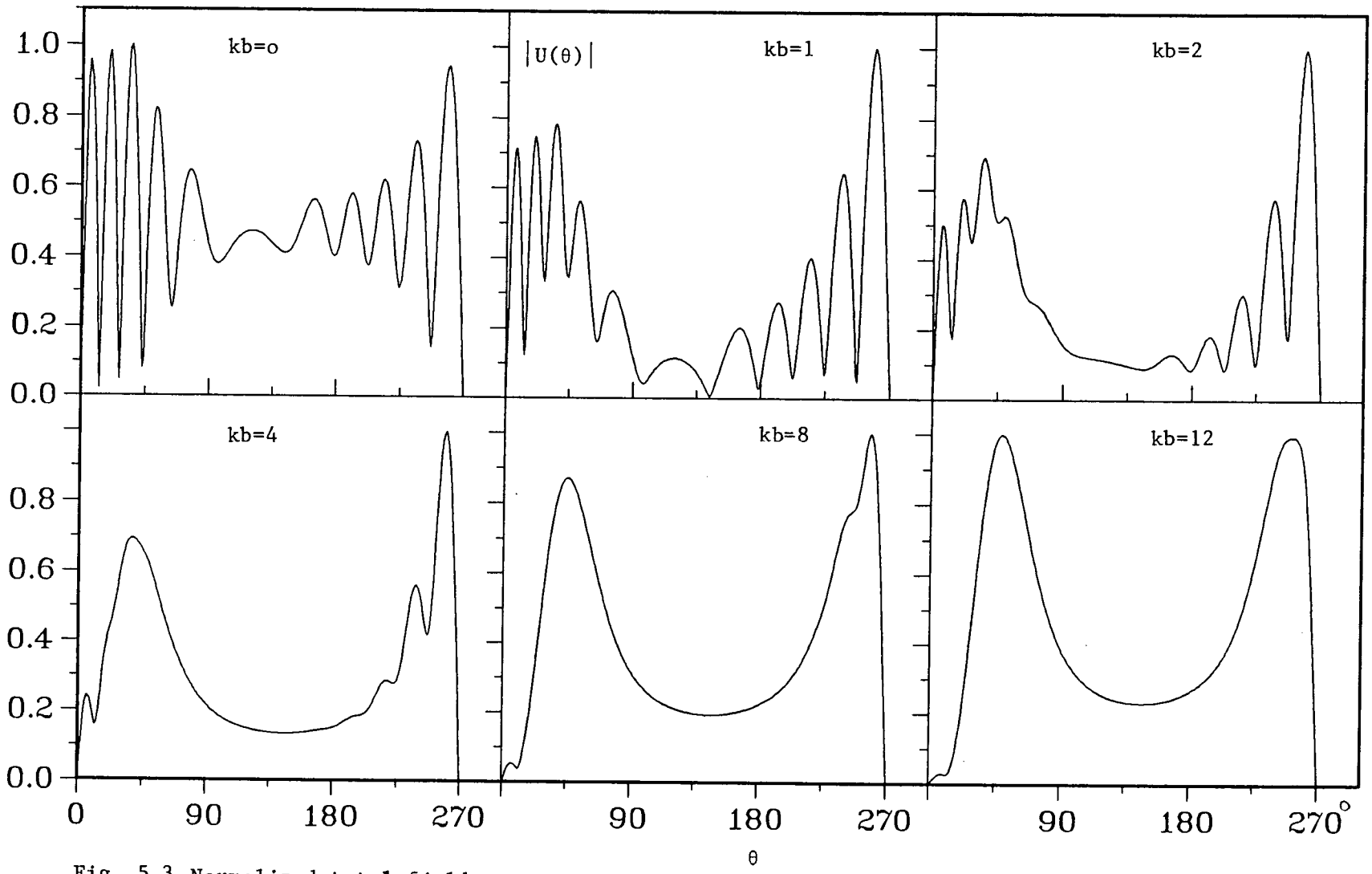

Fig. 5.3 Normalized total field pattern of a beam diffraction by a wedge ($kr_o=16$, $\theta_o=120^o>\theta_{cr}$, $\alpha_w=90^o$, $\beta=180^o$)

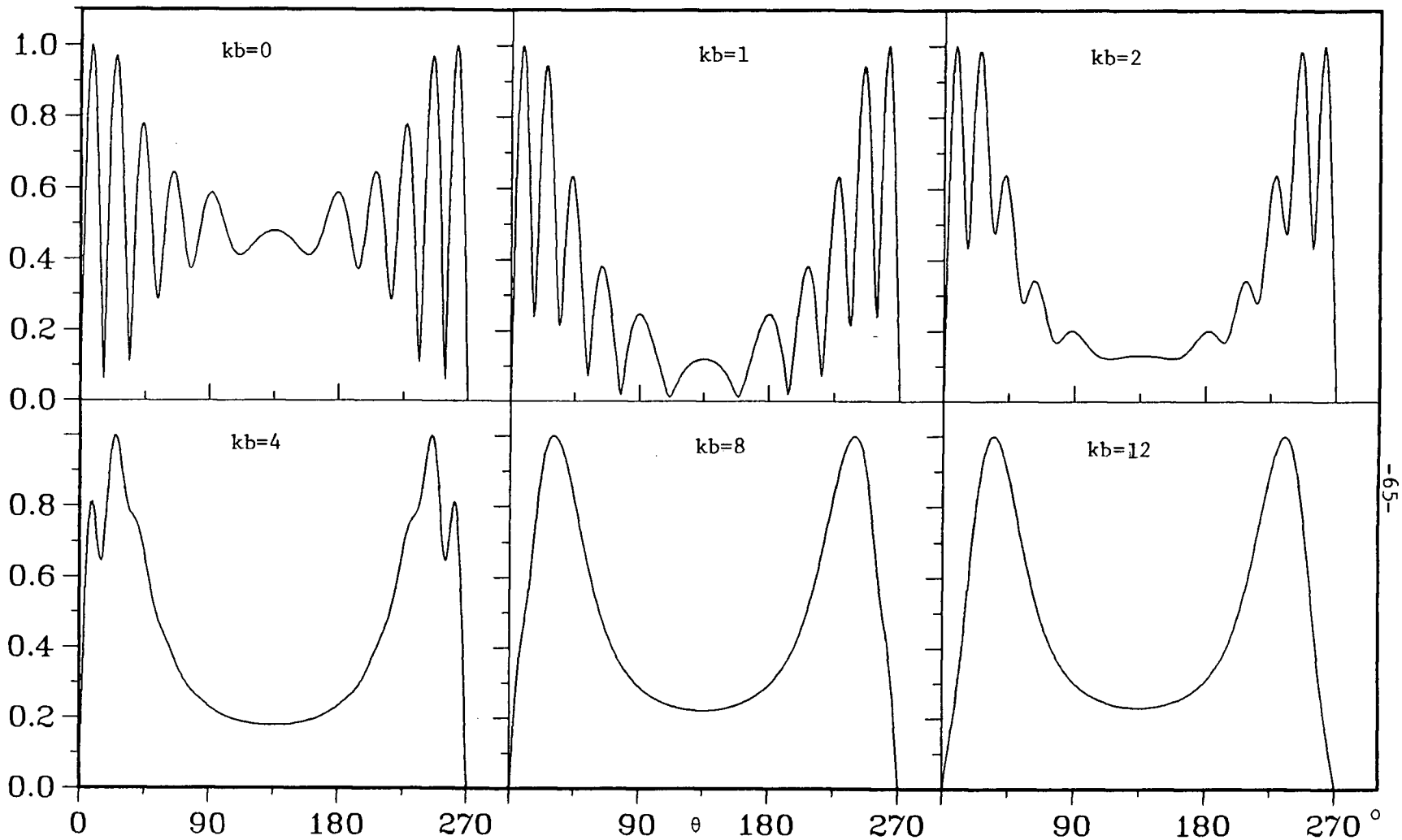

Fig. 5.4 Normalized total field pattern of a beam diffraction by a wedge (kr_o=]6, θ_o=135° = θ_{sym}, α_w = 90°, β = 180° + θ_o)

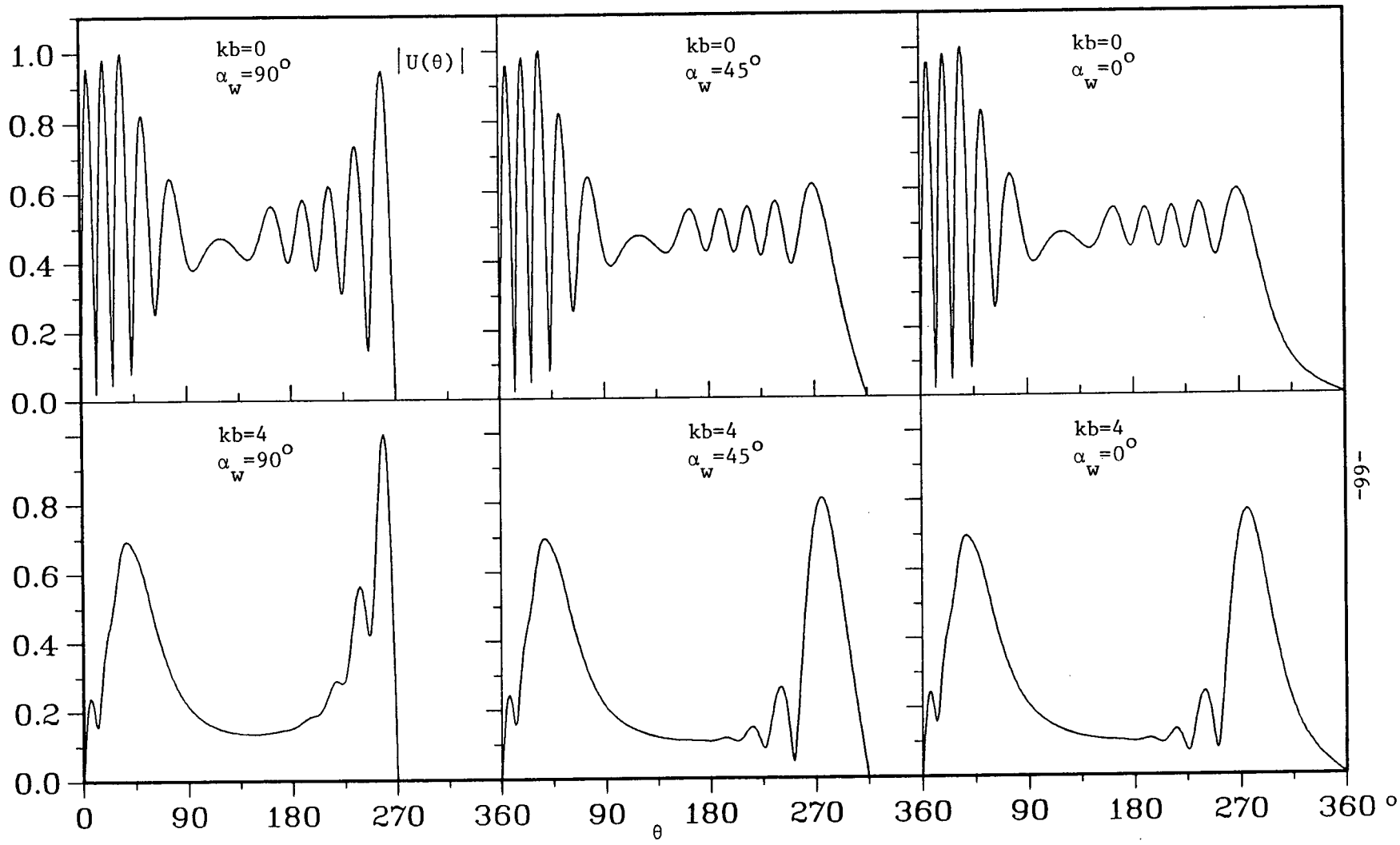

Fig. 5.5 Normalized total field pattern of a beam diffraction by a wedge (kr_o=16, θ_o = 120°, β = θ_o + 180°)

CHAPTER VI

BEAM DIFFRACTION BY A CIRCULAR APERTURE

(NORMAL INCIDENCE)

Fig. 6.1 shows a circular aperture of radius a in a conducting plane (xy-plane) and centred at the origin. For normal incidence, the point source lies on the aperture axis (z-axis). Because of symmetry, without loss of generality the problem can be treated as 2-dimensional.

6.1 Uniform Point-Source Solution

For a point source located at a distance z_o from the origin and r_o from the aperture edges making an angle Θ_o with the aperture plane, as shown in Fig. 6.1, we have the following relations:

$$r_o = \sqrt{z_o^2 + a^2} \tag{6.1}$$

$$\Theta_o = \pi - \cos^{-1}(a/r_o) \tag{6.2}$$

For an observation point in the far field at r,Θ from the origin, or at r_1, Θ_1 from one edge and r_2, Θ_2 from the opposite edge, we have the following approximations:

$$r_{1,2} \simeq r \mp a \cos\Theta \quad ; \quad r>>a, \tag{6.3}$$

$$R \simeq r - z_o \sin\Theta \quad ; \quad r>>z_o . \tag{6.4}$$

Where R is the distance from the source to the observation point.

$$\Theta_1 = \Theta \tag{6.5a}$$

$$\Theta_2 = \pi - \Theta \quad ; \quad 0 \leq \Theta < \pi \quad ; \tag{6.5b}$$

$$\theta_2 = 3\pi - \theta \; ; \quad \pi \leq \theta \leq 2\pi \quad ;$$

$$\theta \simeq 1.5\pi + \phi \; ; \quad -1.5\pi \leq \phi \leq \pi/2. \tag{6.5c}$$

6.1.1 Single Diffraction

The incident and reflected fields at a distant field point (r, θ) due to an isotroptic point source at $(0, z_o)$ and a circular aperture in a conducting plane at z=0 are u^i and u^r, respectively, are given by

$$u^i = \frac{e^{-jkR}}{kR} \simeq e^{jkz_o \sin\theta} \frac{e^{-jkr}}{kr} \tag{6.6}$$

and

$$u^r \simeq -e^{-jkz_o \sin\theta} \frac{e^{-jkr}}{kr} \tag{6.7}$$

The resultant diffracted component of the field by a curved edge is given by Keller (1957) as

$$u^d \simeq u_o^i \cdot D(\theta_o, r_o, \theta) \cdot \sqrt{\rho/r(r+\rho)}\, e^{-jkr} \quad , \tag{6.8}$$

where u_o^i is the incident field at the diffracting edge

$$u_o^i = \frac{e^{-jkr_o}}{kr_o} \quad , \tag{6.9}$$

and $D(\theta_o, r_o, \theta)$ is the diffraction coefficient given by Kouyoumjian and Pathak (1974) as

$$D(\theta_o, r_o, \theta) = \sqrt{\frac{kr_o}{\pi}}\, e^{+j\pi/4} [G(w_i) - G(w_r)] \tag{6.10}$$

G(w) is given by

$$G(w) = \pm e^{jw^2} F[\pm w] \tag{6.11}$$

The (+) sign applies in the shadow region, and (-) sign in the illuminated region. F[w] is the Fresnel integral given by (3.2) with complex arguments $w_{i,r}$ given by

$$w_{i,r} = -\sqrt{2kr_o}\cos\left(\frac{\Theta \mp \Theta_o}{2}\right) \tag{6.12}$$

$\sqrt{\rho/r'(r'+\rho)}$ is the curvature factor with r' as the distance from the diffracting edge to the observation point; i.e. r_1, r_2 in our case.

For normal incidence, Keller(1957) showed

$$\rho = a/\cos\Theta \tag{6.13}$$

and this holds also for a point source on the circular aperture axis. Substituting for ρ and r' in the curvature factor and with the far field approximations in (6.3) one can show that

$$\sqrt{\rho/r_{1,2}(r_{1,2}+\rho)} \simeq \frac{1}{r}\sqrt{a/\cos\Theta_{1,2}} \tag{6.14}$$

Where r is measured from the origin and $\Theta_{1,2}$ given by (6.5).

The singly diffracted component of the far field U_s^d is the sum of the diffracted field component by one edge and its opposite which are given by (6.8).

$$U_s^d \simeq ka\, e^{j\pi/4} U_o^i \left[\frac{D_1 e^{j(ka\cos\Theta-\pi/4)} + D_2 e^{-j(ka\cos\Theta-\pi/4)}}{\sqrt{ka\cos\Theta}}\right] \frac{e^{-jkr}}{kr} \tag{6.15}$$

where

$$D_{1,2} \equiv D(\Theta_o, r_o, \Theta_{1,2}) \tag{6.16}$$

are given by (6.10).

On the axial caustic; i.e. $\Theta = \frac{\pi}{2}$ or $\frac{3\pi}{2}$, (6.15) is singular, so near this axis the field is inaccurate. The singly diffracted far field in (6.15) can be rewritten as

$$U_s^d \simeq ka\, e^{j\pi/4}\, U_o^i \left[(D_1 + D_2) \frac{\cos(ka\cos\Theta - \pi/4)}{\sqrt{ka\cos\Theta}} + j(D_1 - D_2) \frac{\sin(ka\cos\Theta - \pi/4)}{\sqrt{ka\cos\Theta}} \right] \frac{e^{-jkr}}{kr} \qquad (6.17)$$

As $ka\cos\Theta \to 0$, i.e., $\Theta \to \pi/2$ or $3\pi/2$, we use the asymptotic expansion of the Bessel functions

$$\frac{\cos(ka\cos\Theta - \pi/4)}{\sqrt{ka\cos\Theta}} \cong \sqrt{\pi/2}\, J_o(ka\cos\Theta) \qquad (6.18a)$$

$$\frac{\sin(ka\cos\Theta - \pi/4)}{\sqrt{ka\cos\Theta}} \cong \sqrt{\pi/2}\, J_1(ka\cos\Theta) \qquad (6.18b)$$

Here J_o and J_1 are Bessel functions of the first kind, of order zero and one, respectively. Substituting (6.18) in (6.17) gives

$$U_s^d \simeq \sqrt{\frac{\pi}{2}}\, e^{j\pi/4}\, ka\, U_o^i \left[(D_1 + D_2)\, J_o(ka\cos\Theta) + j(D_1 - D_2).J_1((ka\cos\Theta) \right] \frac{e^{-jkr}}{kr} \qquad (6.19)$$

6.1.2 Multiple Diffraction Solution

The diffracted field component at (r,Θ) due to a point source at (r_o,Θ_o) from a curved edge is given by (6.8). To simplify the analysis we rewrite (6.8) as follows:

$$U^d \simeq U_o^i\, D(\Theta_o, r_o, \Theta', r') \qquad (6.20)$$

where r', Θ' are observation point polar coordinates measured from the edge and

$$D(\Theta_o, r_o, \Theta', r') = D(\Theta_o, r_o, \Theta') \sqrt{\frac{ka}{\mp\cos\Theta}} \frac{e^{-jkr'}}{\sqrt{kr.kr'}} ; \Theta \gtrless \frac{3\pi}{2} \quad (6.21)$$

Here $D(\Theta_o, r_o, \Theta')$ is given by (6.10) and r, Θ are measured from the centre of the curved edge. Following the same procedure given by Jull (1981), the multiply diffracted field, excluding single diffracted field, can be written as

$$U_m^d = U_o^1 D^i [(D_o + D_o D_{20} + D_o^2 D_{10} + \ldots\ldots) + (D_o + D_o D_{10} + D_o^2 D_{20} \ldots\ldots\ldots)] , \quad (6.22)$$

where D_o, D^i, D_{10} and D_{20} are given as following:

$$D_o = D(\pi, 2a, \pi, 2a) = \sqrt{4/\pi}\, e^{j(2ka - \pi/4)} F[\sqrt{4ka}] \quad (6.23)$$

$$D^i = D(\Theta_o, r_o, \pi, 2a) = \sqrt{2r_o/\pi a}\, e^{-j(2ka+\pi/4)} e^{jkr_o(1-\cos\Theta_o)} F[\sqrt{2kr_o}\sin(\Theta_o/2)], \quad (6.24)$$

and

$$D_{10}^{20} = D(\pi, 2a, \Theta_2^1, r_2^1)$$

$$D_{10}^{20} = \mp \pi(2ka/\pi)^{3/2} e^{j2ka} \frac{e^{\mp j(ka\cos\Theta - \pi/4)}}{\sqrt{ka\cos\Theta}} F[\sqrt{4ka}\sin(\Theta_2^1/2)] \frac{e^{-jkr}}{kr} \quad (6.25)$$

Now (6.22) can be summed, provided $D_o \neq 1$, giving

$$U_m^d = U_o^i D^i \frac{(D_{10} + D_{20})}{(1-D_o)} \quad (6.26)$$

Again near the axial caustic; i.e. $\Theta = \pi/2$ or $3\pi/2$, the field must be modified as for single diffraction. Following the procedures given before to get the multiply diffracted component, rewrite D_{10}, D_{20} in terms of D_{10}', D_{20}' as

$$D_{\substack{10\\20}} = \mp D'_{\substack{10\\20}} \cdot \frac{e^{\mp j(ka\cos\Theta-\pi/4)}}{\sqrt{ka\cos\Theta}} \quad \frac{e^{-jkr}}{kr}, \tag{6.27}$$

where

$$D'_{\substack{10\\20}} = \pi(2ka/\pi)^{3/2} e^{j2ka} F[\sqrt{4ka}\sin(\theta_1/2)]. \tag{6.28}$$

Then $D_{10} + D_{20}$ can be simplified to

$$D_{10}+ D_{20} = -\left[\frac{D'_{10} e^{-j(ka\cos\Theta-\pi/4)} - D'_{20} e^{j(ka\cos\Theta-\pi/4)}}{\sqrt{ka\cos\Theta}}\right] \frac{e^{-jkr}}{kr} \tag{6.29}$$

$$= -\left[(D'_{10}-D'_{20})\frac{\cos(ka\cos\Theta-\pi/4)}{\sqrt{ka\cos\Theta}} -j(D'_{10}+D'_{20})\frac{\sin(ka\cos\Theta-\pi/4)}{\sqrt{ka\cos\Theta}}\right] \frac{e^{-jkr}}{kr} \tag{6.30}$$

Substituting from (6.18) in (6.30) gives

$$D_{10} + D_{20} = -\sqrt{\pi/2}\left[(D'_{10}-D'_{20})\, J_o(ka\cos\Theta) -j(D'_{10}+D'_{20})\, J_1(ka\cos\Theta)\right] \frac{e^{jkr}}{kr} \tag{6.31}$$

Substitute for (6.31) in (6.26) to get the multiply diffracted field component near the axial caustic as

$$U^d_m \simeq \sqrt{\pi/2}\, \frac{U^i_o D^i}{(D_o-1)} \left[(D'_{10}-D'_{20})\, J_o(ka\cos\Theta) -j(D'_{10}+D'_{20})\, J_1(ka\cos\Theta)\right] \frac{e^{-jkr}}{kr} \tag{6.32}$$

The total field, including single diffraction only, is

$$U^t = U^d_s + U^i\, S(\Theta_{si}-\Theta) + U^r\, S(\Theta_{sr}-\Theta) \tag{6.33a}$$

and including multiple diffraction is

$$U^t = U^d_s + U^d_m + U^i\, S(\Theta_{si}-\Theta) + U^r\, S(\Theta_{sr}-\Theta), \tag{6.33b}$$

where S(x) is the positive unit step function. U^i, U^r, U_s^d and U_m^d are the incident, reflected, singly diffracted and multiply diffracted far fields.

6.2 Uniform Beam Solution

For normal incidence the beam axis is perpendicular to the aperture plane and coincides with the aperture axis.

6.2.1 Far Field Calculation

To change from an isotropic point source solution to a directive beam solution, complex values appropriate to the beam width and beam direction are given to the source coordinates. Then z_o, r_o and Θ_o become complex and are called z_s, r_s and Θ_s, respectively.

$$z_s = z_o - jb \sin\beta \quad ; \; b \geq 0, \; 0 < \beta < 2\pi \tag{6.34}$$

$$r_s = \sqrt{z_s^2 + a^2} \quad ; \; \text{Real}(r_s) \geq 0 \tag{6.35}$$

$$\Theta_s = \pi - \cos^{-1}(a/r_s) \tag{6.36}$$

Where z_o, b and β are real values, defining the source location, beam width and beam direction, respectively. By replacing z_o, r_o and Θ_o by z_s, r_s and Θ_s, respectively in (6.1 to 6.33) we get the beam solution for all above cases, single and multiple diffraction, near or far from the axial caustic.

6.2.2 Shadow and Reflection Boundary Calculations

Since the diffraction phenomena is local, we assume the shadow and reflection boundaries for a curved edge are the same as for a straight edge at the point of diffraction. So the results given in (3.13) and (3.14) are valid here.

The shadow and illuminated regions mentioned in (6.11) and Appendix D are given as, for shadow region:

$$\text{Real}(w_{i,r}) - \text{Imag}(w_{i,r}) > 0 \tag{6.37}$$

and for illuminated region:

$$\text{Real}(w_{i,r}) - \text{Imag}(w_{i,r}) < 0 \tag{6.38}$$

where $w_{i,r}$ are the Fresnel integral arguments given as

$$w_{i,r} = -\sqrt{2kr_s}\,\cos\left(\frac{\theta \mp \theta_s}{2}\right) \tag{6.39}$$

Also the shadow and illuminated regions for incident or reflected fields can be defined, respectively, by

$$\theta \gtrless \theta_{si} \text{ or } \theta_{sr} \tag{6.40}$$

where θ_{si} and θ_{sr} are given by (3.13) and (3.14), respectively.

6.3 Numerical Results

A point source on the circular aperture axis is at a distance $kz_o = 3\pi$ from the centre of the aperture which is of a radius $ka=3\pi$. In the following figures, the horizontal axis, ϕ in degrees, is the angle measured from the aperture axis as shown in Fig. 6.1, and the vertical

axis is the normalized far total field pattern, including single diffraction only or including single and multiple diffraction.

In Fig. 6.2 the dashed curves represent the non-modified solution calculated from (6.25), (6.26) and (6.33b) which is valid far from the axial caustic. The solid curves represent the modified solution near the axial caustic, calculated from (6.32) and (6.33b). This figure shows how the total far field including multiple diffraction, is modified near the axial caustic (z-axis) for two different cases. One is the limiting case of a point source (kb=0) and the other is a directive beam (kb=8).

Fig. 6.3 illustrates the development of the beam solution from the point source (kb=0) to a directive beam (kb=16), and an essentially plane wave (kb=85). When kb is small compared to kz_o interaction between the incident and diffracted fields in the illuminated region is evident because the aperture edge is strongly illuminated, consequently the diffracted field is significant. As kb increases, e.g. kb=16, the incident beam becomes narrower and the edge is weakly illuminated so the diffracted field is insignificant and the interaction decreases. In the shadow region the interaction occurs between the diffracted fields from the two opposite diffracted points on the aperture edge. This interaction is significant when kb small or when $b>>z_o$, eg. kb=85 where the field incident on the aperture becomes uniform, like a plane wave, the edge is strongly illuminated again. In this figure the dashed curves represent the single diffraction solution given by (6.33a), and

the solid curves include for multiple diffraction solution given by (6.33b).

For this choice of aperture radius ($ka=3\pi$), the singly and multiply diffracted fields are very much the same except at the conductor, i.e. $\phi=90°$, the multiply diffracted field vanishes on the conductor, satisfying the boundary condition of a perfect conductor while the singly diffracted field does not.

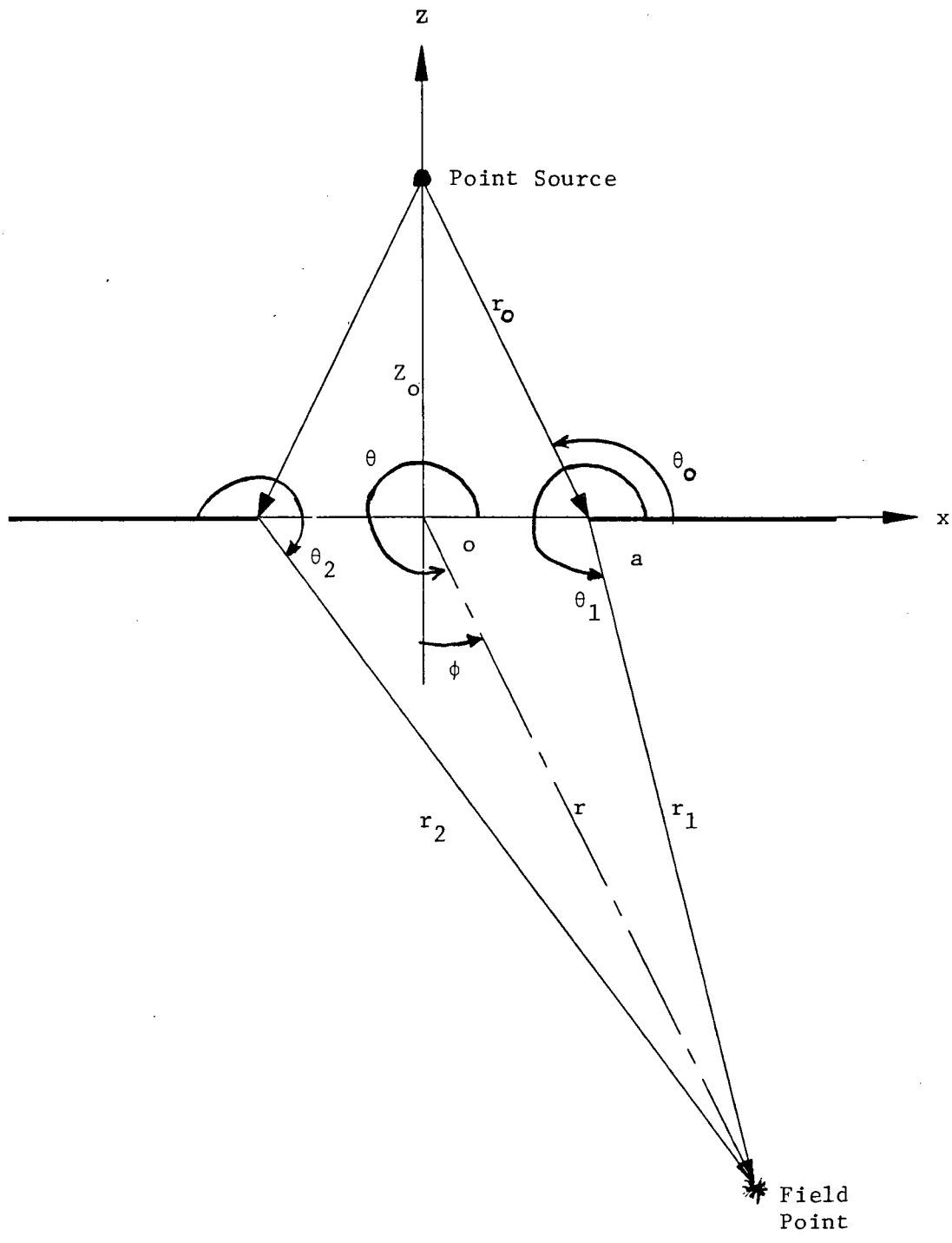

Fig. 6.1 Geometry of a complex point source diffraction by a circular aperture

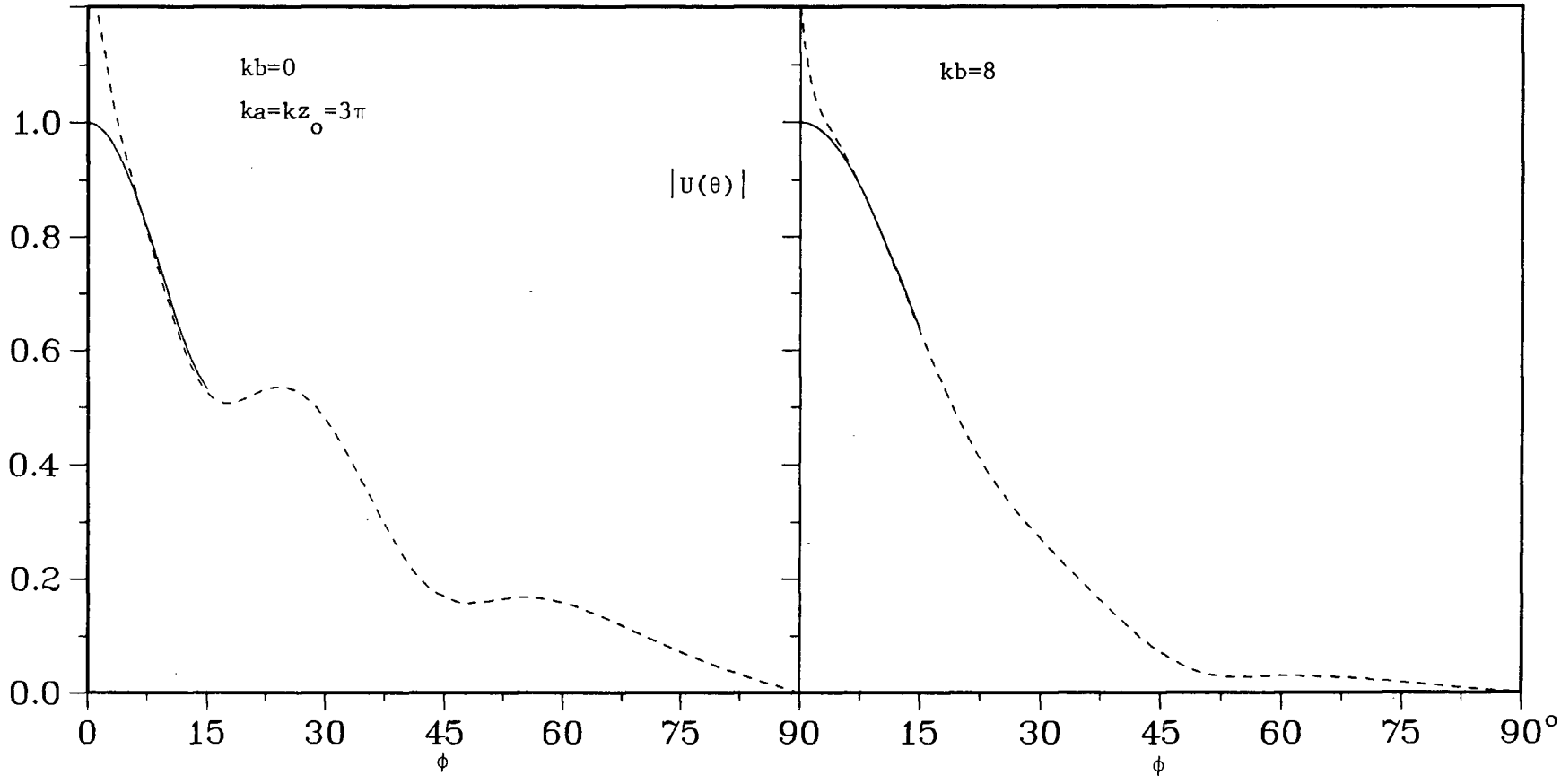

Fig. 6.2 Normalized total field pattern of a point source (kb=0) and moderate beam (kb=8) (solid) modified and (dashed) non-modified on the caustic axis (Normal incidence)

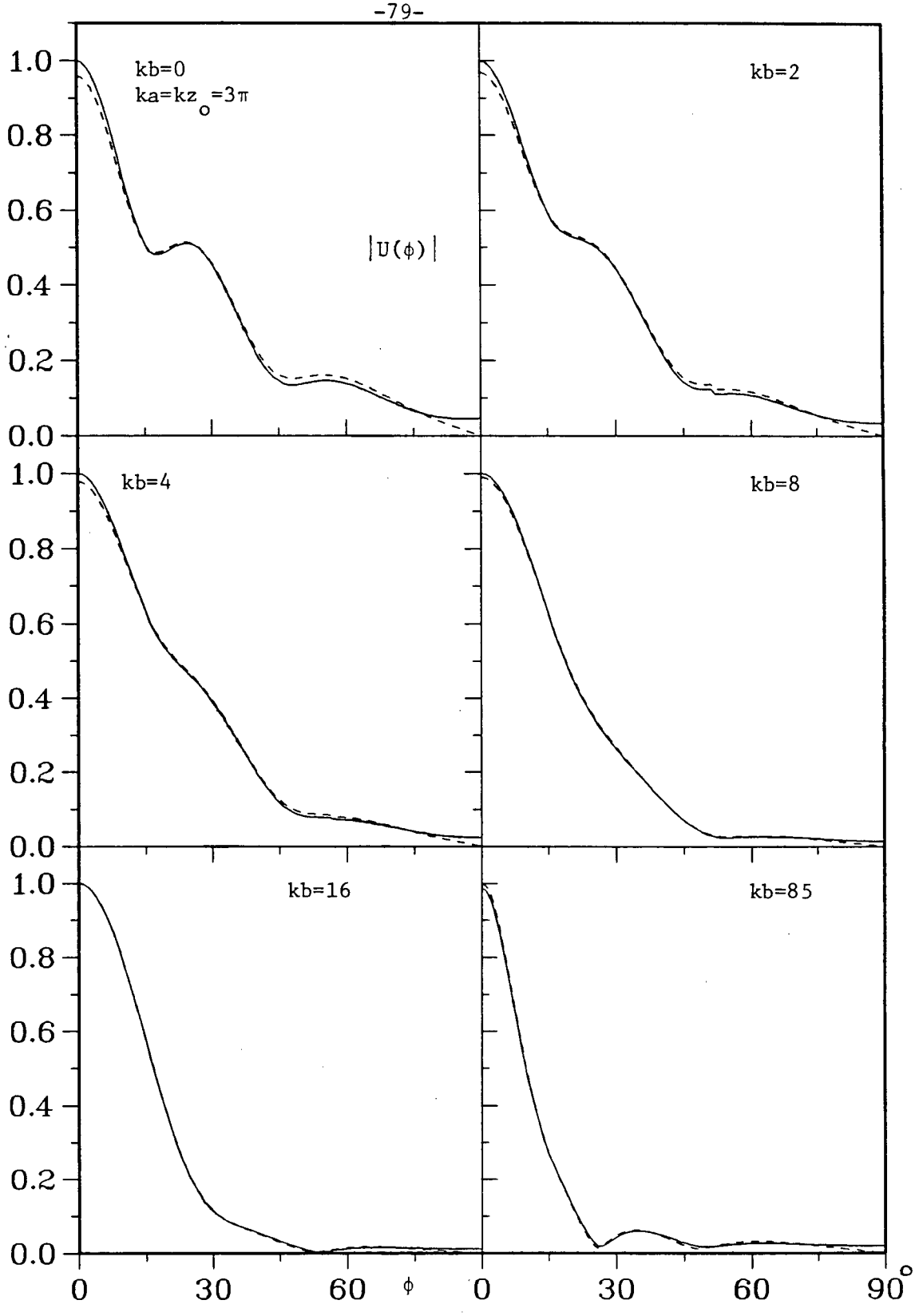

Fig. 6.3 Single (solid) and multiple (dashed) total patterns of a beam diffraction by a circular aperture (Normal incidence)

CHAPTER VII

SUMMARY, CONCLUSIONS AND RECOMMENDATIONS

7.1 Summary

The complex source point method was used to represent a directive beam which is Gaussian in the paraxial region. Uniform solutions for omnidirectional sources were developed and extended analytically to become solutions for directive beams. The geometrical theory of diffraction and equivalent line currents were used to include interaction between the edges of the slit and circular aperture. Numerical results including the limiting cases; e.g. plane wave incidence ($kb \to \infty$) and line or point sources ($kb = 0$), were given for every case studied. Also comparisons with existing solutions were made wherever possible.

In Chapter II, a directive beam was derived in polar coordinates and compared with a Gaussian beam and a typical antenna beam. An expression for the half-power beam width was derived, and a simple discussion of the use of multiple complex source points to derive more complicated beams was given.

The solution of beam diffraction by a half-screen, derived in Chapter III from a simple solution exact in the far field limit, was used to solve the problem of beam diffraction by wide slit and complementary strip. Also a convenient, simple formula was derived for the location of the shadow boundaries of a straight edge.

Beam diffraction by a wedge with its edge on the beam axis was analysed using the uniform theory of diffraction. This uniform solution completes the asymptotic solution, for the same problem, mentioned by Felsen (1976), whose solution is infinite on the shadow boundaries and inaccurate in the transition regions. Also the shadow boundaries are given here for any beam orientation.

Finally, the diffraction by circular aperture when illuminated by normally incident beam, was derived using the uniform theory of diffraction and along the axial caustic, Bessel functions were used to remove the singularity. Multiple diffractions were considered and a closed form expression was derived.

7.2 Conclusions

The beam derived in Chapter II using the complex source point method, can represent a typical antenna beam better than the Gaussian function especially for wide antenna beams (small kb). When the imaginary part (b) of the complex source position vector ($\overline{r}_s=\overline{r}_o-j\overline{b}$) is very large compared to the real part (r_o), i.e. $b>>r_o$, the beam tends to a plane wave.

Other authors assume very narrow beams and solve diffraction problems in the paraxial region. This kind of assumption makes the contribution of the diffracted field negligible, unless the beam axis passes through the diffracting edge. In our analysis this assumption was removed and the range of validity was increased to cover the whole region of interest.

The synthesis of more complicated beams such as one with sidelobes or a nearly square beam, was given in section (2.3) by using multiple complex source points. But the width and sidelobe level of the resultant beam are yet to be calculated and related to the complex coordinates. The study of simulating any beam in terms of Gaussian beams and Complex Source Points, given by Mantica et al (1986), was not rigorous and some assumptions were made to simplify the analysis.

Our solution of beam diffraction by half-screen is accurate, uniform everywhere and valid for all beam orientations and widths. This solution can be used as a reference solution for other uniform or asymptotic solutions which are inaccurate in the transition regions and infinite on the shadow boundaries.

The limiting case kb = 0 of our solution to the strip when illuminated by omnidirectional source, is in very good agreement with solutions of line source diffraction by a strip, given by Vankoughnett and Wong (1981) and by Shafai and Elmoazzen (1972). Tsai et al. (1972) have shown, by comparison with numerical results, that the geometrical theory of diffraction yields satisfactory results for reflector widths as small as 0.2λ (wave length) when double diffraction is included. For our choice of strip width 2.5λ, single diffraction is sufficient. Since the contribution to the diffracted field for directive sources is always less than or equal (for the edge on the beam axis) to that of an omnidirectional source, the accuracy for directive beams is at least as high as that for omnidirectional sources.

In all cases studied here the incident field was normal to the diffracting edge. Solutions can be extended to include oblique incidence on a straight edge or wedge.

The ordinary UTD was used in solving the problems of the wedge and circular aperture. For better accuracy one may use the UTD augmented by slope diffraction (Kouyoumjian et al., 1981) or the improved version (Buyukdhura and Kouyoumjian, 1985), instead.

The diffraction of a beam by parabolic cylinder reflector with an edge was also considered (see appendix E) before we were aware that Ghione et al., (1984) had published their solution to this problem. However, the diffracted field and reflected field, with some approximations, without using the computer search technique is given in Appendix E. The problem was not pursued further, although as they suggest further investigation is needed to clarify and simplify the method.

The uniform theory of diffraction was used to obtain uniform solutions where there were no simple exact solutions, such as for the wedge and circular aperture. Otherwise rigorously correct solutions at high frequencies for far singly diffracted fields were used, such as for the half-screen, slit and strip. All the solutions obtained for the above cases are uniform, for Fresnel integrals provide a smooth transition through shadow and reflection boundary regions.

For simplicity scalar (acoustic) fields were assumed through out this thesis. The results apply directly to two-dimensional electromagnetic fields in the case of the half-plane, slit or strip and wedge. For the circular aperture extension to vector electromagnetic fields can be made by considering the scalar field as one component of

the vector field or as a scalar potential from which vector fields are derived.

7.3 Recommendations for Future Work

So far we have dealt with problems that assume perfect conductors, simple beams and normal incidence, to generalize the incident beam and the reflectors boundary conditions the following may be considered:

i) To make the analysis by the complex ray tracing method more complete, especially for non-planar surfaces, a general a-priori criterion; i.e., one which does not require the study of steepest descents paths used by Ghione et al. (1984), is needed for two-dimensional diffraction.

ii) Diffraction by simple shapes when illuminated by more complicated beams with sidelobes. When these beams are represented by multiple complex source points, solutions may easily be obtained using the superposition principle.

iii) The problem of beam diffraction by straight wedge where the edge does not lie on the beam axis, using the UTD to assess the asymptotic solution by Felsen (1976), is yet to be done. Also diffraction by a conducting curved wedge has not been studied yet. The solution for real source diffraction by a curved wedge by Lee and Deschamps (1976) or Deschamps (1985) may be used.

iv) All existing solutions for beam diffraction by a circular aperture, assume symmetrical incidence; i.e. the beam axis coincides with the aperture axis. The more general non-symmetrical incidence case with the beam axis shifted from the aperture axis by some distance or at some angle, apparently has not been reported yet.

v) To cover a wide range of problems, using the CSP method, a rigorous simulation of an arbitrary beam in terms of complex source points needs to be derived. What exists in the literature now is based on assumptions and experience; i.e. trial and error.

vi) Solutions to beam diffraction by simple shapes such as half-plane, strip and wedge, under impedance boundary conditions may be obtained using the corresponding solutions for omnidirectional sources by Bucci and Franceschetti (1976), and Tiberio et al. (1982 and 1985), respectively.

vii) Extensions of this method to three-dimensional diffraction by curved surfaces with edges need to be addressed.

REFERENCES

ALBERTSEN, N., NIELSEN, Per. and PONTOPPIDAN, K., "New concepts in multi-reflector antenna analysis, final report", TICRA A/S Engineering Consultants, (Copenhagen, Denmark, Sept., 1983), pp. 28-40.

ANDERSON, I. (1978): "The diffraction of an antenna beam by a nearby conducting half-plane", Int. Conf. Ant. Prop. ICAP, UK., pp. 244-246.

ARNAUD, J. (1985): "Representation of Gaussian beams by complex rays", Appl. Opt. 24, pp. 538-543.

BELANGER, P.A. and COUTURE, M. (1983): "Boundary diffraction of an inhomogeneous wave", J. Opt. Soc. Am., Vol. 73, No. 4, pp. 446-450.

BERTONI, H.L., GREEN, A.C. and FELSEN, L.B. (1978): "Shadowing an inhomogeneous plane wave by an edge", J. Opt. Soc. Am., Vol. 68, No. 7, pp. 983-988.

BOERSMA, J. and LEE, S.W. (1977): "High-frequency diffraction of a line-source field by a half-plane: solutions by ray technique", IEEE Trans. Ant. Prop., Vol. AP-25, No. 2, pp. 171-179.

BORN, M. and WOLF, E., "Principles of optics", Pergamon Press, Oxford, 5th edn., 1976.

BOWMAN, J.J., SENIOR, T.B.A. and USLENGHI, P.L.E. (Eds.), "Electromagnetic and acoustic scattering by simple shapes", (North-Holland, 1969).

BUCCI, O.M. and FRANCESCHETTI, G. (1976): "Electromagnetic scattering by a half-plane with two face impedances", Radio Science, Vol. 11, pp. 49-59.

BUYUKDHURA, O.M. and KOUYOUMJIAN, R.G., "An improved UTD solution for wedge diffraction", IEEE, AP-S International Symposium, Vol. II, (UBC Vancouver, CANADA, June, 1985), pp. 439-442.

CHOUDHARY, S. and FELSEN, B.L. (1973): "Asymptotic theory for inhomogeneous waves", IEEE Trans. Ant. Prop., Vol. AP-21, No. 6, pp. 827-842.

CHOUDHARY, S. and FELSEN, L.B. (1974): "Analysis of Gaussian beam propagation and diffraction by inhomogeneous wave tracking", Proc. IEEE, Vol. 62, No. 11, pp. 1530-1541.

CLEMMOW, P.C. (1950): "A note on the diffraction of a cylindrical wave by a perfectly conducting half-plane", Quart, Journ. Mech. and Appl. Math., Vol. 3, Pt. 3, pp. 377-384.

CLEMMOW, P.C. and MUNFORD, C.M. (1952): "A table of $\sqrt{\pi/2}\ \exp\left(\frac{i\pi\rho^2}{2}\right) . \int_{\rho}^{\infty} \exp\left(\frac{-i\pi\lambda^2}{2}\right) d\lambda$ for complex values of ρ", Philosophical Trans. Royal Soc. London [A], Vol. 245, pp. 189-211.

COUTURE, M. and BELANGER, P. (1981): "From Gaussian beam to complex-source-point spherical wave", Phys. Review A, Vol. 24, No. 1, pp. 355-359.

DESCHAMPS, G.A. (1971): "Gaussian beam as a bundle of complex rays", Electronics Letters, Vol. 7, No. 23, pp. 684-685.

DESCHAMPS, G.A. (1972): "Ray techniques in electromagnetics", Proc. IEEE, Vol. 60, No. 9, pp. 1022-1035.

DESCHAMPS, G.A. (1985): "High frequency diffraction by wedges", IEEE Trans. Ant. Prop., Vol. AP-33, No. 4, pp. 357-368.

EINZIGER, P. and RAZ, S. (1980): "On the asymptotic theory of inhomogeneous wave tracking", Radio Science, Vol. 15, No. 4, pp. 763-771.

EINZIGER, P.D. and FELSEN, L.B. (1982): "Evanescent waves and complex rays", IEEE Trans. Ant. Prop, Vol. AP-30, No. 4, pp. 594-605.

EINZIGER, P.D. and RAZ, S. (1987): "Wave solutions under complex space-time shifts", J. Opt. Soc. Am. A, Vol. 4, No. 1, pp. 3-10.

FELSEN, L.B. and MARCUVITZ, N., "Radiation and scattering of waves", (Prentice-Hall, Inc., Englewood Cliffs, N.J., 1973).

FELSEN, L.B. (1976): "Complex source point solutions of the field equations and their relation to the propagation and scattering of Gaussian beams", Symposia Mathematica, Vol. XVII, (Academic Press, New York), pp. (31-33, 45-46, 67-69).

FELSEN, L.B. (1976): "Evanescent waves", J. Opt. Soc. Am., Vol. 66, No. 8, pp. 751-760.

FELSEN, L.B. (1984): "Geometrical theory of diffraction, evanescent waves, complex rays and Gaussian beams", Geophys. J.R. Astr. Soc., Vol. 79, pp. 77-88.

GAUTSCHI, W., "Error function and Fresnel integrals", in "Handbook of mathematical functions", Eds. M. Abramowitz and I. Stegun, NBS Appl. Math. Ser. 55, (Nat. Bur. of Stand. Washington, D.C., 9th Print, 1970).

GHIONE, G., MONTROSSET, I. and ORTA, R., "Complex rays in hybrid formulation of wave propagation and scattering", Ed. L.B. Felsen, NATO ASI, Series E, No. 86, (Martinus Nijhoff publishers, the Netherlands, 1984).

GHIONE, G., MONTROSSET, I. and FELSEN (1984), "Complex Ray Analysis of Radiation from Large Aperture with Tapered Illumination", IEEE Trans. Ant. Prop., Vol. AP-32, No. 7, pp. 684-693.

GREEN, A.C., BERTONI, H.L. and FELSEN, L.B. (1979), "Properties of the shadow cast by a half-screen when illuminated by a Gaussian beam", J. Opt. Soc. Am., Vol. 69, No. 11, pp. 1503-1508.

HASHIMOTO, M. (1985): "Beam waves with sources at complex location", Electronics Letters, Vol. 21, No. 23, pp. 1006-1007.

HASSELMANN, F. (1980): "Asymptotic analysis of parabolic reflector antennas", Ph.D. Thesis, Polytechnique Instit. of New York, pp. 106-107.

HASSELMAN, F.J. and FELSEN, B.L. (1982): "Asymptotic analysis of parabolic reflector antennas", IEEE Trans. Ant. Prop., Vol. AP-30, No. 4, pp. 677-685.

JONES, D.S., "Methods in electromagnetic wave propagation", (Clarendon Press, Oxford, 1979).

JULL, E.V., "Aperture antennas and diffraction theory", (Peter Peregrinus, U.K., 1981).

KARP, S.N. and KELLER, J.B. (1961): "Multiple diffraction by an aperture in a hard screen", Optica Acta, 8, pp. 61-72.

KELLER, J.B. (1957): "Diffraction by an aperture", J. Appl. Phys., Vol. 28, No. 4, pp. 426-444.

KELLER, J.B. (1962): "Geometrical theory of diffraction", J. Opt. Soc. Am., Vol. 52, No. 2 pp. 116-130.

KELLER, J.B. and STREIFER, W. (1971): "Complex rays with an application to Gaussian beams", J. Opt. Soc. Am., Vol. 61, No. 1, pp. 40-43.

KOGELNIK, H.W. and LI, T. (1966): "Laser beams and resonators", App. Opt. Vol. 5, No. 10, pp. 1550-1567.

KOUYOUMJIAN, R.G. and PATHAK, P.H. (1974): "A uniform geometrical theory of diffraction for an edge in a perfectly conducting surface", Proc. IEEE, Vol. 62, No. 11, pp. 1448-1461.

KOUYOUMJIAN, R.G., PATHAK, P.H. and BURNSIDE, W.D., "A uniform GTD for the diffraction by edges, vertices and convex surfaces", Theoretical Methods for Determining the Interaction of Electromagnetic Waves with Structures, ed. J.K. Skwirzynski (Sijthoff and Noordhoff, Alphen aan den Rijn, The Netherlands, 1981).

LEE, S. and DESCHAMPS, G. (1976): "A uniform asymptotic theory of electromagnetic diffraction by a curved wedge", IEEE Trans. Ant. Prop., Vol. AP-24, No. 1, pp. 25-34.

LUK, K. and YU, P. (1985): "Generation of Hermite-Gaussian beam modes by multipoles with complex source points", J. Opt. Soc. Am. A, Vol. 2, No. 11, pp. 1818-1820.

MANTICA, P.G., MONTROSSET, I., TASCONE, R. and ZICH, R. (1986): "Source-field representation in terms of Gaussian beam", J. Opt. Soc. Am. A, Vol. 3, No. 4, pp. 497-507.

MITTRA, R. and LEE, S.W., "Analytic techniques in the theory of guided waves", (Macmillan, New York, 1971).

MITTRA, R., RAHMAT-SAMII, Y. and KO, W.L. (1976): "Spectral theory of diffraction", J. App. Phys., Vol. 10, pp. 1-13.

MIYAMOTO, K. and WOLF, E. (1962): "Generalization of the Maggi-Rubinowicz theory of the boundary diffraction wave, part I", J. OPt. Soc. Am., Vol. 52, No. 6, pp. 615-625.

MIYAMOTO, K. and WOLF, E. (1962): "Generalization of the Maggi-Rubinowicz theory of the boundary diffraction wave, part II", J. OPt. Soc. Am., Vol. 52, No. 6, pp. 626-637.

OTIS, G. (1974): "Application of the Boundary-Diffraction-Wave theory to Gaussian beams", J. OPt. Soc. Am., Vol. 64, No. 11, pp. 1545-1550.

OTIS, G. and LIT, J.W.Y. (1975): "Edge-on diffraction of a Gaussian laser beam by a semi-infinite plane", App. Opt., Vol. 14, No. 5, pp. 1156-1160.

OTIS, G., LACHAMBRE, J.L., LIT, J.W.Y. and LAVIGNE, P. (1977): "Diffracted waves in the shadow boundary region", J. Opt. Soc. Am., Vol. 67, No. 4, pp. 551-553.

PEARSON, J.E., McGILL, T.C., KURTIN, S. and YARIV, A. (1969): "Diffraction of Gaussian laser beam by a semi-infinite plane", J. Opt. Soc. Am., Vol. 59, No. 11, pp. 1440-1445.

SHAFAI, L. and EL-MOAZZEN, Y.S. (1972): "Radiation patterns of an antenna near a conducting strip", IEEE Trans. Ant. Prop. pp. 642-644.

SHIN, S.Y. and FELSEN, L.B. (1977): "Gaussian beam modes by multipoles with complex source points", J. Opt. Soc. Am., Vol. 67, No. 5, pp. 699-700.

SIEGMAN, A.E., "An introduction to lasers and masers", (McGraw-Hill, New York, 1971), ch. VIII.

TAKENAKA, T., KAKEYA, M. and FUKUMITSU, O. (1980): "Asymptotic representation of the boundary diffraction wave for a Gaussian beam incident on a circular aperture", J. Opt. Soc. Am., Vol. 70, No. 11, pp. 1323-1328.

TAKENAKA, T. and FUKUMITSU, O. (1982): "Asymptotic representation of the boundary-diffraction wave for a three-dimensional Gaussian beam incident upon a Kirchhoff half-screen", J. Opt. Soc. Am. Vol. 72, No. 3, pp. 331-336.

TIBERIO, R., BESSI, F., MANARA, G. and PELOSI, G. (1982): "Scattering by a strip with face impedances at edge on incidence", Radio Sci., Vol. 17, pp. 1199-1210.

TIBERIO, R., PELOSI, G. and MANARA, G. (1985): "a uniform GTD formulation for the diffraction by a wedge with impedance faces", IEEE Trans. Ant. Prop., Vol. AP-33, No. 8, pp. 867-873.

TSAI, L.L., WILTON, R.D., HARRISON, M.G. and WRIGHT, E.H. (1972): "A comparison of geometrical theory of diffraciton and integral equation formulation for analysis of reflector antennas", IEEE Trans. Ant. Prop., Vol. AP-20, No. 6, pp. 705-712.

WANG, W.Y.D. and DESCHAMPS, G.A. (1974): "Application of complex ray tracing to scattering problems", Proc. IEEE, Vol. 62, No. 11, pp. 1541-1551.

WILLIAMS, C.S. (1973), "Gaussian beam formulas from diffraction theory", J. App. Opt. Vol. 12, No. 4, pp. 872-876.

APPENDIX A

THE FRESNEL INTEGRAL WITH A COMPLEX ARGUMENT

A.1 Evaluation of Fresnel Integrals from Error Functions

For a real or complex argument w, Fresnel Integral F[w] is defined as

$$F[w] = \int_{w}^{\infty} e^{-j\tau^2} d\tau \qquad (A.1)$$

By changing variables

$$\tau = y\, e^{-j\pi/4}, \qquad d\tau = e^{-j\pi/4} dy \qquad (A.2)$$

$$F[w] = e^{-j\pi/4} \int_{we^{j\pi/4}}^{\infty} e^{-y^2} dy \qquad (A.3)$$

The complementary error function is defined as

$$\operatorname{erfc}(v) = \frac{2}{\sqrt{\pi}} \int_{v}^{\infty} e^{-y^2} dy = 1 - \operatorname{erf}(v) \qquad (A.4)$$

where v can be real or complex and erf(v) is the error function.

$$\operatorname{erf}(v) = \frac{2}{\sqrt{\pi}} \int_{o}^{v} e^{-y^2} dy \qquad (A.5)$$

From (A.3) and (A.4) with $v = w\, e^{j\pi/4}$ we can write

$$F[w] = \sqrt{\pi}/2\; e^{-j\pi/4} \operatorname{erfc}(we^{j\pi/4}) \qquad (A.6)$$

Subroutines for complementary error functions with complex arguments are available in UBC Computing Centre Library.

A.2 Some Properties of Fresnel Integrals:

i) Symmetry relation

$$F[w] + F[-w] = \sqrt{\pi}\, e^{j\pi/4} \qquad (A.7)$$

ii) Special values

$$F[-\infty] = \sqrt{\pi}\, e^{-j\pi/4} \quad , \quad F[0] = \frac{1}{2} F[-\infty] \text{ and } F[\infty] = 0 \qquad (A.8)$$

iii) Asymptotic expansion.

$$F[w] \sim S(-w) + F[w] \quad ; \quad |w| \to \infty \quad , \qquad (A.9)$$

where $S(x)$ is the unit step function, and

$$F[w] = \frac{-j\, e^{-jw^2}}{2w\sqrt{\pi}} \sum_{n=0}^{\infty} \Gamma(n + 1/2)(-jw)^{-n} \qquad (A.10)$$

where $\Gamma(x)$ is the gamma function.

$$\Gamma(n + 1/2) = \sqrt{\pi}\,(1/2)(3/2) \ldots\ldots (n - 1/2) \qquad (A.11)$$

APPENDIX B

CALCULATION OF REAL AND IMAGINARY PARTS OF r_s

B.1 Analysis

Using (2.5) which is rewritten here as

$$r_s = [r_o^2 + 2r_o\,(-jb)\cos(\beta-\Theta_o) + (-jb)^2]^{1/2} \quad ; \quad \mathrm{Re}(r_s)>0 \qquad (B.1)$$

Let us write r_s as

$$r_s = R - jI \quad ; \quad R \geq 0 \qquad (B.2)$$

Where R and I are real. By squaring (B.1) and (B.2) and equating the real parts and the imaginary parts, respectively, we get

$$R^2 - I^2 = r_o^2 - b^2 \qquad (B.3)$$

and

$$R.I = r_o b \cos(\beta-\Theta_o) \qquad (B.4)$$

Solving (B.3) and (B.4) for R and I gives

$$R = \left[\left(\frac{r_o^2 - b^2}{2}\right) + \frac{1}{2}\sqrt{(r_o^2 - b^2)^2 + [2r_o b\cos(\beta-\Theta_o)]^2}\,\right]^{1/2}; \qquad (B.5)$$

and

$$I = \frac{r_o b}{R}\cos(\beta - \Theta_o) \qquad (B.6)$$

From (B.6) we notice that:

$$I \gtrless 0 \quad \text{if} \quad |\beta - \Theta_o| \lessgtr \pi/2. \qquad (B.7)$$

B.2 Special Cases:

i) $b=0$ gives $R=r_o$ and $I=0$; (B.8)

ii) $b=r_o$ gives $R=r_o\sqrt{|\cos(\beta-\Theta_o)|}$,

and $I = \mp R$; $|\beta-\Theta_o| \gtrless \pi/2$ (B.9)

iii) $\beta = \Theta_o$ or $\Theta_o+\pi$ gives $R = r_o$

and $I = \pm b$ (B.10)

iv) $|\beta - \Theta_o| = \pi/2$ gives

$R = \sqrt{r_o^2 - b^2}$ and $I = 0$ if $r_o > b$;

$R = 0$ and $I = 0$ if $r_o = b$; (B.11)

$R = 0$ and $I = \sqrt{b^2-r_o^2}$ if $r_o < b$.

APPENDIX C

GAUSSIAN BEAM DIFFRACTION BY HALF-SCREEN

(ASYMPTOTIC SOLUTION)

The asymptotic solution given by Green et al. (1979) for a Gaussian beam diffraction by a half-screen is summarized here with some changes in coordinates and notation for comparison with the solution given in Chapter 3. By replacing Θ', Θ, ρ', ρ and E by $(\frac{\pi}{2} - \Theta_s)$, $(\frac{3\pi}{2} - \Theta)$, r_s, r and U, respectively, we can write the incident U^i, reflected U^r, diffracted $U^d$and total U^t far fields as

$$U^i \simeq e^{jkr_s \cos(\Theta-\Theta_s)} \frac{e^{-jkr}}{\sqrt{kr}} \tag{C.1}$$

$$U^r \simeq - e^{jkr_s\cos(\Theta+\Theta_s)} \frac{e^{-jkr}}{\sqrt{kr}} \tag{C.2}$$

$$U^d \simeq \frac{e^{-j(kr_s-3\pi/4)}}{2\sqrt{2\pi kr_s}} \left[\sec\left(\frac{\Theta-\Theta_s}{2}\right) (1-\Delta^+) - \sec\left(\frac{\Theta+\Theta_s}{2}\right) (1-\Delta^-)\right] \frac{e^{-jkr}}{\sqrt{kr}}$$

where (C.3)

$$\Delta^{\pm} \simeq \frac{-j}{4kr_s} \sec^2\left(\frac{\Theta \mp \Theta_s}{2}\right) \quad ; \; r >> |r_s| \tag{C.4}$$

$$U^t \simeq U^d + U^i.S(\Theta_{si} - \Theta) + U^r.\, S(\Theta_{sr} - \Theta) \tag{C.5}$$

where S(x) is the unit step function, and Θ_{si} and Θ_{sr} are the shadow and

reflection boundaries measured from the illuminated side of the half-screen.

$$\Theta_{si} = \pi + \mathrm{Re}(\Theta_s) + \tan^{-1}\left[\frac{\sinh[\mathrm{Im}(\Theta_s)] \cdot \mathrm{Re}(r_s)}{|r_s| + \mathrm{Im}(r_s) \cdot \cosh[\mathrm{Im}(\Theta_s)]}\right] \qquad (C.6)$$

$$\Theta_{sr} = 2\pi - \Theta_{si} \qquad (C.7)$$

where Re(x) and Im(x) are the real and imaginary parts. The accuracy of the above solution depends on how small is $|\Delta^{+}_{-}|$ compared to 1.

APPENDIX D

THE SINGULARITY CANCELLATION IN THE WEDGE DIFFRACTION COEFFICIENT

One of the cotangent functions of the diffraction coefficient given by (5.9) is singular on the shadow or reflection boundaries, at the same time the corresponding G(w) function is zero. So the term cot(t).G(w) is finite everywhere. Therefore the singularity is cancelled and the diffraction coefficient is finite everywhere.

Near the shadow boundary or reflection boundary from the upper wedge surface, we can write from (5.3a,b),

$$\Theta \mp \Theta_o = \pi + \varepsilon \tag{D.1}$$

where $\varepsilon \to \pm 0$. $\varepsilon>0$ and $\varepsilon<0$ define the shadow and illuminated regions, respectively. Substituting (D.1) in (5.13a) gives

$$M_1^{\mp} = 0 \tag{D.2}$$

and (D.1), (D.2) in (5.11a) and (5.12a) gives

$$\cot(T_{1,2}) = \cot\left(\frac{-\varepsilon}{2n}\right) \simeq \frac{2n}{\varepsilon} \tag{D.3}$$

$$w_{1,2} = -\sqrt{2kr_o}\,\cos\left(\frac{\pi+\varepsilon}{2}\right) \simeq \sqrt{2kr_o}\cdot\frac{\varepsilon}{2} \tag{D.4}$$

Substitute (D.4) in (D.10) to get

$$G(w_{1,2}) = 2j\, e^{j\left(\frac{kr_o\varepsilon^2}{2}\right)} \cdot \left(\pm\sqrt{2kr_o}\,\frac{\varepsilon}{2}\right) F\left[\pm\sqrt{2kr_o}\,\frac{\varepsilon}{2}\right], \quad \varepsilon \lessgtr 0 \tag{D.5}$$

From (D.3) and (D.5) we get as $\varepsilon \to \pm 0$

$$\cot(T_{1,2}).G(w_{1,2}) = \mp n\sqrt{2\pi kr_o}\, e^{-j\pi/4} \tag{D.6}$$

Where (-) for shadow region and (+) for illuminated region. Similarly, near the reflection boundary due to the lower wedge surface, we can write from (5.3c)

$$\Theta + \Theta_o = (2n - 1)\,\pi - \varepsilon \tag{D.7}$$

Again $\varepsilon \to \overset{+}{-}0$. $\varepsilon>0$ and $\varepsilon<0$ define the shadow and illuminated regions of the reflected field, respectively. Inserting (D.7) in (5.13b) gives

$$M_2^+ = 1 \tag{D.8}$$

and substituting (D.7) and (D.8) in (5.11b), (5.12b) and (5.10) gives

$$\cot(T_4) = \cot(\pi - \frac{\varepsilon}{2n}) \simeq \frac{-2n}{\varepsilon} \tag{D.9}$$

and

$$\cot(T_4)\; G(w_4) = \mp\, n\sqrt{2\pi k r_o}\; e^{j\pi/4} \tag{D.10}$$

where (-) and (+) refer to the shadow and illuminated regions of the reflected field, respectively. Notice that the third term of the diffraction coefficient is finite everywhere, because of the restriction on Θ_o, $(0<\Theta_o<\frac{n\pi}{2})$. Therefore, all singularities of the diffraction coefficient are cancelled and the diffraction coefficient is finite everywhere.

APPENDIX E

BEAM DIFFRACTION BY A PARABOLIC REFLECTOR

The calculation of the reflected field from a conducting parabolic cylinder when illuminated by a Gaussian beam is given by Hasselmann & Felsen (1982). In their analysis, they assumed a very sharp Gaussian beam and an infinite parabolic reflector. so they did not include the diffracted field from the edge of a finite reflector. They used the method of computer search for the complex reflection points.

To include the diffracted field from the edges, half-plane tangent to the reflector at its edges are used instead. Also in the far field, with some approximation, the reflected field can be calculated without computer research for the reflection points.

Fig. E.1, shows a line source parallel to the reflector axis at a complex point $S(r_s, \Theta_s)$. $A(r,\Theta)$ is a far field point, $P(r_p,\Theta_p)$ is a typical point on the reflector, $E(r_e,\Theta_e)$ is the edge of the reflector and $O(0,0)$ is its focus. The equation of the parabola of a focal length F is given by

$$r_p = 2F/(1 + \cos\Theta_p) \tag{E.1}$$

and the slope of the tangential half-plane is given as

$$\left.\frac{dy_p}{dx_p}\right|_{y_e} = \frac{2F}{y_e} = \tan\Theta_t \tag{E.2a}$$

and $$\Theta_t = (\pi - \Theta_e)/2 \ . \tag{E.2b}$$

From the geometry of Fig. E.1 and the far field approximations, we have

$$r_i \simeq r - r_s \cos(\Theta - \Theta_s) \ , \tag{E.3a}$$

$$r_r \simeq r + r_p \cos(\theta + \theta_p) \ , \tag{E.3b}$$

$$r_1 \simeq r + r_e \cos(\theta + \theta_e) \ , \tag{E.3c}$$

$$r_2 \simeq r + r_e \cos(\theta - \theta_e) \ . \tag{E.3d}$$

Using the complex source point method, an incident field of a beam which makes an angle β with the x-axis is given as

$$U^i \simeq \frac{e^{-jkr_i}}{\sqrt{kr_i}} \simeq e^{-jk[r - r_o\cos(\theta - \theta_o)]} \cdot e^{kb\cos(\theta - \beta)} \ , \tag{E.4}$$

Here r_o, θ_o are the real coordinates of the line source. The reflected field at A from point P is

$$U^r \simeq \frac{e^{-jk(r_{sp} + r_r)}}{\sqrt{k(r_r + r_z)}} \ , \tag{E.5}$$

where r_r and r_{sp} are shown in Fig. E.1 and

$$r_z = - \frac{r_p R_c \cos\theta_i}{(2r_p - R_c\cos\theta_i)} \ . \tag{E.6}$$

Here R_c is the local radius of curvature and θ_i is the angle between the incident ray (r_{sp}) and the normal (R_c) at the reflection point P.

$$R_c = 2F/\cos^3(\theta_p/2) \tag{E.7}$$

$$\theta_i = \pm(\theta_p/2 - \theta_{sp}) \quad ; \quad \text{Real}(\theta_i) > 0. \tag{E.8}$$

To calculate the complex reflection point (r_p, θ_p), we apply the stationary phase condition

$$\frac{d}{dx_p}(r_{sp} + r_r) = 0 \ , \tag{E.9}$$

where

$$r_{sp} = [(x_p - x_s)^2 + (y_p - y_s)^2]^{1/2} \quad , \tag{E.10a}$$

$$r_r = [(x - x_p)^2 + (y - y_p)^2]^{1/2} \quad . \tag{E.10b}$$

Substituting (E.10) in (E.9), gives

$$\cos\Theta_r + \sin\Theta_r \cdot \cot(\Theta_p/2) = -[\cos\Theta_{sp} - \sin\Theta_{sp} \cdot \mathrm{Cot}(\Theta_p/2)], \tag{E.11}$$

where

$$\cos\Theta_r = \frac{x - x_p}{r_r} \quad , \quad \sin\Theta_r = \frac{y - y_p}{r_r} \quad , \tag{E.12a}$$

$$\cos\Theta_{sp} = \frac{x_p - x_s}{r_{sp}} \quad , \quad \sin\Theta_{sp} = \frac{y_p - y_s}{r_{sp}} \quad , \tag{E.12b}$$

$$\cot(\Theta_p/2) = \frac{dy_p}{dx_p} = 2F/y_p \quad . \tag{E.12c}$$

After some manipulations on (E.11), one gets

$$\sin(\Theta_r + \Theta_p/2) = -\sin(\Theta_p/2 - \Theta_{sp}) \tag{E.13}$$

or

$$\Theta_r = -(\Theta_p - \Theta_{sp}) \tag{E.14}$$

From Fig. E.1, (E.1) and the sine law,

$$\sin(\Theta_{sp} + \Theta_s)\cos(\Theta_p) = \frac{2F}{r_s}\sin(\Theta_p + \Theta_{sp}) \tag{E.15}$$

Inserting (E.14) in (E.15) and after some manipulations, one gets

$$\Theta_p = -\frac{1}{2}\{\Theta_s + \Theta_r + \sin^{-1}[\frac{4F}{r_s}\sin(\Theta_r) + \sin(\Theta_s + \Theta_r)]\} \qquad (E.16)$$

In the far field $\Theta_r \simeq \Theta$ and Θ_p is derived.

The diffracted field U^d at A is the sum of the diffracted field (U_1^d and U_2^d) of each edge

$$U^d = U_1^d\,[St(\Theta-\pi+\Theta_t) + St(\pi-\Theta_e-\Theta)] + U_2^d\,[St(\Theta+\pi-\Theta_t) + st(\pi+\Theta_e+\Theta)] \qquad (E.17)$$

where St( ) is a unit step function,

$$U_1^d = \frac{e^{-j(kr_1-\pi/4)}}{\sqrt{\pi kr_1}}\{e^{jkr_{s1}\cos(\Theta_1-\Theta_{s1})}\,F[-\sqrt{2kr}_{s1}\cos(\frac{\Theta_1-\Theta_{s1}}{2})] - e^{jkr_{s1}\cos(\Theta_1+\Theta_{s1})}\,F[-\sqrt{2kr}_{s1}\cos(\frac{\Theta_1+\Theta_{s1}}{2})]\} \qquad (E.18)$$

and U_2^d is given by (E.18) with subscript 2 replacing 1.

$$\Theta_1 \simeq (\pi-\Theta_t) + \Theta \quad ; \quad 0 < \Theta_1 < 2\pi \quad , \qquad (E.19a)$$

$$\Theta_2 \simeq (\pi-\Theta_t) - \Theta \quad ; \quad 0 < \Theta_2 < 2\pi \quad , \qquad (E.19b)$$

and

$$r_{s1} = [r_e^2 + r_s^2 + 2r_e r_s\cos(\Theta_e + \Theta_s)]^{1/2} \quad , \qquad (E.20a)$$

$$\Theta_{s1} = \Theta_t + \sin^{-1}[\frac{r_s\sin(\Theta_e + \Theta_s)}{r_{s1}}] \quad , \qquad (E.20b)$$

where r_s and Θ_s are given by (2.5) and (2.6), respectively.

Fig E.2 shows the normalized diffracted field component for a beam represented by the Complex Source Point method with its axis directed to the apex of the reflector. The incident and reflected fields are not included. In the region $\Theta>120°$, the diffracted field is the total field.

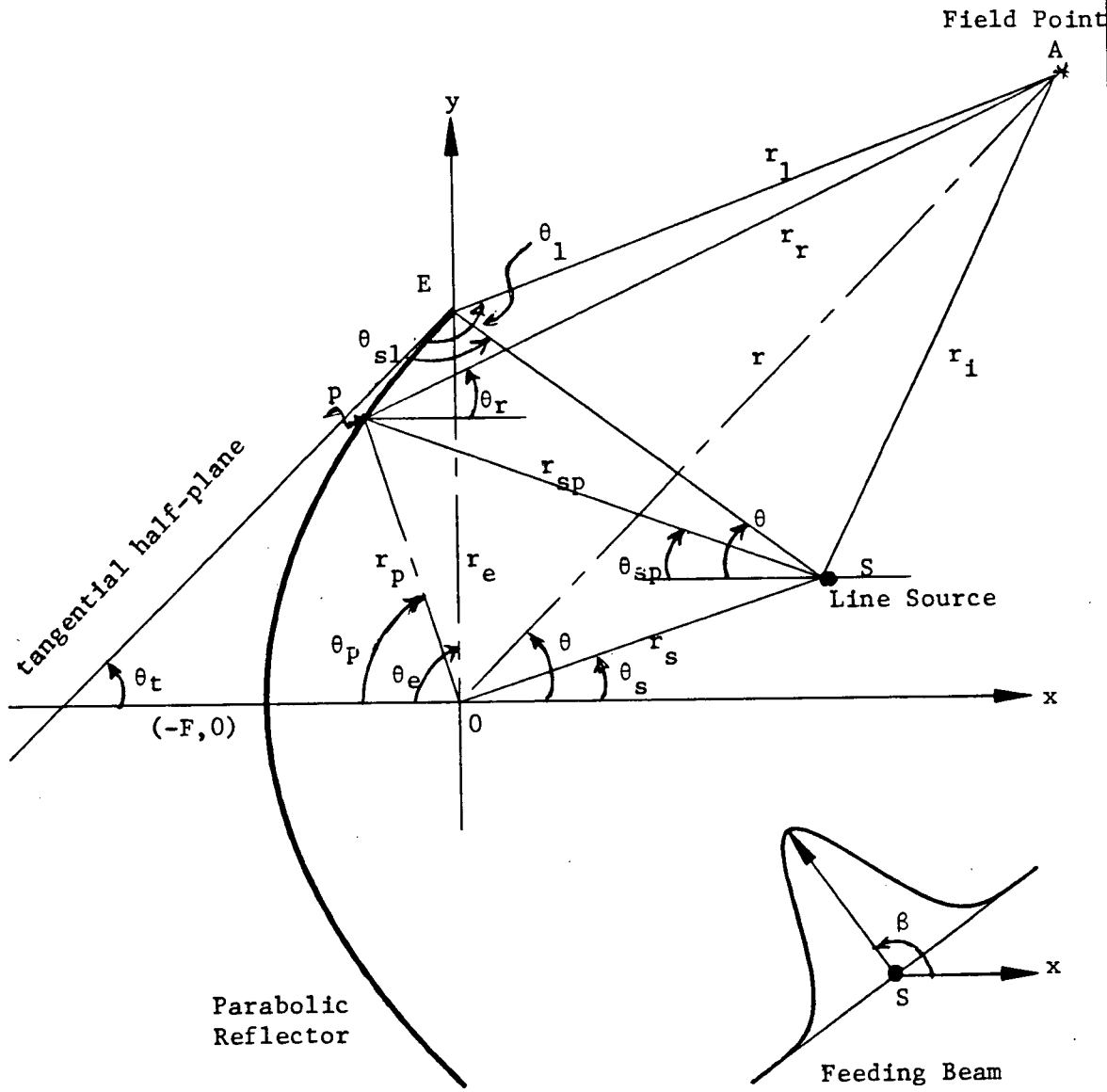

Fig. E.1 Geometry of a beam diffraction by a parabolic cylinder

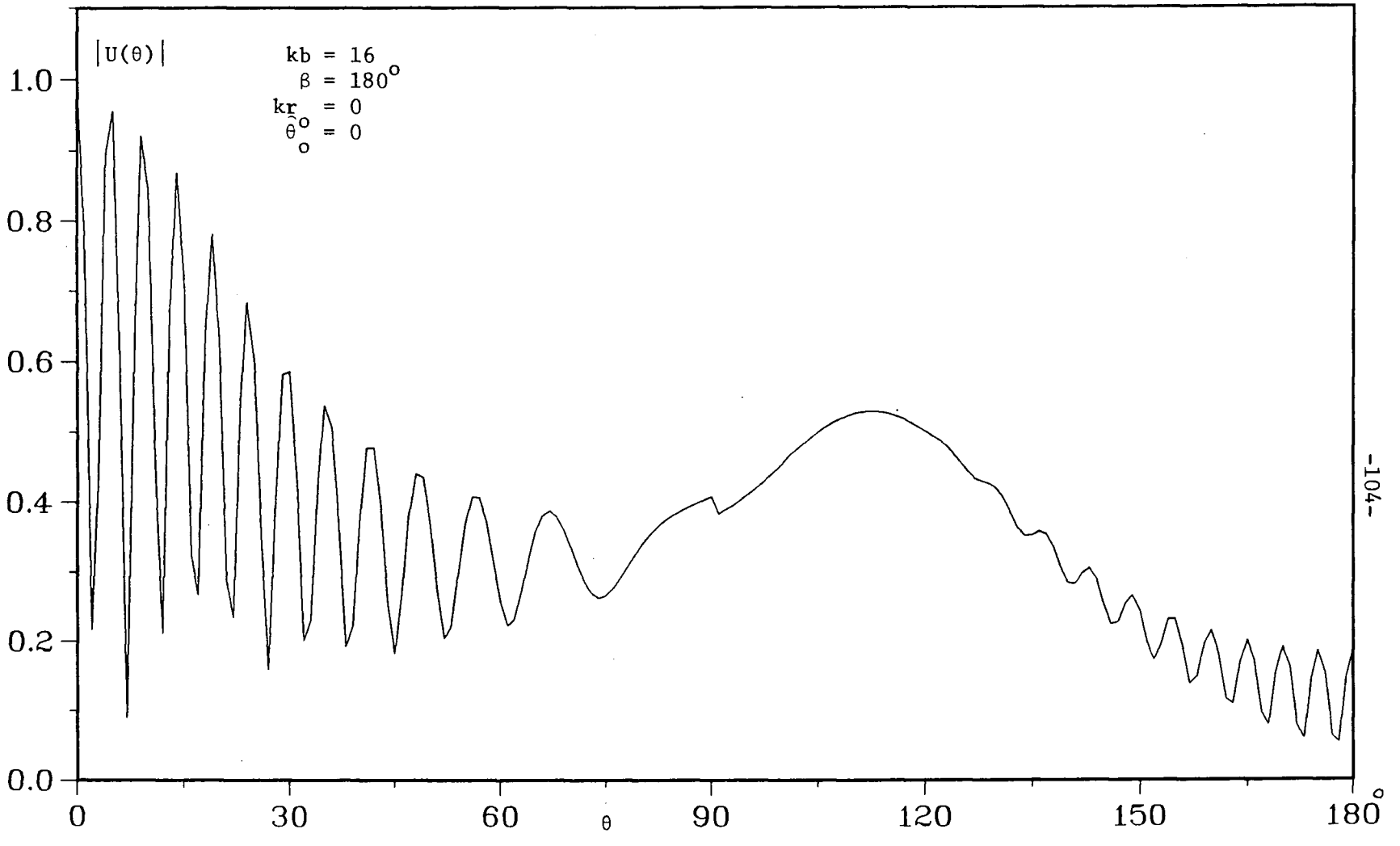

Fig. E.2 Normalized diffracted field component of a beam diffraction by a parabolic cylinder ($kF = 10\pi$, $\theta_e = 60^\circ$)

APPENDIX F

EVALUATION OF ARCTANGENT OF A COMPLEX NUMBER

To calculate the complex angle Θ in the proper quadrant; i.e. $-\pi<\text{Real}(\Theta) \leq \pi$, which a complex position vector makes with the x-axis

$$\tan\Theta = \frac{y}{x} \quad , \tag{F.1}$$

or

$$\tan(\Theta_R + j\Theta_I) = R_t + jI_t \tag{F.2}$$

where Θ_R and Θ_I are the real and imaginary parts of Θ, and R_t and I_t are the real and imaginary parts of (y/x). Also we can write

$$\cos(\Theta_R + j\Theta_I) = \frac{X}{\sqrt{x^2+y^2}} = R_c - jI_c \tag{F.3}$$

where R_c and $-I_c$ are the real and imaginary parts of $\left(\frac{x}{\sqrt{x^2+y^2}}\right)$. Expanding (F.3) and equating the real parts of both sides and the imaginary parts of both sides, gives

$$\cos\Theta_R \cdot \cosh\Theta_I = R_c \tag{F.4}$$

and

$$\sin\Theta_R \cdot \sinh\Theta_I = I_c \tag{F.5}$$

Also by expanding the left side of (F.2), one gets

$$\frac{\tan\Theta_R + j\tanh\Theta_I}{1 - j\tan\Theta_R \cdot \tanh\Theta_I} = R_t + jI_t \tag{F.6}$$

After some manipulations on (F.6) we can write

$$\tanh\Theta_I \cdot \frac{\sec^2\Theta_R}{(1 + \tan^2\Theta_R \cdot \tanh^2\Theta_I)} = I_t \qquad (F.7)$$

and

$$\tan\Theta_R \cdot \frac{\operatorname{sech}^2\Theta_I}{(1 + \tan^2\Theta_R \cdot \tanh^2\Theta_I)} = R_t \qquad (F.8)$$

From (F.7) we can say

$$\Theta_I \lessgtr 0 \quad \text{if} \quad I_t \lessgtr 0 \qquad (F.9)$$

Now let Θ_s be given as

$$\Theta_s = \cos^{-1}(R_c - j|I_c|) \qquad (F.10)$$

the arccosine of a complex number of form (F.10) is available in the UBC Computer Library. Using (F.4), (F.5) and (F.9) we get

$$\Theta = \mp \Theta_s \quad ; \quad I_t \lessgtr 0 \quad , \quad I_c > 0 \qquad (F.11)$$

and

$$\Theta = \pm \Theta_s^* \quad ; \quad I_t \lessgtr 0 \quad , \quad I_c < 0 \qquad (F.12)$$

where Θ_s^* is the complex conjugate of Θ_s.

APPENDIX G

LIST OF COMPUTER PROGRAMS FOR CSP ANALYSIS

All the programs used in the Complex Source Point analysis and listed below are written in the language of FORTRAN.

G.1 Comparison of CSP, Gaussian and Typical Antenna Beams

This program makes use of expressions (2.10), (2.16) and (2.18) with ka=4, kb=3 and HPBW=55.7^{o} to compare the normalized far fields of CSP, Gaussian, and typical antenna beams. Also it uses (2.20) with different weighting factors (Q_1, Q_2, Q_3) and beam parameters (b_1, b_2, b_3 and β_{o1}, β_{o2}, β_{o3}) to calculate far fields of different beams.

```
C*************************************************************************
C PROGRAM CALCULATES AND COMPARES THE FIELDS OF THE CSP, GAUSSIAN AND
C TYPICAL ANTENNA BEAMS. THIS PROGRAM IS CALLED "CSP.FTNC".
C =======================================================================
C     The Time Harmonic Factor " exp(-iwt) " is suppressed .
C     The Common Factor " exp(ikr)/Sqrt(kr) " is supperessed.
C =======================================================================
      KK = 181
      KM = (KK+1)/2
      H  = 1.0
C     ===============
      PI  = 3.1415926
      DTR = PI/180.0
      C   = CMPLX(0.0,1.0)
C     -------------------
      A   = 4.0
      B   = 3.0
      IF ( B .LT. 0.25*ALOG(2.0) )                                    STOP
C =======================================================================
C      HPBW IS THE HALH-POWER BEAM WIDTH
C =======================================================================
      HPBW= 2.0*ACOS( 1.0 - 0.5*ALOG(2.0)/B )
C     ---------------------------------------
      DO 111 K=1,KK
      Y   = H*(K-KM)
      FI  = Y*DTR
C     ---------------------------------
      CSP = ABS( EXP(B*(COS(FI)-1.0)) )
      GB  = EXP( -ALOG(4.0)*(FI/HPBW)**2 )
C     -----------------------------------
      U   = A*SIN(FI)
      IF ( ABS(U) .EQ. PI/2.0 )  GO TO 11
      CD  = COS(U)/( 1.0 - (2.*U/PI)**2 )
      GO TO 22
11    CD  = PI/4.0
C     --------------------------
22    WRITE(6,1)  Y , CD ,CSP ,GB
C     ==========================
111   CONTINUE
C     ============================
1     FORMAT( F6.1 ,3(1X, E14.7) )
      STOP
      END
C*************************************************************************
C*************************************************************************
```

```
C*********************************************************************
C PROGRAM FOR DEVELOPING A BEAM FROM SINGLE OR MULTIPLE LINE SOURCE(S)
C LOCATED AT COMPLEX POINT(S). THIS PROGRAM CALLED "CSP.FTNM".
C ------------------------------------------------------------------
C         THE TIME HARMONIC FACTOR "exp(-iwt)" IS SUPPRESSED.
C         THE COMMON FACTOR "exp(ikr)/Sqrt(kr)" IS SUPPRESSED.
C==================================================================
      COMPLEX*8   C ,U1 ,U2 ,U3 ,CASIN ,CACOS ,CATAN ,ARKTAN
      REAL   *4   Y(361) ,AUT(361)      ,AU1(361) ,AU2(361) ,AU3(361)
C     ------------------------------------------------------------
      KK  = 361
      H   = 1.0
      C   = CMPLX(0.0,1.0)
      PI  = 3.1415926
      DTR = PI/180.0
C     ==============
      Q2  = 1.0
      B2  = 4.0
      BET2= PI
      R02 = 0.0
      TH02= PI/2.0
C     ============
      Q1  =-1.0
      B1  = B2
      R01 = 1.0
      DLTA= PI/4.0
      GAMA= PI/2.0
C     ------------
      Q3  = Q1
      B3  = B1
      R03 = R01
C     -----------------
      TH01= TH02 - GAMA
      TH03= TH02 + GAMA
C     -----------------
      BTA1= BTA2 - DLTA
      BTA3= BTA2 + DLTA
C     -----------------
      BIG = 0.0
C
      DO 111 K=1,KK
      Y(K)= H*(K-1)
      TH  = Y(K)*DTR
C     ------------------------------------------------
      U1 = CEXP( B1*COS(TH-BTA1) - C*R01*COS(TH-TH01) )
      U2 = CEXP( B2*COS(TH-BTA2) - C*R02*COS(TH-TH02) )
      U3 = CEXP( B3*COS(TH-BTA3) - C*R03*COS(TH-TH03) )
C     ------------------------------------------------
      AUT(K)= CABS( Q1*U1 + Q2*U2 + Q3*U3 )
      IF( AUT(K) .GT. BIG )                BIG = AUT(K)
C     ------------------------------------------------
CC    AU1(K)= CABS( Q1*U1 )
CC    AU2(K)= CABS( Q2*U2 )
CC    AU3(K)= CABS( Q3*U3 )
C     --------------------
111   CONTINUE
C     ============
      DO 222 K=1,KK
```

```
      AUTN= AUT(K)/BIG
      WRITE(6,1) Y(K) , AUTN
CC    AUN1= AU1(K)/BIG
CC    AUN2= AU2(K)/BIG
CC    AUN3= AU3(K)/BIG
CC    WRITE(6,2) Y(K) ,AUN1 ,AUN2 ,AUN3 ,AUN
222   CONTINUE
C     -------------------------
1     FORMAT( F6.1 , 1X, E14.7 )
C2    FORMAT( F6.1 ,4(1X, E14.7) )
      STOP
      END
C*******************************************************************************
C*******************************************************************************
```

G.2 Beam Diffraction by a Half-Plane

This program uses expressions (3.3) and (C.5) to compare the total (asymptotic and uniform) far fields of beam diffraction by a half-plane with $kr_o = 16$, $\theta_o = 90^o$ and different values of the beam parameters kb and $\beta = \pi + \theta_o - \delta$.

```
C*********************************************************************
C  Program for calculating Antenna Beam Diffraction by a Half Screen.
C  The Complex Source Point Solution compared with Asymptotic solution
C  by Green et al.(1979). Program called "HP.FTN1".
C=====================================================================
C  The Time Harmonic Factor " exp(-iwt) " is suppressed .
C  The Common Factor " exp(i.kr)/Sqrt(kr) " is suppressed .
C=====================================================================
      COMMON      C , PI
C     ---------------------------------------------------
      COMPLEX*8   WI ,WR ,UI ,UR ,UTG ,UDF          ,CACOS ,CFR
      COMPLEX*8   C ,RS ,THS ,DL1 ,DL2 ,SC1 ,SC2 ,QST
      REAL*4      Y(181) ,AUF(181) ,AUG(181)
C     ---------------------------------------------------
      KK = 181
      KM = (KK+1)/2
      H  = 1.0
C     --------------------
      C   = CMPLX(0. ,1. )
      PI  = 3.1415926
      DTR = PI/180.
C     --------------
      R0  = 16.
      TH0 = PI/2.
C
      DO 999 J=1,3
      B   = 2**(J+1)
CC    IF( J .LE. 1 )      B = 0.0
CC    IF( J .GE. 6 )      B = 12.0
C
CC    DO 999 J=1,3
CC    BETA= TH0 + PI - J*PI/12.
      BETA= TH0 + PI -PI/6.
C     ---------------------------------------------------
      IF( BETA .EQ. (TH0+PI) )                      GO TO 11
C
      RS  = CSQRT( R0**2 + 2.0*R0*C*B*COS(BETA-TH0) - B**2 )
      IF( REAL(RS) .LE. 0.0 )                        RS = -RS
      THS = CACOS( (R0*COS(TH0) + C*B*COS(BETA)) /RS )
C     ------------------------------------------------
CC    U   = REAL(THS)
CC    V   = AIMAG(THS)
CC    RSA = CABS(RS)
CC    RSR = REAL(RS)
CC    RSI = AIMAG(RS)
CC    THSI= PI + ( U + ATAN( SINH(V)*RSR/(RSA + RSI*COSH(V)) ) )
C =====================================================================
C "THSI" and "THSR" are the shadow boundary angles for incident and
C  reflected fields respectively (measured from the half-screen) .
C =====================================================================
      THSI= PI + TH0 + ACOS( REAL(RS)/R0 )
      IF( BETA .GT. (TH0+PI) )  THSI = 2.*(PI+TH0) - THSI
      GO TO 22
C
11    RS  = R0 - C*B
      THS = TH0
```

```
      THSI= PI + TH0
22    THSR= 2.0*PI - THSI
C ===================================================================
C "TH" the observation angle measured from the half-screen ( X-axis ).
C "FI" is the observation angle measured from beam axis in anticlock .
C ===================================================================
      QST = CEXP( C*(RS - 0.75*PI) ) / CSQRT(8.0*PI*RS)
C     ------------------------------------------------
      AMX = 0.0
      DO 111  K=1,KK
C
      Y(K)= H*(K-KM)
      FI  = Y(K)*DTR
      TH  = 1.5*PI + FI
C ===================================================================
C The far field distance "R" is not used in calculating the pattern.
C "UI" and "UR" are the incident and reflecteds field, respectively .
C ===================================================================
      UI  = CEXP( -C*R0*COS(TH-TH0) + B*COS(TH-BETA) )
      UR  =-CEXP( -C*R0*COS(TH+TH0) + B*COS(TH+BETA) )
C     ------------------------------------------------
      WI  = -CSQRT(2.0*RS) * CCOS((TH-THS)/2.0)
      WR  = -CSQRT(2.0*RS) * CCOS((TH+THS)/2.0)
C
      UTG = ( UI*CFR(WI) + UR*CFR(WR) ) * CEXP(-C*PI/4.)/SQRT(PI)
      AUG(K)= CABS(UTG)
C     ------------------------------------------------------------------
      IF( (AIMAG(THS).EQ. 0.).AND.(REAL(TH-THS) .EQ. PI) )   GO TO 33
      IF( (AIMAG(THS).EQ. 0.).AND.(REAL(TH+THS) .EQ. PI) )   GO TO 33
C
      SC1 = 1.0/CCOS(.5*(TH-THS))
      SC2 = 1.0/CCOS(.5*(TH+THS))
      DL1 = C*SC1**2/(4.*RS)
      DL2 = C*SC2**2/(4.*RS)
      UDF = QST * ( SC1*(1.- DL1) - SC2*(1.- DL2) )
C     ------------------------------------------------------
      IF( TH .LE. THSI )   UDF = UDF + UI
      IF( TH .LE. THSR )   UDF = UDF + UR
      AUF(K)= CABS(UDF)
C
CC     IF((AUG(K).GT.AMX).OR.(AUF(K).GT.AMX)) AMX=AMAX1(AUG(K),AUF(K))
      IF( AUG(K) .GT. AMX )                                  AMX= AUG(K)
      GO TO 111
C     ----------------
33    AUF(K)= 100.0*AMX
C     ================
111   CONTINUE
C     ==============
      DO 222  K=1,KK
      UGN = AUG(K)/AMX
      UFN = AUF(K)/AMX
      IF( UFN .GT. 1.1 )   UFN = 1.1
      WRITE(6,1) Y(K) , UGN , UFN
222   CONTINUE
C     ========
999   CONTINUE
C     ============================
1     FORMAT( F6.1 ,2(1X ,E14.7) )
      STOP
      END
```

```
C ===================================================================
C  PROGRAM FOR CALCULATING FRESNEL INTEGRAL "CFR" OF COMPLEX ARGUMENT.
C ===================================================================
      COMPLEX FUNCTION   CFR(X)
C     ------------------------
      COMMON       C , PI
      COMPLEX*8    C , X
      COMPLEX*16   Z , ERFZ
      Z     = X*CEXP(-C*PI/4.0)
      CALL CERF(Z,ERFZ)
      CFR   = 0.5*SQRT(PI)*CEXP(C*PI/4.0)*(1.0-ERFZ)
      RETURN
      END
C*******************************************************************************
C*******************************************************************************
```

G.3 Beam Diffraction by a Wide Slit

Using expressions (4.5), (4.10) and (4.15), the total diffracted far field including interaction between the edges is calculated for $kr_o = ka = 8$, $\theta_o = 90^o$, $\beta = 270^o$ and different values of the beam parameter, kb.

```
C*********************************************************************
C PROGRAM FOR CALCULATING ANTENNA BEAM (SINGLE & MULTIPLE) DIFFRACTION
C BY A SLIT USING HALF-PLANE SOLUTION.THE PROGRAM IS CALLED "SLIT.FTN"
C           " NON-SYMETRICAL INCIDENCE "
C ------------------------------------------------------------------
C TIME DEPENDCE exp(-iwt) & COMMON FACTOR exp(i(kr-PI/4))/Sqrt(PI*kr).
C ==================================================================
      COMMON       C ,PI
      COMPLEX*8    WI1 ,WI2 ,WR1 ,WR2          ,CFR  ,FR ,CACOS ,CASIN
      COMPLEX*8    D0 ,DI1 ,DI2 ,DF1 ,DF2        ,UI ,UDD ,UDM ,US
      COMPLEX*8    UE1 ,UE2 ,U1 ,U2 ,UI0 ,UI1 ,UI2 ,UR1 ,UR2
      COMPLEX*8    C ,F0 ,RS ,RS1 ,RS2 ,THS ,THS1 ,THS2 ,CMPLX
      REAL         Y(181) , AUS(181) , AUT(181)
C      ---------------------------------------------------------------
       KK = 181
       KM = (KK+1)/2
       H  = 1.
C      --------------------
      C   = CMPLX(0.0,1.0)
      PI  = 3.1415926
      DTR = PI/180.
      F0  = SQRT(PI)*CEXP(C*PI/4.0)
C
      A   = 8.
      R0  = 8.
      TH0 = PI/2.
      B   =         ??
      BETA1= TH01 + PI
      BETA2= 3*PI - BETA1
C
      RS  = CSQRT( R0**2 + 2.*R0*C*B*COS(BETA1-TH0) - B**2 )
      IF( REAL(RS) .LE. 0.0 )  RS = -RS
      THS = CACOS( (R0*COS(TH0) + C*B*COS(BETA1)) /RS )
C
      R01 =  SQRT( R0**2 + A**2 - 2.*R0*A* COS(TH0) )
      R02 =  SQRT( R0**2 + A**2 + 2.*R0*A* COS(TH0) )
      TH01= PI - ASIN(R0*SIN(TH0)/R01)
      TH02= PI - ASIN(R0*SIN(TH0)/R02)
C
      RS1 = CSQRT( RS**2 + A**2 - 2.*RS*A*CCOS(THS) )
      IF( REAL(RS1) .LE. 0.0 )     RS1 = -RS1
      RS2 = CSQRT( RS**2 + A**2 + 2.*RS*A*CCOS(THS) )
      IF( REAL(RS2) .LE. 0.0 )     RS2 = -RS2
C
      THS1= PI - CASIN(RS*CSIN(THS)/RS1)
      THS2= PI - CASIN(RS*CSIN(THS)/RS2)
C
CC     THSI1= PI + TH01 + ACOS(REAL(RS1)/R01)
CC     THSI2= PI + TH02 + ACOS(REAL(RS2)/R02)
CC     IF( BETA1 .GT. TH01+PI )      THSI1 = 2.*(PI+TH01) - THSI1
CC     IF( BETA2 .GT. TH02+PI )      THSI2 = 2.*(PI+TH02) - THSI2
CC     THSR1 = 2.*PI - THSI1
CC     THSR2 = 2.*PI - THSI2
C
      UE1 = CEXP(C*RS1) /CSQRT(RS1)
      UE2 = CEXP(C*RS2) /CSQRT(RS2)
C
```

```
      IF( REAL( CSQRT(2.*RS1) *CSIN(THS1/2.) ) .LT. 0. )          STOP
      IF( REAL( CSQRT(2.*RS1) *CSIN(THS1/2.) ) .LT. 0. )          STOP
C
      D0  = -SQRT(4./PI) * CEXP(-C*(2.*A+PI/4.) ) * FR( SQRT(4.*A) )
C
      DI1 = -CSQRT(2.*RS1/(PI*A))* CFR( CSQRT(2.*RS1)*CSIN(THS1/2.) )
      DI1 = DI1 * CEXP( C*(2.*A + RS1*CCOS(THS1) - RS1 - PI/4.) )
C
      DI2 = -CSQRT(2.*RS2/(PI*A))* CFR( CSQRT(2.*RS2)*CSIN(THS2/2.) )
      DI2 = DI2 * CEXP( C*(2.*A + RS2*CCOS(THS2) - RS2 - PI/4.) )
C ---------------------------------------------------------------------
C ALL ANGLES ARE IN RADIANS EXCEPT Y(K) IN DEGREES.
C ---------------------------------------------------------------------
      BIG = 0.0
      DO 111 K=1,KK
      Y(K)= H*(K-KM)
      FI  = Y(K)*DTR
      TH1 = 1.5*PI + FI
C
      TH2 = 3*PI - TH1
      IF( TH1 .LT. PI )          TH2 = PI - TH1
C ---------------------------------------------------------------------
C THE DISTANCES R1,R2 ARE NOT USED IN CALCULATING THE PATTERN.
C       R1 = R-A*COS(TH1)
C       R2 = R+A*COS(TH1)
C       RS*COS(TH1-THS) = R0*COS(TH1-TH0) + C*B*COS(TH1-BETA)
C THE UI,S AND UR,S ARE EXPONENTIAL FUNCTIONS.
C FOR SYMMETRICAL NORMAL INCIDENCE " UI0 = UI1 = UI2  &  UR1 = UR2 "
C ---------------------------------------------------------------------
      UI0 = CEXP( -C*R0 *COS(TH1-TH0 ) + B*COS(TH1-BETA1) )
      UI1 = CEXP( -C*R01*COS(TH1-TH01) + B*COS(TH1-BETA1) )
      UR1 = CEXP( -C*R01*COS(TH1+TH01) + B*COS(TH1+BETA1) )
      UI2 = CEXP( -C*R02*COS(TH2-TH02) + B*COS(TH2-BETA2) )
      UR2 = CEXP( -C*R02*COS(TH2+TH02) + B*COS(TH2+BETA2) )
C
      WI1 = -CSQRT(2.0*RS1) * CCOS((TH1-THS1)/2.0)
      WR1 = -CSQRT(2.0*RS1) * CCOS((TH1+THS1)/2.0)
      WI2 = -CSQRT(2.0*RS2) * CCOS((TH2-THS2)/2.0)
      WR2 = -CSQRT(2.0*RS2) * CCOS((TH2+THS2)/2.0)
C
C THE CFR(W) IS A SUBROUTINE CALCULATES FRESNEL INTEGRALS WITH COMPLEX
C ARGUMENTS.
      UI = UI0*F0
      U1 = ( UI1*CFR(WI1) - UR1*CFR(WR1) ) * CEXP(-C*A*COS(TH1))
      U2 = ( UI2*CFR(WI2) - UR2*CFR(WR2) ) * CEXP(-C*A*COS(TH2))
C---------------------------------------------------------------------
C UI ,UD AND US ARE THE INCIDENT, DIFFRACTED AND TOTAL SINGLE DIFFRAC-
C TION FAR FIELD PATTERNS, RESPECTIVELY.
C---------------------------------------------------------------------
      US = U1 + U2 - UI
      AUS(K)= CABS(US)
C
      DF1 = -SQRT(8.*A/PI) *CEXP( C*(A*COS(TH1)-2.*A-PI/4.))
      DF1 = DF1 * FR( SQRT(4.*A)*SIN(TH1/2.) )
C
      DF2 = -SQRT(8.*A/PI) *CEXP( C*(A*COS(TH2)-2.*A-PI/4.))
      DF2 = DF2 * FR( SQRT(4.*A)*SIN(TH2/2.) )
C
CC     UDD =  UE1*DI1*DF2 + UE2*DI2*DF1
      UDM =( UE1*DI1*(D0*DF1+DF2) + UE2*DI2*(D0*DF2+DF1) )/(1.-D0**2)
```

```
      AUT(K)= CABS(US+UDM)
C      ------------------------------------------------------------------
      IF((AUT(K).GE.BIG).OR.(AUS(K).GE.BIG)) BIG=AMAX1(AUT(K),AUS(K))
C      ------------------------------------------------------------------
111   CONTINUE
C      -------------
      DO 222 K=1,KK
      USN= AUS(K)/BIG
      UTN= AUT(K)/BIG
      WRITE(6,1) Y(K) , USN , UTN
222   CONTINUE
C      ----------------------------
1     FORMAT( F6.1 ,2(1X ,E14.7) )
      STOP
      END
C ======================================================================
C PROGRAM FOR CALCULATING FRESNEL INTEGRAL "CFR" OF COMPLEX ARGUMENTS.
C ----------------------------------------------------------------------
      COMPLEX  FUNCTION  CFR(X)
C      ========================
      COMMON       C , PI
      COMPLEX*8    C , X
      COMPLEX*16   Z , ERFZ
C ----------------------------------------------------------------------
C THE CERF(W,ERF) IS A SUBROUTINE CALCULATES ERROR FUNCTIONS WITH
C COMPLEX ARGUMENTS.
C ----------------------------------------------------------------------
      Z    = X*CEXP(-C*PI/4.0)
      CALL CERF(Z,ERFZ)
      CFR = 0.5 * SQRT(PI) * CEXP(C*PI/4.0) * (1.0-ERFZ)
      RETURN
      END
C ======================================================================
C PROGRAM FOR CALCULATING FRESNEL INTEGRAL "FR" OF REAL ARGUMENTS.
C ----------------------------------------------------------------------
      COMPLEX  FUNCTION   FR(X)
C      ========================
      COMMON       C , PI
      COMPLEX*8    C
      COMPLEX*16   Z , ERFZ
C ----------------------------
      Z    = X*CEXP(-C*PI/4.0)
      CALL CERF(Z,ERFZ)
      FR  = 0.5 * SQRT(PI) * CEXP(C*PI/4.0) * (1.0-ERFZ)
      RETURN
      END
C **********************************************************************
C**********************************************************************
```

G.4 Beam Diffraction by a Strip

This program calculates the total far field of a normally incident beam diffraction by a conducting strip, neglecting the interaction between the edges, using expression (4.18) with $kr_o = ka = 8$, $\theta_o = 90^o$ and different values of beam parameters kb and $\beta = \pi + \theta_o - \delta$.

```
C*********************************************************************
C PROGRAM FOR CALCULATING ANTENNA BEAM SINGLY DIFFRACTED BY A STRIP
C USING HALF-PLANE SOLUTION. THE PROGRAM IS CALLED " STRP.FTN ".
C =====================================================================
C           TIME DEPENDCE  " exp(-iwt) " .
C           COMMON FACTOR  " exp(ikr)/Sqrt(kr) " .
C THE ANGLES (THS,THS1,THS2,TH1,TH2,FI,BETA) ALL ARE IN RADIANS.
C =====================================================================
      COMMON      C , PI
      COMPLEX*8   C ,F0 ,WI1 ,WR1 ,WI2 ,WR2        ,CASIN ,CACOS ,CFR
      COMPLEX*8   U1 ,U2 ,UI ,UR ,UD ,UT
      COMPLEX*8   RS ,RS1 ,RS2   ,THS ,THS1 ,THS2
C     ---------------------------------------------------------------
      REAL*4      Y(361) ,AUT(361) ,AUD(361) ,AUI(361) ,AUR(361)
C     ---------------------------------------------------------------
      Y0  = 00.0
      H   = 1.0
      KK  = 361
C     --------------------
      C   = CMPLX(0.0,1.0)
      PI  = 3.1415926
      DTR = PI/180.0
      F0  = CEXP(-C*PI/4.0)/SQRT(PI)
C     ------------------------------
      R0  = 8.0
      A   = 8.0
      TH0 = PI/2.0
C
      B   = 8.0
CC     DO 999 I=1,6
CC     B   = 2.0**(I-2)
CC     IF( (I .LE. 1).OR.(I .GE. 6) )   B = 2.4*(I-1)
C     ------------------------------------------
      DO 999 J=1,5
      BETA= TH0 + PI - PI*(J-1)/12.
      IF( J .GE. 5 )   GO TO 11
C
       GO TO 22
11    A   = 10.*A
      BETA= TH0+PI-PI/4.
C
CC     BET1= 3.0*PI - BETA
CC     IF( BETA .LT. PI )          BET1 = PI - BETA
CC     BET2= BETA
C     ------------------------------------------
CC     R01 = SQRT( R0**2 + A**2 - 2.0*R0*A*COS(TH0) )
CC     R02 = SQRT( R0**2 + A**2 + 2.0*R0*A*COS(TH0) )
CC     TH01= ASIN( R0*SIN(TH0) /R01 )
CC     TH02= ASIN( R0*SIN(TH0) /R02 )
C     ------------------------------------------------
22    RS  = CSQRT( R0**2 - B**2 + 2.0*C*B*R0*COS(BETA-TH0) )
      IF( REAL(RS) .LE. 0.0 )    RS  = -RS
      THS = CACOS( (R0*COS(TH0) + C*B*COS(BETA)) /RS )
C     ------------------------------------------------
      RS1 = CSQRT( RS**2 + A**2 - 2.0*RS*A*CCOS(THS) )
      RS2 = CSQRT( RS**2 + A**2 + 2.0*RS*A*CCOS(THS) )
      IF( REAL(RS1) .LE. 0.0 )            RS1 = -RS1
```

```
      IF( REAL(RS2) .LE. 0.0 )            RS2 = -RS2
      THS1= CASIN( RS*CSIN(THS) /RS1 )
      THS2= CASIN( RS*CSIN(THS) /RS2 )
C     ------------------------------------
CC     TH11= PI + TH01 + ARCOS(REAL(RS1)/R01)
CC     IF( BET1 .GT. (TH01+PI) )  TH11= 2.0*(PI+TH01) - TH11
CC     THR1= 2.0*PI - TH11
C     ------------------------------------
CC     TH12= PI + TH02 + ARCOS(REAL(RS2)/R02)
CC     IF( BET2 .GT. (TH02+PI) )  TH12= 2.0*(PI+TH02) - TH12
CC     THR2= 2.0*PI - TH12
C     ==================
      BIGT = 0.0
      DO 111  K=1 , KK
      Y(K) = H*(K-1)
      TH   = Y(K)*DTR
C      ---------------
      TH2  = TH
      TH1  = PI - TH
      IF( TH1 .LT. 0. )  TH1 = TH1 + 2*PI
C ===================================================================
C THE DISTANCE "R" IS NOT USED IN CALCULATING THE PATTERN.
C      R1 = R+A*COS(TH)
C      R2 = R-A*COS(TH)
C      Ri = R-RS*CCOS(TH-THS)
C      Rr = R-RS*CCOS(TH+THS)
C ===================================================================
      WI1 = -CSQRT(2.0*RS1)*CCOS( (TH1-THS1)/2.0 )
      WR1 = -CSQRT(2.0*RS1)*CCOS( (TH1+THS1)/2.0 )
      WI2 = -CSQRT(2.0*RS2)*CCOS( (TH2-THS2)/2.0 )
      WR2 = -CSQRT(2.0*RS2)*CCOS( (TH2+THS2)/2.0 )
C -----------------------------------------------
CC     ARI1= ABS( ATAN( AIMAG(WI1)/REAL(WI1) ) )
CC     IF( ARI1 .GT. PI/4.0 )                STOP
CC     ARR1= ABS( ATAN( AIMAG(WR1)/REAL(WR1) ) )
CC     IF( ARR1 .GT. PI/4.0 )                STOP
CC     ARI2= ABS( ATAN( AIMAG(WI2)/REAL(WI2) ) )
CC     IF( ARI2 .GT. PI/4.0 )                STOP
CC     ARR2= ABS( ATAN( AIMAG(WR2)/REAL(WR2) ) )
CC     IF( ARR2 .GT. PI/4.0 )                STOP
C ===================================================================
C "UT" IS THE TOTAL SINGLE DIFFRACTION PATTERN BY STRIP.
C "U1,E2" ARE THE TOTAL DIFF. PATTERN BY HALF PLANES FORMING THE STRIP
C "UI & ER" ARE INCIDENT AND REFLECTED FIELD PATTERN RESPECTIVELY.
C ===================================================================
      UI   =+CEXP( -C*RS*CCOS(TH-THS) )
      UR   =-CEXP( -C*RS*CCOS(TH+THS) )
      U1   = UI*CFR(WI1) + UR*CFR(WR1)
      U2   = UI*CFR(WI2) + UR*CFR(WR2)
C     ------------------------------
      UT   = F0*(U1+U2)
      IF( TH .LT. PI )    UT = UT - (UI+UR)
C     ------------------------------------
CC     UD   = UT - UI
CC     IF( (TH1 .LT. THR1).AND.(TH2 .LT. THR2) )    UD = UT - (UI+UR)
CC     IF( (TH1 .GT. THI1).AND.(TH2 .GT. THI2) )    UD = UT
C     ------------------------------------------------
      AUT(K)= CABS(UT)
CC     AUD(K)= CABS(UD)
CC     AUI(K)= CABS(UI)
```

```
CC      AUR(K)= CABS(UR)
        IF( AUT(K) .GT. BIGT )   BIGT = AUT(K)
C       ======================================
111     CONTINUE
C        ==============
        DO 222  K=1,KK
        UTN = AUT(K)/BIGT
        WRITE(6,1)  Y(K) , UTN
222     CONTINUE
C       ========================
999     CONTINUE
C       ========================
1       FORMAT( F6.1 ,1X, E14.7 )
        STOP
        END
C ===================================================================
C PROGRAM FOR CALCULATING FRESNEL INTEGRAL "CFR" OF COMPLEX ARGUMENTS.
C -------------------------------------------------------------------
        COMPLEX FUNCTION   CFR(X)
C       ========================
        COMMON       C , PI
        COMPLEX*8    C , X
        COMPLEX*16   Z , ERFZ
        Z     = X*CEXP(-C*PI/4.0)
        CALL CERF(Z,ERFZ)
        CFR  = 0.5*SQRT(PI)*CEXP(C*PI/4.0)*(1.0-ERFZ)
        RETURN
        END
C ********************************************************************
C********************************************************************
```

G.5 Beam Diffraction by a Wedge

The total diffracted field given by (5.15) or (5.17) is calculated using this program with $kr_o = 16$, $\beta = \theta_o + \pi$ for different angles of incidence, θ_o and wedge angles, α_w.

```
C*********************************************************************
C PROGRAM FOR CALCULATING BEAM DIFFRACTION BY A CONDUCTING WEDGE USING
C THE UNIFORM THEORY OF DIFFRACTION (KOUYOUMJIAN & PATHAK 1974). THE
C EDGE LIES ON THE BEAM AXIS. THIS PROGRAM CALLED " WEDG.FTN ".
C =====================================================================
C     The time harmonic factor " Exp(+jwt) " is suppressed .
C     Common factor is " Exp(-j.kr)/Sqrt(kr) " .
C =====================================================================
      COMPLEX*8   C ,RS ,WI1 ,WI2 ,WR1 ,WR2    ,GR ,CFR ,CASIN ,CACOS
      COMPLEX*8   U0 ,UE ,UI ,UR1 ,UR2 ,UD1 ,UD2 ,UD ,UT
      REAL        Y(361) ,AUT(361) ,N
C     ---------------------------------------------------------------
      KK  = 361
      H   = 1.0
      N   = 1.50
      ERR = 0.01
C     --------------------
      C   = CMPLX(0.0,1.0)
      PI  = 3.1415926
      DTR = PI/180.0
      THSY= N*PI/2.0
      THCR= (N-1.0)*PI
C     ----------------
      R0  = 16.0
      TH0 =          ?
      BETA= TH0 + PI
C =====================================================================
C     ALW is the wedge interior angle.
CC    ALW = (2.0 - N)*PI
C =====================================================================
      IF( (TH0  .LT. 0.).OR.(TH0  .GT. THSY   ) )   STOP
CC    IF( (BETA .LE. PI).OR.(BETA .GT. 2.0*PI ) )   STOP
C     ---------------------------------------------------
      DO 999 J = 1,4  ?
      B   =  2.0*(J-1) ?
C     ================
      RS  = R0 + C*B
      THS = TH0
C =====================================================================
C "THSI" and "THSR" are the shadow boundary angles for incident and
C  reflected fields respectively (measured from wedge upper surface).
C =====================================================================
      THSI = PI + TH0
      THSR1= PI - TH0
      THSR2= (2.0*N - 1.0)*PI - TH0
C     ----------------------------
      UE = CEXP(-C*RS)/CSQRT(RS)
      U0 = -CEXP(-C*PI/4.0) / ( N * SQRT(8.0*PI) )
C ---------------------------------------------------------------------
C "TH" the observation angle measured from the half-screen ( X-axis ).
C ---------------------------------------------------------------------
      DO 111  K=1,KK
C
      Y(K)= H*(K-1)
      TH  = Y(K)*DTR
C =====================================================================
C  The distance "R" is not used in calculating the pattern.
```

```
C  " UI, UR1, UR2 " are the incident and reflected fields from upper
C  and lower Wedge surfaces, respectively.
C ================================================================
      THI = TH - THS
      THR = TH + THS
      UI  = CEXP( C*RS*COS(THI) )
      UR1 =-CEXP( C*RS*COS(THR) )
      UR2 =-CEXP( C*RS*COS(2.0*N*PI-THR) )
C     ----------------------------------
      IF( TH .GT. N*PI )       GO TO 88
C     ---------------------------------
      MR1 = 0.0
      MI1 = 0.0
      MR2 = 0.0
      MI2 = 0.0
      IF( (THI .GT. -THSY).AND.(THI .LT.    -THCR) )   MI1= -1.0
      IF( (THI .GT.  THCR).AND.(THI .LT.     N*PI) )   MI2= +1.0
      IF( (THR .GT.  THCR).AND.(THR .LT. 1.5*N*PI) )   MR2= +1.0
C     ------------------------------------------------------------
      WI1 = -CSQRT(2.0*RS) * COS( 0.5*(2*N*PI*MI1 - THI) )
      WR1 = -CSQRT(2.0*RS) * COS( 0.5*(2*N*PI*MR1 - THR) )
      WI2 = -CSQRT(2.0*RS) * COS( 0.5*(2*N*PI*MI2 - THI) )
      WR2 = -CSQRT(2.0*RS) * COS( 0.5*(2*N*PI*MR2 - THR) )
C     ------------------------------------------------
      TI1 = 0.5*(PI-THI) / N
      TR1 = 0.5*(PI-THR) / N
      TI2 = 0.5*(PI+THI) / N
      TR2 = 0.5*(PI+THR) / N
C     ---------------------------------------
      IF( ABS(TH-THSI ) .LE. ERR )   GO TO 11
      IF( ABS(TH-THSR1) .LE. ERR )   GO TO 22
C
      UD1 = GR(WI1)/TAN(TI1) - GR(WR1)/TAN(TR1)
      GO TO 33
C
11    UD1 = N * CSQRT(2.0*PI*RS) * CEXP(C*PI/4.0) - GR(WR1)/TAN(TR1)
      GO TO 33
C
22    UD1 = GR(WI1)/TAN(TI1) - N * CSQRT(2.0*PI*RS) * CEXP(C*PI/4.0)
C     ------------------------------------------------------------
33    IF( ABS(TH-THSR2) .LE. ERR )   GO TO 44
C
      UD2 = GR(WI2)/TAN(TI2) - GR(WR2)/TAN(TR2)
      GO TO 55
C
44    UD2 = GR(WI2)/TAN(TI2) + N * CSQRT(2.0*PI*RS) * CEXP(C*PI/4.0)
C
55    UD  = U0 * UE * (UD1+UD2)
C     ------------------------------------------------------------
      IF( (TH0 .GT. (N-1.0)*PI).AND.(TH0 .LE. N*PI/2.0) )  GO TO 66
C     ------------------------------------------------------------
      UT  = UD
      IF(  TH .LE. THSR1 )                          UT = UD + UI + UR1
      IF( (TH .GT. THSR1).AND.(TH .LE. THSI) )  UT = UD + UI
      GO TO 99
C
66    UT  = UD + UI
      IF( TH .LE. THSR1 )    UT = UT + UR1
      IF( TH .GT. THSR2 )    UT = UT + UR2
      GO TO 99
```

```
C
88    UT  = 0.0
C
99    AUT(K)= CABS(UT)
      IF( AUT(K) .GT .BIG )   BIG = AUT(K)
C     ====================================
111   CONTINUE
C     ===============
      DO  222  K=1,KK
      UTN = AUT(K)/BIG
      WRITE(6,1) Y(K) , UTN
222   CONTINUE
C      ==========
999   CONTINUE
C     =========================
1     FORMAT( F6.1 ,1X, E14.7 )
      STOP
      END
C ======================================================================
C PROGR. FOR CALCULATING MODIFIED FRESNEL INTEGRAL OF COMPLEX ARGUMENT
C ----------------------------------------------------------------------
      COMPLEX FUNCTION  GR(X)
C     ======================
      COMPLEX*8  C , X , CFR
      C    = CMPLX(0.0,1.0)
      PI   = 3.1415926
C     ------------------------------------------
      IF( REAL(X*CEXP(C*PI/4.0)) .LT. 0.0 )   X = -X
      GR   = 2.0 * C * X * CEXP(C*X*X) *CFR(X)
      RETURN
      END
C ======================================================================
C PROGRAM FOR CALCULATING FRESNEL INTEGRAL "CFR" OF COMPLEX ARGUMENT.
C ======================================================================
      COMPLEX FUNCTION   CFR(X)
C     ========================
      COMPLEX*8   C , X
      COMPLEX*16  Z , ERFZ
C      --------------------
      C    = CMPLX(0.0,1.0)
      PI   = 3.1415926
C      -------------------------
      Z    = X * CEXP(C*PI/4.0)
      CALL CERF(Z,ERFZ)
      CFR  = 0.5 * SQRT(PI) * CEXP(-C*PI/4.0) * (1.0 - ERFZ)
      RETURN
      END
C**********************************************************************
C**********************************************************************
```

G.6 Beam Diffraction by a Circular Aperture

This program makes use of expressions (6.33a,b) to calculate the single and multiple diffraction total fields modified on the caustic axis with $kz_0 = ka = 3\pi$, $\theta_0 = 90^o$, $\beta = 270^o$ and different values of the beam parameter, kb.

```
C**********************************************************************
C PROGRAM CALCULATES SINGLE AND MULTIPLE BEAM DIFFRACTION BY CIRCULAR
C APERTURE (NORMAL INCIDENCE), MODIFIED ON THE CAUSTIC AXIS, USING THE
C UNIFROM THEORY OF DIFFRACTION & COMPLEX SOURCE-POINT REPRESENTATION.
C THIS PROGRAM IS CALLED " CRCL.FTN2 ".
C ======================================================================
C THE TIME DEPENDENCE "exp(-iwt)" AND A COMMON FACTOR "exp(ikr)/kr"
C ARE SUPPRESSED.
C======================================================================
      COMMON      C ,PI ,THSI
C     ----------------------------------------------------------
      COMPLEX*8   C  ,CASIN ,CACOS ,CATAN     ,DC  ,FR  ,CFR
      COMPLEX*8   ZS ,RS1 ,THS1 ,WI              ,B0S ,B1S ,B0M ,B1M
      COMPLEX*8   UE ,UI ,UR ,U1 ,U2 ,USD ,UMD ,US
      COMPLEX*8   D0 ,D1 ,D2 ,DI ,DF1 ,DF2
      REAL   *4   Y(181) , AUS(181) , AUT(181)
C     ----------------------------------------------------------
            JJ = 16
            KK = 91
            H  = 1.0
C     ======================
      C     = CMPLX(0.0,1.0)
      PI    = 3.1415926
      DTR   = PI/180.
C     ---------------
      A     = 3*PI
      Z0    = A
      BETA  = 1.5*PI
C     ===========================
      R01  = SQRT( Z0**2 + A**2 )
      TH01 = PI - ATAN( Z0/A )
C
         DO 999 I=1,6
         B  = 2.**(I-1)
      IF ( I .LE. 1 )   B = 0.0
      IF ( I .GE. 6 )   B = 85.0
C     -------------------------
      ZS   = Z0 - C*B
C     -----------------------------
      RS1  = CSQRT( ZS**2 + A**2 )
      IF ( REAL(RS1) .LE. 0.0 )  RS1 = -RS1
      THS1 = PI - CATAN( ZS/A )
C ======================================================================
C       THSI, THSR ARE THE SHADOW AND REFLECTION BOUNDARY ANGLES.
C ======================================================================
      THSI = PI + TH01 + ACOS( REAL(RS1)/R01 )
      IF( BETA .GT. TH01+PI )  THSI = 2.*(PI+TH01) -THSI
      THSR = 2.0*PI - THSI
C     ------------------------
      UE   = CEXP(C*RS1) / RS1
C     ----------------------------------------------------------
      D0   = SQRT(4./PI) * CEXP( C*(PI/4 - 2.*A) ) * FR( SQRT(4.*A) )
C
      WI    = CSQRT(2.0*RS1) *CSIN(THS1/2.0)
      IF( REAL( WI*CEXP(-C*PI/4.) ) .LT. 0.0 )     TOP
      DI   = CSQRT(2.*RS1/(PI*A)) *CEXP(C*(PI/4.+2.*A))
      DI   = DI * CEXP(-C*WI**2) *CFR(WI)
```

```
C     ==================================
         BG = 0.0
C     --------------
      DO 111  K=1,KK
      Y(K) = H*(K-1)
      FI   = Y(K)*DTR
C     ------------------
      TH1  = 1.5*PI + FI
      TH2  = 1.5*PI - FI
C     ---------------------------------
      WF1  = SQRT(4.0*A) * SIN(TH1/2.0)
      WF2  = SQRT(4.0*A) * SIN(TH2/2.0)
      DF1  = CEXP(-C*WF1**2) * FR(WF1)
      DF2  = CEXP(-C*WF2**2) * FR(WF2)
C     ---------------------------------
      D1   = DC(THS1,RS1,TH1)
      D2   = DC(THS1,RS1,TH2)
C     ---------------------------------
      UI   =  CEXP( C * ZS * COS(FI) )
      UR   = -CEXP(-C * ZS * COS(FI) )
C     ----------------------------------
      IF( K .GT. JJ )            GO TO 11
C     -----------------------------------
      B0S  = (D2 + D1) * BESJ0(A*SIN(FI),I)
      B1S  = (D2 - D1) * BESJ1(A*SIN(FI),I)
      USD  = A * SQRT(PI/2.0) * CEXP(-C*PI/4.0) * UE * (B0S + C*B1S)
C     ------------------------------------------------------------
      B0M  = (DF1 + DF2) *BESJ0(A*SIN(FI),I)
      B1M  = (DF1 - DF2) *BESJ1(A*SIN(FI),I)
      UMD  = 2. * (A**1.5) * UE * DI * (B1M + C*B0M) / (1.0-D0)
C     ------------------------------------------------------
      GO TO 22
C     ------------------------------------
11    U1   = CEXP( -C*(A*SIN(FI) - PI/4.) )
      U2   = 1.0/U1
      USD  = SQRT(A/SIN(FI)) *CEXP(-C*PI/4.) *UE *(U1*D1 + U2*D2)
C     ----------------------------------------------------------
      UMD  = C *A *SQRT( 8.0 /(PI*SIN(FI)) )
      UMD  = UMD *UE *DI *( U1*DF1 + U2*DF2 ) / (1.0-D0)
C     ---------------------------------------------------
      US   = USD
22    IF( (TH1 .LT. THSI).AND.(TH2 .LT. THSI) )  US = USD + UI
C
      AUS(K)= CABS(US)
      AUT(K)= CABS(US+UMD)
      IF( (AUS(K).GT.BG).OR.(AUT(K).GT.BG) ) BG=AMAX1(AUT(K),AUS(K))
C     ==============================================================
111   CONTINUE
C     ====================
      DO  222   K = 1 , KK
      USN  = AUS(K)/BG
      UTN  = AUT(K)/BG
      WRITE(6,1) Y(K) , USN , UTN
222   CONTINUE
C     ========
999   CONTINUE
C     ==============================
1     FORMAT( F6.1 , 2(1X , E14.7) )
      STOP
      END
```

```
C ==========================================================================
C       PROGRAM FOR CALCULATING DIFFRACTION COFFICIENT .
C ==========================================================================
      COMPLEX   FUNCTION  DC(THS,RS,TH)
C     ==================================
      COMMON      C ,PI ,THSI
      COMPLEX*8   C ,RS ,THS ,WI ,WR ,DI ,DR ,CFR
C     ------------------------------------------
      WI    = -CSQRT(2.0*RS) * CCOS( (TH-THS)/2.0 )
      WR    = -CSQRT(2.0*RS) * CCOS( (TH+THS)/2.0 )
      DI    = CFR(WI)
      DR    = CFR(WR)
C     ------------------------------------------------------
CC     IF( REAL(WI*CEXP(-C*PI/4.)) .LT. 0. )   DI = -CFR(-WI)
      IF( TH .LT. THSI )                      DI = -CFR(-WI)
      DC    = CSQRT(RS/PI) *CEXP(-C*PI/4.0)
      DC    = DC *( DI*CEXP(-C*WI**2) - DR*CEXP(-C*WR**2) )
      RETURN
      END
C ==========================================================================
C PROGRAM FOR CALCULATING FRESNEL INTEGRAL "CFR" OF COMPLEX ARGUMENTS.
C==========================================================================
      COMPLEX   FUNCTION  CFR(X)
C     ==========================
      COMMON      C ,PI
      COMPLEX*8   C , X
      COMPLEX*16  Z , ERFZ
C      ----------------------
      Z     = X*CEXP(-C*PI/4.0)
      CALL CERF(Z,ERFZ)
      CFR   = 0.5*SQRT(PI)*CEXP(C*PI/4.0)*(1.0-ERFZ)
      RETURN
      END
C ==========================================================================
C   PROGRAM FOR CALCULATING FRESNEL INTEGRAL "FR" OF REAL ARGUMENTS.
C==========================================================================
      COMPLEX   FUNCTION  FR(X)
C     =========================
      COMMON      C ,PI ,THSI
      COMPLEX*8   C
      COMPLEX*16  Z , ERFZ
C     ----------------------
      Z     = X*CEXP(-C*PI/4.0)
      CALL CERF(Z,ERFZ)
      FR    = 0.5*SQRT(PI)*CEXP(C*PI/4.0)*(1.0-ERFZ)
      RETURN
      END
C **************************************************************************
C**************************************************************************
```

G.7 Beam Diffraction by a Parabolic Reflector

The following program uses (E.17) to calculate the diffracted field component for a beam of parameters (kb=16, $\beta=180^{o}$), located at ($kr_{o}=0$, $\theta_{o}=0^{o}$) incident on a conducting parabolic reflector (kF=10π, $\theta_{e}=60^{o}$). Also, the program can be used to calculate the reflected and total far fields using (E.5), (E.4) and (E.17), without using the computer search technique.

```
C*********************************************************************
C PROGRAM CALCULATES ANTENNA BEAM DIFFRACTION BY A PARABOLIC REFLECTOR
C NO COMPUTER SEARCH FOR REFLECTION POINTS.
C THE PROGRAM IS CALLED "PRBL.FTN.NS".
C =====================================================================
C           TIME DEPENDCE " Exp(-iwt) ".
C           COMMON FACTOR " Exp(ikr)/Sqrt(kr) ".
C =====================================================================
      COMPLEX*8   C ,UI ,UR ,UD1 ,UD2 ,UD ,UT  ,CD ,CFR ,CASIN ,CACOS
      COMPLEX*8   THP ,THS ,THSP ,THS1 ,THS2 ,THI ,TH1P ,THS1P ,WP
      COMPLEX*8   F0 ,RI ,RR ,RS ,RP ,RSP ,RS1 ,RS2 ,RC ,RX ,XP ,YP
      COMPLEX*8   XS ,YS
      REAL*4      Z(361) ,AUI(361) ,AUR(361) ,AUD(361) ,AUT(361)
C     ---------------------------------------------------------------
                  KK = 181
                  H  = 1.0
C                 =======
      C   = CMPLX(0.0,1.0)
      PI  = 3.1415926
      DTR = PI/180.
      F0  = CEXP(-C*PI/4.)/SQRT(PI)
C     ----------------------------
      R0  = 0.0
      TH0 = 0.0
      F   = 10*PI
      THE = PI/3.0
      BET = PI+TH0
      B   = 16.0
C =====================================================================
C     BW IS THE HALF-POWER BEAM WIDTH
C =====================================================================
CC    BW  = 66.*DTR
CC    B   = 0.5*ALOG(2.0)/(1.0 - COS(BW/2.0))
C     ---------------------------------------
      THT = (PI-THE)/2.
      RE  = 2*F/(1.0+COS(THE))
      R01 = SQRT( RE**2 + R0**2 + 2*RE*R0*COS(THE+TH0) )
      TH01= THT + ASIN( R0*SIN(THE+TH0) /R01 )
C     -----------------------------------------------
      IF( BET .EQ. TH0+PI )                    GO TO 11
      RS  = CSQRT( R0**2 - 2*C*R0*B*COS(BET-TH0) - B**2 )
      IF( REAL(RS) .LE. 0.0 )                  RS  = -RS
      THS = CCOS( ( R0*COS(TH0) + C*B*COS(BET) ) /RS )
      GO TO 22
C
11    RS  = R0 - C*B
      THS = TH0
C     -----------------------------------------------
22    RS1 = CSQRT( RE**2 + RS**2 + 2*RE*RS*CCOS(THE+THS) )
      IF( REAL(RS1) .LE. 0.0 )    RS1 = -RS1
      THS1= THT + CASIN( RS*CSIN(THE+THS) /RS1 )
      RS2 = RS1
      THS2= THS1
C =====================================================================
C      THBI, THBR ARE THE SHADOW AND REFLECTION BOUNDARY ANGLES
C =====================================================================
      THBI= TH01 + PI + ACOS(REAL(RS1)/R01)
      IF( BET .GT. (TH01+THT) )   THBI = 2*(PI+TH01) - THBI
      THBR= 2*PI - THBI
```

```
C     ================
         BIG = 0.0
      DO 111  K = 1,KK
      Z(K)= H*(K-1)
      TH  = Z(K)*DTR
C     ------------------
      TH1 = (PI-THT) + TH
      IF( TH1 .GT. 2.0*PI )                TH1 = TH1 - 2.0*PI
      TH2 = (PI-THT) - TH
      IF( TH2 .LT. 0.0 )                   TH2 = TH2 + 2.0*PI
C     ------------------------------------------------------
      UD1 = F0 * CEXP( C*RE*COS(TH+THE) ) * CD(RS1,THS1,TH1)
      IF( (TH .GT. PI/2.).AND.(TH .LT. (PI-THT)) )  GO TO 33
      UD2 = F0 * CEXP( C*RE*COS(TH-THE) ) * CD(RS2,THS2,TH2)
         GO TO 44
33    UD2 = 0.0
C     ---------------
44    UD  = UD1 + UD2
      AUD(K)= CABS(UD)
      IF( AUD(K) .GT. BIG )  BIG = AUD(K)
C ==========================================================================
C      TO CALCULATE THE DIFFRACTED FIELD COMPONENT ONLY GO TO 111
C ==========================================================================
      GO TO 111
C     ------------------------------------------------------------------
110   IF( TH .GT. (PI-THE) )                                    GO TO 55
      THR = TH
      THP =-.5 *( THS+THR + CASIN(4.*F*SIN(THR)/RS + CSIN(THS+THR)) )
C     ------------------------------------------------------------------
      RP  = 2.*F/(1.+CCOS(THP))
      IF( REAL(RP) .LE. 0.0 )   RP  = -RP
C
      RSP = CSQRT( RP**2 + RS**2 + 2.*RP*RS*CCOS(THP+THS) )
      IF( REAL(RSP) .LE. 0.0 )  RSP = -RSP
      THSP= THR+THP
C
      TH1P = (PI+THP)/2. + TH
      THS1P= (PI+THP)/2. - THSP
      WP  = -CSQRT(2.*RSP) * CCOS((TH1P+THS1P)/2.)
      RWP = REAL( WP * CEXP(-C*PI/4.) )
      IF( RWP .GT. 0.0 )  GO TO 55
C     ----------------------------
      THI = THP/2.0 - THSP
      IF( REAL(THI) .LT. 0. )   THI =-THI
      RC  = 2.0*F/CCOS(THP/2.0)**3
      RX  = -RC*CCOS(THI)*RSP/( 2.0*RSP-RC*CCOS(THI) )
C     ------------------------------------------------
      UR  = CEXP( C*(RSP + RP*CCOS(TH+THP)) )
         GO TO 66
55    UR  = 0.0
66    AUR(K)= CABS(UR)
CC    IF( AUR(K) .GT. BIG )  BIG = AUR(K)
C     ----------------------------------
      IF( TH1 .GT. THBI )       GO TO 77
      UI  = CEXP( B*COS(TH-BET) - C*R0*COS(TH-TH0) )
      GO TO 88
77    UI  = 0.0
88    AUI(K)= CABS(UI)
C     ----------------------------------
      UT  = UI + UR + UD
```

```
      AUT(K)= CABS(UT)
CC    IF( AUT(K) .GT. BIG )  BIG = AUT(K)
C     ----------------------------------
111   CONTINUE
C     ==========
      DO 222  K = 1 , KK
CC    UIN  = AUI(K)/BIG
CC    URN  = AUR(K)/BIG
      UDN  = AUD(K)/BIG
CC    UTN  = AUT(K)/BIG
222   WRITE(6,1)  Z(K) ,UDN
C     -------------------------
1     FORMAT( F6.1 ,1X, E14.7 )
      STOP
      END
C=======================================================================
C PROGRAM CALCULATES THE DIFFRACTED FIELD COMPONENT BY A HALF SCREEN.
C =======================================================================
      COMPLEX  FUNCTION  CD(R0,TH0,TH)
C     ================================
      COMPLEX*8   C ,TH0 ,R0 ,WI ,WR ,EI ,ER ,DI ,DR ,CFR
C     ---------------------------------------------------
      PI  = 3.1415926
      C   = CMPLX(0.0,1.0)
C     ---------------------------------
      EI  = CEXP( -C*R0 *CCOS(TH-TH0) )
      ER  = CEXP( -C*R0 *CCOS(TH+TH0) )
      WI  =-CSQRT(2.0*R0) * CCOS((TH-TH0)/2.0)
      WR  =-CSQRT(2.0*R0) * CCOS((TH+TH0)/2.0)
      RWI = REAL( WI *CEXP(-C*PI/4.) )
      RWR = REAL( WR *CEXP(-C*PI/4.) )
C     -------------------------------
      DI  = CFR(WI)
      DR  = CFR(WR)
      IF ( RWI .LT. 0.0 )   DI = -CFR(-WI)
      IF ( RWR .LT. 0.0 )   DR = -CFR(-WR)
      CD = EI*DI - ER*DR
      RETURN
      END
C=======================================================================
C PROGRAM CALCULATES THE FRESNEL INTEGRAL "CFR" OF COMPLEX ARGUMENTS.
C =======================================================================
      COMPLEX  FUNCTION   CFR(X)
C     ==========================
      COMPLEX*8   C , X
      COMPLEX*16  Z , ERFZ
C     --------------------
      PI   = 3.1415926
      C    = CMPLX(0.0,1.0)
C
      Z    = X * CEXP( -C*PI/4.0 )
      CALL CERF(Z,ERFZ)
      CFR  = 0.5 * SQRT(PI) * CEXP(C*PI/4.0) * (1.0 - ERFZ)
      RETURN
      END
C***********************************************************************
C***********************************************************************
```